TOXIC SUBSTANCES FROM COAL COMBUSTION -- PHASE I COAL SELECTION AND CHARACTERIZATION

TOPICAL REPORT

Reporting Period: Start Date:10/01/1995 End Date: 09/30/1997

Authors:
C.L. Senior (1)
F.E. Huggins, G.P. Huffman, N. Shah (2)
S.Crowley, A. Kolker, C.A. Palmer, R. Finkelman(3)"
A. Sarofim, I. Olmez, T. Zeng (4)

Report Issue Date: 07/16/1998

DE-AC22-95PC95101--09

Physical Sciences Inc.
20 New England Business Center
Andover, MA 01810-1077

University of Kentucky
Lexington, KY 40506-0059

U.S. Geological Survey
Eastern Energy Resources
National Center
Reston, VA 20192"

Massachusetts Institute of Technology
Cambridge, MA 02139

Disclaimer

TABLE OF CONTENTS

TABLE OF CONTENTS (Continued)

LIST OF GRAPHICAL MATERIALS

LIST OF GRAPHICAL MATERIALS (Continued)

LIST OF GRAPHICAL MATERIALS (Continued)

LIST OF TABLES

LIST OF TABLES (Continued)

SECTION 1

EXECUTIVE SUMMARY

1. EXECUTIVE SUMMARY

1.1 Introduction

The Clean Air Act Amendments of 1990 identify a number of hazardous air pollutants (HAPs) as candidates for regulation. Should regulations be imposed on HAP emissions from coal-fired power plants, a sound understanding of the fundamental principles controlling the formation and partitioning of toxic species during coal combustion will be needed. Over the past decade, a large database identifying the partitioning and emitted concentrations of several toxic metals on the list of HAPs has been developed. Laboratory data have also been generated to help define the general behavior of several elements in combustion systems. These data have been used to develop empirical and probabalistic models to predict emissions of trace metals from coal-fired power plants.

While useful for providing average emissions of toxic species, these empirically based models fail when extrapolated beyond their supporting database. This represents a critical gap; over the coming decades, new fuels and combustion systems will play an increasing role in our nation's power generation system. For example, new fuels, such as coal blends or beneficiated fuels, new operating conditions, such as low-NO_x burners or staged combustion, or new power systems, for example, those being developed under the DoE sponsored Combustion 2000 programs and integrated gasification combined cycle (IGCC) systems, are all expected to play a role in power generation in the next century.

The need for new predictive tools is not limited to new combustion systems, however. Existing combustion systems may have to employ controls for HAPs, should regulations be imposed. Testing of new control methods, at pilot and full scale, is expensive. A sound understanding of the chemical transformations of both organic and inorganic HAPs will promote the development of new control methods in a cost-effective manner. To ensure that coal-fired power generation proceeds in an environmentally benign fashion, methods for the prediction and control of toxic species in a broad range of coal fired systems must be developed.

1.2 Objective

In Phase I of this program, a team led by Physical Sciences Inc. (PSI), and involving researchers from the University of Kentucky (UKy), U.S.Geological Survey (USGS), Massachusetts Institute of Technology (MIT), the University of Arizona (UA), the University of Connecticut, and Princeton University have begun a detailed research program with three major objectives: (1) to elucidate the important mechanisms of toxics formation and partitioning; (2) develop submodels for the appropriate trace toxic species transformations; and (3) to incorporate these mechanisms into an Engineering Model to predict trace toxic formation, partitioning, and fate based upon coal and combustion parameters. In the 2-year Phase I program described here, preliminary experiments were performed to decide upon the relevant mechanisms for trace element transformations. The 3-year Phase II program which follows will contain more detailed experiments and model developement activities.

1.3 Coal Selection and Characterization

We chose four coals for detailed study in Phase I. Variation in source and coal mineralogy were criteria for selection, as well as economic importance. The four coals are as follows: Pittsburgh Seam, Northern Appalachian bituminous coal; Elkorn and Hazard Seams, Eastern Kentucky, low sulfur, "compliance" coal; Illinois 6 Seam, Illinois basin bituminous coal; and Wyodak Seam: Powder River Basin sub-bituminous coal. Pulverized samples were procured and characterized by traditional analyses as well as advanced analyses such as Computer-Controlled Scanning Electron Microscopy (CCSEM), Mössbauer spectroscopy, and X-Ray Absorption Fine Structure (XAFS) spectroscopy at the University of Kentucky and selective leaching and microprobe at USGS. Of particular interest were the forms of occurrence of the trace elements Hg, As, Se, and Cr in the coals. All experimentalists in the program received samples from the same lot of pulverized coal.

The coals that were selected for study in Phase I had a variety in the forms of occurrence of key HAP metals, As, Se, Cr, and Hg. Forms of occurence of trace metals were determined by different methods employed at the University of Kentucky and the USGS. There was good quantitative agreement between the results of the two groups. Key results can be summarized as follows:

- Arsenic was associated with pyrite (or oxidized pyrite) in the bituminous coals but was organically associated in the subbituminous coal.

- Selenium was assocated with pyrite in the Pittsburgh coal, but split between pyrite and organic association in the other two bituminous coals.

- Chromium was primarily found as amorphous CrOOH in the bituminous coals, although a significant fraction was found as clays, particularly in the Pittsburgh and Elkorn/Hazard seam coals. Chromium was organically associated in the Wyodak coal.

- Mercury was difficult to detect, but seemed to be found both in organic form and in sulfides in the bituminous coals.

SECTION 2

INTRODUCTION AND PROGRAM OVERVIEW

2. INTRODUCTION AND PROGRAM OVERVIEW

Before electric utilities can plan or implement emissions minimization strategies for hazardous pollutants, they must have an accurate and site-specific means of predicting emissions in all effluent streams for the broad range of fuels and operating conditions commonly utilized. Development of a broadly applicable emissions model useful to utility planners first requires a sound understanding of the fundamental principles controlling the formation and partitioning of toxic species during coal combustion (specifically in Phase I, As, Se, Cr, and possibly Hg). Physical Sciences Inc. (PSI) and its team members will achieve this objective through the development of an "Engineering Model" that accurately predicts the formation and partitioning of toxic species as a result of coal combustion. The "Toxics Partitioning Engineering Model" (ToPEM) will be applicable to all conditions including new fuels or blends, low-NO_x combustion systems, and new power systems being advanced by DOE in the Combustion 2000 program.

Based on a goal of developing and delivering this ToPEM model, a 5-year research program was proposed. This program is divided into a 2-year Phase I program and a 3-year Phase II program. The objective of the Phase I program is to develop an experimental and conceptual framework for the behavior of selected trace elements (arsenic, selenium, chromium, and mercury) in combustion systems. This Phase I program was undertaken by a team of researchers from the Massachusetts Institute of Technology (MIT), the University of Arizona (UA), the University of Kentucky (UKy), Princeton University, the University of Connecticut, and PSI. Model development and commercialization will be carried out by PSI.

Our general approach to the development of the ToPEM model is to break the process for toxic formation into sub-processes, each of which will be addressed by team members who are experts in the area. Ultimately, this will result in new sub-models which will be added to the existing Engineering Model for Ash Formation (EMAF) to create ToPEM. Figure 2-1 illustrates the relationship between the elements of the Phase I Work Breakdown Structure and the sub-processes. Characterization of the coal mineralogy and of the forms of occurrence of trace elements in coal is the cornerstone of this program. A significant effort was carried out in the Phase I program to procure, prepare, and characterize representative coal samples.

One of the most important questions to be answered in the program as a whole is whether the form of a particular element in the coal affects its form of emission at the end of the process. The answer to this question will determine the shape of the sub-models that must be developed in this program. Thus, a detailed understanding of the forms of individual trace elements in coal provides a foundation for much of the rest of the program. Key issues that were addressed in Phase I are the specific mineral associations of individual elements and the relationship between trace metal form and “standard” analyses.

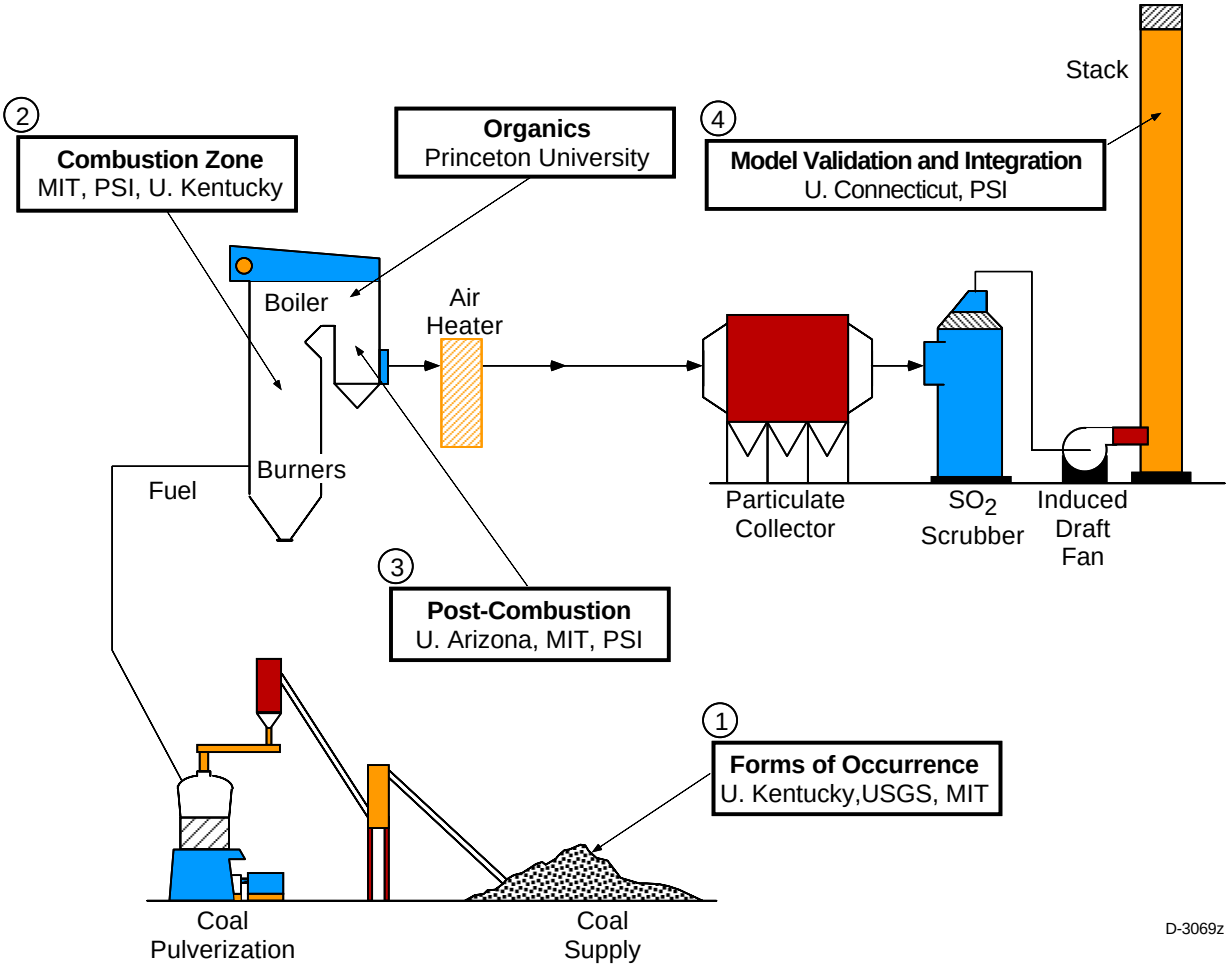

Figure 2-1. Project organization.

SECTION 3

RESULTS AND DISCUSSION

3. RESULTS AND DISCUSSION

3.1 Coal Selection

One of the primary goals of this program is to determine the mechanisms that govern the partitioning of trace elements into forms that may be emitted from commercial power plants, with the ultimate goal of developing a model framework to predict potential emissions. For this reason it is extremely important that the coals (and the experimental conditions) used in this program be directly applicable to commercial systems. By studying coals that are either currently in widespread use, for which a great deal of operational information exists, or are potentially attractive as 'compliance coals,' we can facilitate the use of the information obtained in this program in the full scale systems.

Another important criterion for coal selection is the mode-of-occurrence of the trace elements in the coals. As one of the technical objectives of the Phase I program is to explore the link between the mode-of-occurrence of a given element in coal and its partitioning into potentially emitted phases (i.e., submicron fume or vapor), it is important to pick coals which have a wide range of modes of occurrence for selected elements. As this information is not always readily apparent, at least two coals were selected based on either knowledge gained in previous programs at PSI or knowledge of the general trends of trace elements with other coal parameters, such as ash yield and sulfur content. In addition, in order to facilitate XAFS analysis of the coals, efforts were taken to maximize the arsenic concentrations in the coal, while still only utilizing those coals that are suitable for use in commercial power plants. In summary, the following criteria were used to select the coals:

- Diversity of coal and mineral types
- All coals currently burned by utilities
- One low sulfur eastern bituminous coal and one PRB coal
- Maximize concentrations of arsenic in the coal.

The Phase I coal samples were obtained from the following beds:

1. Illinois No. 6
2. Pittsburgh seam (washed)
3. A low sulfur bituminous coal, a mixture of the Elkhorn and Hazard seams from eastern Kentucky
4. Wyodak subbituminous

Samples of the Illinois No. 6 coal were studied under previous DOE funded programs at PSI. This represents a coal for which PSI has background information and a commonly used coal for power production. Although use of Illinois basin coals has decreased over the last 5 years, primarily due to the increased use of low sulfur Powder River Basin coals, coals from this seam have been used for many years by the power industry. Therefore, many utilities have operating experience with these coals. For this reason, the combustion characteristics and mineral matter transformations of Illinois No. 6 coals have been studied extensively. In addition, coal samples

from this seam are commonly used as design coals for novel power systems (such as the Combustion 2000 program) as they provide a ready link between the operating characteristics of the new unit and the operating characteristics familiar to many utilities.

The washed Pittsburgh seam coal was also studied under previous DOE funded programs. For example, this coal was utilized in the DOE program to collect data on trace element partitioning in full scale units (these data were evaluated as part of Task 7 in the current program). Although trace element concentration does vary within a particular mine, the use of this coal in our current program allowed qualitative comparisons to be drawn between the data trends observed in the small scale program with the full scale data. In addition, a PSI-led team (including many members of the current research team) studied a highly washed version of the coal from this mine to explore the effect of reducing conditions on mineral transformations during combustion (DE-AC22-93PC92190). This coal sample was also studied at PSI under a Phase I DOE SBIR program (DE-FG02-94ER81834) to study arsenic, selenium, and mercury partitioning during combustion. This study (Bool and Helble, 1995) explored the effect of forms-of-occurrence of these elements on their partitioning under a single combustion system. This preliminary information provided important guidance for the more detailed experiments carried out in this program.

The next coal, the low-sulfur eastern Kentucky coal, represents a compliance coal that is currently in use by utilities to meet the CAAA Title IV regulations. The coal comes from a single mine in eastern Kentucky, but is a mixture of the Elkhorn and Hazard seams. The Wyodak coal is another important coal for this program. ABB-Combustion Engineering examined this coal in a separate DOE program on enhanced ESP performance by burning the coal in a pilot-scale combustor. We have teamed with ABB to investigate a common coal in the two DOE funded programs. This collaboration allowed us to evaluate trace element partitioning at the pilot scale for this coal - data needed for extrapolating results obtained on the smaller scale facilities to full scale boilers.

The three bituminous coals were obtained from CONSOL. Coals were received at the CONSOL R&D Center in Library, PA and pulverized there. PSI received approximately one ton of each coal. Samples were sent to each of the team members and the drums were purged with argon to prevent changes in coal properties due to oxidation. Approximately twenty tons of the Wyodak coal was received at ABB and a one ton subsample sent to PSI for distribution to program participants. In addition, a small sample of each coal was sent to a commercial laboratory for analysis.

After the USGS received the program coals, they were shipped to Geochemical Testing of Somerset, Pennsylvania (May, 1996) for grinding of samples to -20 mesh splits (to be used in petrographic, SEM, and microprobe analysis) and -60 mesh splits (for analysis by ICP-MS, ICP-AES, hydride generation, and cold vapor atomic absorption). Geochemical Testing also provided sulfur form analyses. The USGS received the Pittsburgh and Elkhorn/Hazard coals in May 1996; the Illinois No. 6 coal in June 1996; and the Wyodak coal in February 1997.

3.2 Coal Composition and Mineralogy

3.2.1 *Ultimate, Proximate, and Ash Chemistry Analyses*

Table 3-1 shows the ultimate, proximate, and ash composition for the program coals. As can be seen from this table, the ash yields of the Pittsburgh and the Elkhorn/Hazard coal are very similar. The Pittsburgh coal contains 7.01% ash, and the Elkhorn/ Hazard coal contains 7.41%. The Illinois No. 6 has a higher ash yield, 10.26%. This coal also has a much higher sulfur content that the other two bituminous coals. The ash composition of the Pittsburgh and Illinois No. 6 coals are very similar. The ash from these two coals is fairly typical of American bituminous coals, containing primarily silica, alumina, and iron oxide. The Elkhorn/ Hazard coal, however, is somewhat atypical as it contains a relatively low iron concentration in the ash. This, and the lower sulfur content of this coal, suggest that the pyrite content of the coal is low.

The ash yield for the Wyodak coal is similar to the other program coals. The moisture content is much higher for this coal than the bituminous coals. Moisture in the raw, crushed, coal obtained by ABB was much higher, approximately 30%, than the as-received coal at PSI which had already been pulverized. The drop in moisture content indicates that the coal was dried during pulverization at ABB. Another parameter that is much different than the bituminous coals is the high calcium content of the Wyodak coal. This high calcium content, and low iron content, is typical of coals from the Powder River Basin. Experiments with this coal provided valuable insight on the role of calcium on arsenic retention in the fly ash.

The forms of sulfur analyses for the Phase I coals were reported by the USGS and presented in Table 3-2. The data in Table 3-2 indicate that the Illinois No. 6 coal contains significant amounts of both pyritic and organic sulfur. The Elkhorn/Hazard and Wyodak coals contain primarily organic sulfur.

3.2.2 *SEM and XRD Analyses*

The USGS prepared samples of the raw coals for analysis by Scanning Electron Microscope (SEM) and X-Ray Diffraction (XRD) analyses. The pellet formation procedure follows the ASTM D2797-85 technique for anthracite and bituminous coal (ASTM, 1993). In the casting procedure, approximately 7 to 8 g of crushed sample are impregnated, under pressure, with Armstrong C4 epoxy. The resultant mold is cured overnight at room temperature. A label is incorporated with the sample.

The pellet block is ground and polished using ASTM D2797-85 procedures (ASTM, 1993). In this process, the epoxy-coal pellet is ground with a 15 µm diamond platen and 600-grit

Table 3-1. Coal Properties Phase I Program Coals

	Elkhorn/Hazard		Pittsburgh		Illinois No. 6		Wyodak	
	Dry Basis	As Received	Dry Basis	As Received	Dry Basis	As Received	Dry Basis	As Received
Proximate (wt %):								
Fixed Carbon	57.80	56.46	62.23	61.99	54.98	53.16	49.62	43.14
Volatile Matter	34.61	33.80	30.66	30.22	34.41	33.27	41.91	36.44
Moisture	0.00	2.33	0.00	1.44	0.00	3.31	0.00	13.06
Ash	7.59	7.41	7.11	7.01	10.61	10.26	8.47	7.36
Ultimate (wt %):								
Carbon	76.66	74.87	77.74	76.62	70.02	67.70	61.19	53.20
Hydrogen	4.70	4.59	4.87	4.80	4.89	4.73	5.28	4.59
Nitrogen	1.46	1.43	1.50	1.48	1.22	1.18	0.95	0.83
Sulfur	0.84	0.82	1.66	1.64	3.72	3.60	0.25	0.22
Oxygen	8.58	8.38	7.01	6.91	9.50	9.20	23.86	20.74
Chlorine	0.17	0.17	0.099	0.098	0.035	0.034	NA	NA
Moisture	0.00	2.33	0.00	1.44	0.00	3.31	0.00	13.06
Ash	7.59	7.41	7.11	7.01	10.61	10.26	8.47	7.36
Ash Composition (wt%):								
SiO_2	55.83		42.92		44.38		31.76	
Al_2O_3	34.27		22.87		17.35		18.04	
Fe_2O_3	5.18		19.18		19.80		5.81	
TiO_2	1.71		1.08		0.91		1.80	
CaO	1.84		4.51		4.00		24.35	
MgO	0.60		0.97		0.85		2.61	
Na_2O	0.32		1.28		0.63		0.90	
K_2O	1.53		1.21		1.80		0.70	
SO_3	1.45		5.40		4.62		12.93	
P_2O_5	0.23		0.57		0.12		1.10	

Table 3-2. Forms of Sulfur in Phase I Program Coals

	Elkhorn/Hazard		Pittsburgh		Illinois No. 6		Wyodak	
Sulfur (wt%, dry basis)	0.87		2.12		3.82		0.46	
Forms of sulfur:	Wt % in Coal (Dry Basis)	Percent of Total Sulfur	Wt % in Coal (Dry Basis)	Percent of Total Sulfur	Wt % in Coal (Dry Basis)	Percent of Total Sulfur	Wt % in Coal (Dry Basis)	Percent of Total Sulfur
Sulfate	0.03	3.4	0.01	0.5	0.04	1.0	0.02	4.3
Pyritic	0.12	13.8	0.91	42.9	1.57	41.1	0.03	6.5
Organic	0.72	82.8	1.2	56.6	2.21	57.9	0.41	89.1

SiC paper until flat and smooth. Rough polishing is done with 1 µm alumina and final polishing is completed with 0.06 µm colloidal silica. Ultrasonic cleaning between and after the various steps insures a final product free of extraneous abrasive material. Two pellets are prepared from each sample. The pellets are sectioned with a thin, slow-speed diamond saw and carbon-coated for SEM and microprobe analysis (Section 3.3.2).

Scanning Electron Microscope Analysis.

A JEOL-840[1] scanning electron microscope equipped with a Princeton Gamma-Tech.[1] energy-dispersive X-ray analytical system and/or an Autoscan ETEC[1] with Kevex EDX were used for SEM examination of project coals. Mineral identifications were made on the basis of grain morphology and major-element composition. Both secondary electron imaging (SEI) and back-scattered electron imaging (BSE) modes were used in coal sample characterization. The BSE mode is especially sensitive to variation in mean atomic number, and is useful for showing within-grain compositional variation. By optimizing the BSE image, the presence of high-atomic number trace phases can be revealed. Samples were scanned initially to obtain an overall view of the phases present, as with a petrographic microscope. This initial scanning was followed by a series of overlapping traverses in which the relative abundance of the phases was assessed. EDX analysis provides information on elements having concentrations at approximately a tenth-of-weight-percent level or greater. Typical operating conditions for SEM analysis were: accelerating potential of 10 to 30 kV, magnifications of ~ 50 to 10,000x and working distances ranging from 15 to 20 mm (ETEC) and 25 or 39 mm (JEOL).

Scanning electron microscopy preceded electron microprobe analysis which will be discussed in Section 3.3.2. SEI or BSE images taken at low magnification were used as a guide to locate phases of interest for microprobe analysis. SEM images taken at higher magnifications provided records of the points analyzed. Images at higher magnifications commonly reveal the presence of interstices or other imperfections in mineral grains that are not visible in reflected light microscopy. SEI/BSI mapping enabled us to avoid features that would adversely affect the quantitative analysis using the microprobe.

[1]Use of trade names is for information purposes only and does not constitute an endorsement by USGS

Table 3-3. Mineralogy of the Three Program Coals Inferred from SEM Analysis

Pittsburgh		
	Major:	Illite, kaolinite, quartz, pyrite, calcite, iron oxide
	Minor/trace:	Barite, TiO_2, calcium sulfate (probably gypsum)
Elkhorn/Hazard		
	Major:	Illite, kaolinite, quartz, pyrite
	Minor/trace:	Iron oxide, chalcopyrite, TiO_2, barite, apatite, monazite (REE phosphate), zircon.
Illinois No. 6		
	Major:	Illite, kaolinite, quartz, pyrite, calcite
	Minor/trace:	none observed
Wyodak		
	Major:	Quartz, illite, kaolinite, mixed layer clays
	Minor/trace:	Pyrite

SEM analyses indicate the presence of the major minerals illite, kaolinite, quartz, calcite, and pyrite in the Pittsburgh and Illinois No. 6 coals (Table 3-3). The Elkhorn/Hazard coal contains the same major phases, with the exception of calcite. (However, trace amounts of calcite were detected in the Elkhorn/Hazard with XRD analysis, as discussed below). Iron oxides were also found to be a major constituent of the Pittsburgh coal. Other minerals were found in minor or trace amounts in each of the coals. In the Wyodak coal, major minerals detected include quartz, illite, kaolinite, and possibly mixed-layer clays. Pyrite was found only in very minor amounts in the Wyodak coal. A range of pyrite morphologies was observed in the program coals using the SEM, including subhedral, euhedral, composite, and framboidal grains.

X-Ray Diffraction Analysis

In order to obtain semi-quantitative information on minerals present in the study coals, samples of low-temperature (< 473 K) ash were pressed onto powdered plastic backings to form wafers which were X-rayed using an automated diffractometer. The samples were diffracted over an interval from 4^o to 60^o 2θ at a step interval of 0.02^o 2θ. Counts were collected for 0.5 s per step. The data were processed using a computer program for semi-quantitative mineral analysis by X-ray diffraction (Hosterman and Dulong, 1985).

Results of X-ray diffraction analysis of low-temperature ash are presented in Table 3-4, together with semi-quantitative estimates of the mineral content of the coal on a dry, whole-coal basis. Quartz and kaolinite are dominant in each of the four program coals. Illite is dominant in the Pittsburgh, Elkhorn/Hazard, and Illinois No. 6 coals; however, it occurs only in trace amounts in the Wyodak coal. Bassanite (a form of calcium-sulfate), which is formed from calcium and

Table 3-4. Semi-Quantitative Ash Mineralogy by XRD*

Sample	% Ash	Quartz	Feldspar	Calcite	Siderite	Ankerite	Illite	Kaolinite	Pyrite	Gypsum and Bassanite	Sphalerite	Analcime	Hematite
Pittsburgh	7.3	20	trace**	trace	trace	trace	10	45	20				
		[1.5]***					[0.7]	[3.3]	[1.5]				
Elkhorn/ Hazard	8.0	15	trace	trace	trace		10	65	trace				
		[1.2]					[0.8]	[5.2]					
Illinois #6	10.3	25		trace	trace		10	35	20	trace	trace		trace
		[2.6]					[1.0]	[3.6]	[2.1]				
Wyodak	7.9	30		< 5			< 5	60		10		< 5****	
		[2.6]		[1.0]			[1.0]	[3.6]				[< 0.4]	

* Analyst F. Dulong, USGS-Reston

** Values less than 5% are termed "trace." Because there are no "trace" amounts in Wyodak, numbers add up to 100% for this coal. The other coals have "trace" amounts of several minerals.

*** Numbers in brackets indicate percent values recalculated to a dry, whole-coal basis.

**** Analcime is indicated in a trace amount at the lowest level of probability.

sulfur in the ashing process, is dominant only in the Wyodak coal. XRD analysis indicates pyrite concentrations of 1.5 and 2.1% on a whole-coal basis in the Pittsburgh and Illinois No. 6 coals, respectively. In the Elkhorn/Hazard coal, only trace amounts of pyrite were detected by XRD. Although pyrite was not detected by XRD analysis in the Wyodak coal, it was observed with SEM analysis. Trace amounts of calcite are present in the Pittsburgh, Elkhorn/Hazard, and Illinois No. 6 coals.

The XRD data are in general agreement with SEM analysis, with a several exceptions. For example, trace amounts of feldspar were detected in the Pittsburgh and Elkhorn/Hazard coals with XRD analysis, but not detected with SEM analysis. In the Pittsburgh coal, iron metal or iron oxide was detected with SEM analysis, however, it was not detected by XRD analysis. Because the XRD is dependent on the crystallinity of the minerals, iron oxides are not easily detected. Both the XRD data and SEM data indicate the dominance of kaolinite over illite in each of the four program coals.

3.2.3 *Computer-Controlled Scanning Electron Microscopy (CCSEM) and Mössbauer Analyses*

CCSEM

Computer-controlled scanning electron microscopy has been used for about 17 years for the determination of the discrete mineral matter in coals. The original concept (Lee et al. , 1981; Huggins and Huffman, 1982) has not changed significantly over the years, although improvements in SEM technology and computer capabilities have greatly improved the operation of the CCSEM and data handling. The basis for coal minerals analysis by CCSEM is the statistical determination of the types and relative quantities of different minerals in a random, representative coal sample. The coal sample is pulverized and divided according to ASTM procedures to generate a sufficient quantity (5 to 10 g) of a finely ground (< 100 mesh) representative sample of the coal, from which a 1 in. diameter by 2 in.-long pellet can be pressed. The pellet is prepared by mixing the fine coal with a small amount of epoxy that is allowed to set in a cylindrical die under pressure. The resulting cylinder of coal is sectioned, ground, and polished to provide a flat surface with a minimum of relief that is suitable for examination in the SEM.

The sectioned pellet is placed in the SEM after the polished surface has been given a thin carbon coating in an evaporator. The SEM operating voltage is set to 25 keV and the section is examined in the back-scattered electron (BSE) mode. In this mode, any physical differences in relief of the mineral particles vis-à-vis the epoxy/maceral matrix are minimized and the mineral particles are distinguished from the matrix almost entirely by their brightness in the BSE image. The brightness of a mineral in the BSE image is a function of its chemical composition: the higher the average atomic number (Z) of the mineral, the brighter it will appear in the BSE image. A threshold level in the BSE brightness is defined so that all of the minerals are brighter

than this level, whereas the maceral/epoxy matrix falls below the level. This level is used by the computer to discriminate between mineral and maceral and to define the edges of mineral particles in the carbon-rich matrix. Hence, it is a simple matter to determine the physical extent of mineral grains in the cross-section of the coal and hence the area of cross-section of each mineral grain. This measurement is done automatically by the computer, and other physical parameters, such as the perimeter, minimum and maximum diameters, aspect ratio, etc., are also determined at the same time. The computer then locates the electron beam at the center of the particle and an energy dispersive X-ray (EDX) spectrum is recorded from the particle for four seconds. The computer records the intensity of the 14 most common inorganic elements (Na, Mg, Al, Si, P, S, Cl, K, Ca, Ti, Fe, Cu, Zn, Ba). The relative intensities of the X-rays for these elements are used (with only application of a minor correction procedure for the low Z elements - Na, Mg, and Al) to identify the mineral that gives rise to the grain in the cross-section. A quantitative analysis is not done; the rationale being that nearly all common minerals in coal can be readily identified from their uncorrected EDX spectra. The few ambiguities that might remain from this procedure are (i) either unimportant (e.g. kaolinite vs. halloysite) or (ii) would probably not be resolved in an quantitative analysis (e.g. siderite, $FeCO_3$, vs. iron oxides, Fe_3O_4 or Fe_2O_3, vs. iron oxyhydroxide, FeOOH, which would give identical EDX spectra) in any case.

Once the computer has located a mineral particle, determined its size parameters, and recorded the EDX spectrum, it seeks out a new mineral particle and the size and chemistry determinations are repeated. The beam-control software in the CCSEM includes routines that minimize the possibility of multiple counting of particles. In current practice, the CCSEM is programmed to determine 400 particles at each of three different magnifications, so that a total of 1200 particle analyses constitute the complete analysis. The data are then down-loaded to an off-line computer for data reduction, statistical analysis, and archival storage. Off-line, there are a number of additional analysis programs that provide summaries of the data and various sophisticated graphical representations of the data, including both binary and ternary plots (Shah et al., 1992; Shah, 1996).

Mössbauer Spectroscopy

Iron-57 Mössbauer spectroscopy provides complementary information to both CCSEM and XAFS spectroscopy in two important areas: (i) it provides detailed information regarding the iron minerals in coal and iron phases in ash, and (ii) it gives an indication of the degree of oxidation of pyrite, the major coal mineral most sensitive to oxidation, and, hence, of the overall coal as a whole. Also, many key HAPs elements (As, Se, Hg, Ni?) are likely to have a strong association with pyrite (Swaine, 1990; Finkelman, 1994).

Mössbauer spectroscopy is a powerful, element-specific technique for iron in complex materials. In the area of coal characterization, it has been used for identification of iron minerals, quantitative estimates of pyritic sulfur, oxidation and weathering studies, conversion of iron minerals during coal combustion, liquefaction, and gasification, iron-based catalysis in coal conversion, etc.

At the University of Kentucky, the Mössbauer spectrometer consists of a driving unit (Halder Elektronik, GmbH) interfaced to a 286-PC via PHA/MCS add-in boards (Canberra/Nuclear Data). The data are recorded as a function of the velocity of the oscillating ^{57}Co(Pd) γ-ray source (DuPont Radiochemicals) relative to the stationary absorber by means of a proportional counter tube gated to the energy of the 14.4 keV Mössbauer transition in ^{57}Fe. The synchronization of the drive and data collection in the MCA memory is controlled by a start signal from the 286 computer. Iron foil calibration spectra are recorded simultaneously with the data acquisition for the coal or ash sample by utilization of a second Mössbauer system located at the opposite end of the driving unit. The spectra are usually collected over a velocity range of ±4 mm/s for coal samples or ±12 mm/s for ash samples. Spectra are normally recorded for at least 48 h, depending on the absorption effect, which is generally a function of the total amount of iron in the γ-ray beam. Further details of Mössbauer spectroscopy as applied to coal have been discussed elsewhere (Huffman and Huggins, 1978; Huggins and Huffman, 1979).

Analysis of Mössbauer spectra is based on using a least-squares fitting procedure built around a lorentzian peak shape. Mössbauer absorption features are fit as single peaks, two-line quadrupole doublets, or six-line magnetic hyperfine sextets. The parameters derived from the Mössbauer spectrum are the center of position of the absorption feature, which is known as the isomer shift (I.S.) and is reported in mm/s relative to metallic iron (defined as having an I.S. of 0.0 mm/s), the separation of the quadrupole components, which is known as the quadrupole splitting (Q.S.) and is also reported in mm/s, and the separation of peaks 1 and 6 in a magnetic sextet, which is known as the magnetic hyperfine splitting (H_0) and is reported in kGauss (for iron, 1 mm/s is equivalent to 30.98 kG). These three parameters derived in the computer fitting are usually sufficient to identify and determine the iron-bearing mineral species present in virtually all coal samples. Fairly extensive databases now exist as to the Mössbauer parameters of iron-bearing minerals likely to be found in coal (Huffman and Huggins, 1978; Huggins and Huffman, 1979). Following the method and procedures described elsewhere (Huffman and Huggins, 1978; Huggins and Huffman, 1979), direct determinations of the pyritic sulfur content (Spyr) of the coals and derived fractions have been made from the Mössbauer data.

Sample Preparation for Spectroscopic Examination

The approach we are taking to determine elemental modes of occurrence in this project is to examine not just the coal itself but also ash-rich and ash-poor fractions generated from the coal by float/sink or other physical separative method. We have found (Huggins et al., 1997a) that such an approach is much more definitive in establishing the mode of occurrence, particularly when the mode of occurrence consists of more than one significant elemental form. Furthermore, this approach clearly ties in well with investigation of removal of HAPs using physical coal cleaning methods.

The overall sample splitting scheme is shown in Figure 3-1. The sample of the as-received coal has typically been given a standard pulverized-coal grind and is approximately 70% below 200 mesh. A small fraction of the as-received coal was then separated by splitting to constitute the "RAW " sample. The remaining major fraction of the as-received sample is then subjected to either a float/sink separation in perchloroethylene (PCE, 1.62 specific gravity) or

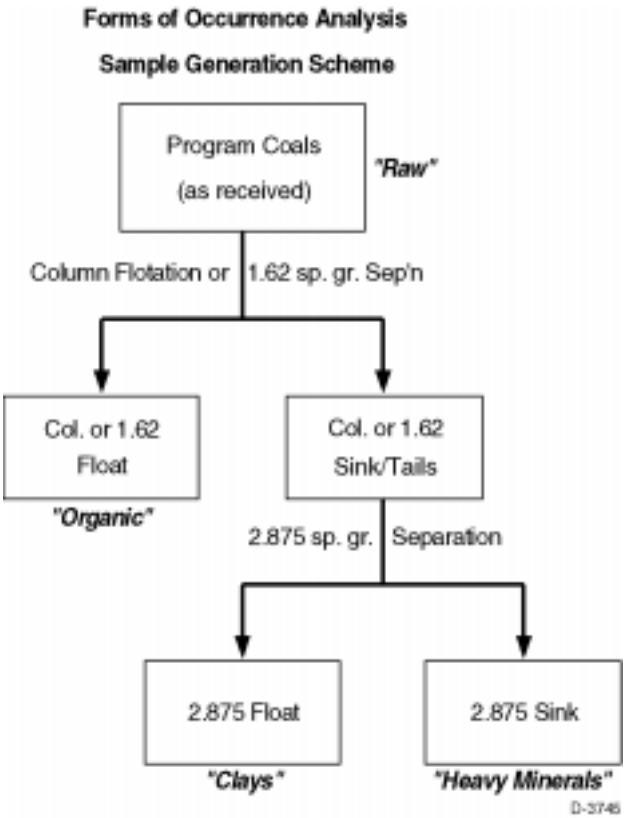

Figure 3-1 Sample separation scheme for coal fractions for Mössbauer and XAFS speciation analysis.

separation in a Denver cell flotation machine into a float and a tailings fractions. We are most grateful to Dr. B.K. Parekh, U.K. Center for Applied Energy Research and his staff for performing the Denver Cell flotation separations for this study. These separations provide an ash-poor fraction, designated as the organic ("ORG ") fraction, and an ash-rich fraction. The ash-rich fraction was then subjected to a second separation in bromoform (BROMO, 2.875 specific gravity) to generate two further fractions: the PCE sink, BROMO float fraction, which will be referred to as the "CLAY " fraction, and the PCE sink, BROMO sink fraction, which will be referred to as the "HYM" fraction for the heavy minerals concentrated in this fraction. Although the individual fractions were not quantified, it should be noted that the separate fractions were quite different in mass: the "ORG" fraction constituted 75% to 90% of the sample subjected to separation, whereas the "CLAY" fraction constituted 5% to 20% of the mass, and the "HYM" fraction constituted only 0% to 5% of the mass. Almost no material was found as the "HYM" fraction for the Wyodak sample after the bromoform separation and consequently no measurements could be made on this particular fraction. The "RAW", "ORG", "CLAY", and "HYM" fractions have been individually examined by both XAFS and Mössbauer spectroscopies for the other three coals.

Table 3-5. CCSEM Mineralogical Determinations for As-received Coals

Mineral Species	Elk./Hazard	Pittsburgh	Illinois #6	Wyodak
Quartz	12	11	13	27
Kaolinite	26	9	5	19
Illite	15	13	11	8
Montmorillonite		0.5		2
K-Feldspar				2
Misc. Silicates	29	29	23	29
Pyrite	6	18	30	1
Fe^{2+} sulfate				
Jarosite				
Misc. sulf.	0.5		2	1
Siderite	1	0.5	0.5	0.5
Calcite	1	6	3	
Misc. carbonates	2	2	1	0.5
Ti oxide				0.5
Apatite				
Misc. phosphates	2			3
Unclassified	5	11	12	6

Mineralogical Determinations

The individual mineral weight fractions of the discrete mineral matter in the four project coals are summarized and compared in Table 3-5. It should be noted that mineral matter accounts for most (> 90 wt%) of the inorganic matter present in the three bituminous coals, but only about 60% to 70% of the inorganics present in the Wyodak coal. The remaining 30% to 40% of the inorganics in the Wyodak coal is present principally as dispersed cationic species, mainly Ca^{2+}, with minor Mg^{2+}, and Na^{+}, bound to the organic macerals via carboxyl groups. The complete summary listings from the CCSEM technique for each coal can be found in Appendix A. Size distributions over the seven CCSEM size bins are shown in Figure 3-2 for all minerals and for pyrite. The size distributions for all minerals are not greatly different among the four coals, however individual mineral entities, especially pyrite, differ significantly among the four coals.

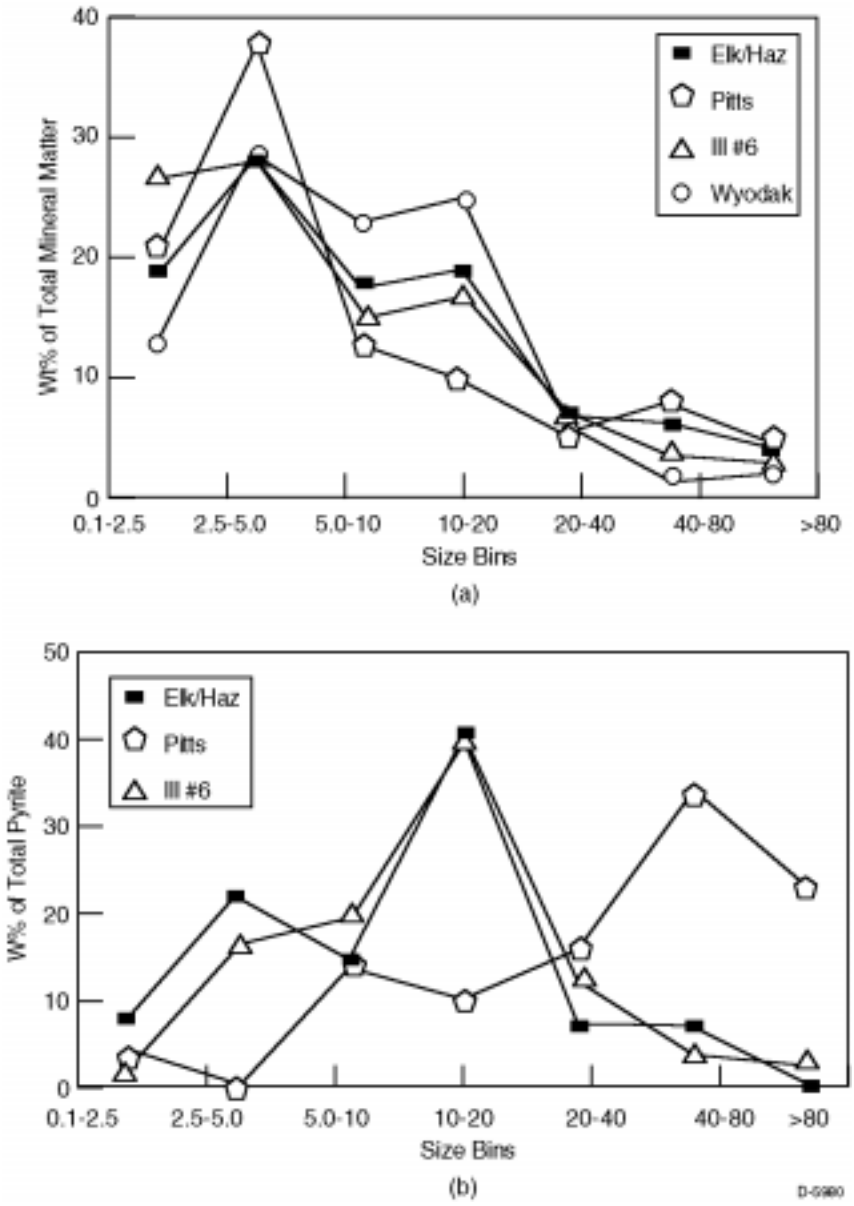

Figure 3-2 Summary of CCSEM size distribution data for (top) all minerals and (bottom) pyrite only. Size bins are in microns.

Mössbauer data are summarized in Tables 3-6 to 3-9 for each coal and its fractions derived according to the scheme shown in Figure 3-1. Owing to the very low amount of iron in the Wyodak coal, separate fractions were not examined for this coal. Figure 3-3 shows the Mössbauer spectra of the Elkhorn/Hazard and Pittsburgh as-received coals. The Mössbauer spectrum of the Wyodak coal is shown in Figure 3-4, while the Mössbauer spectrum exhibited by the as-received Illinois #6 coal (not shown) is very similar to that for the Pittsburgh coal. The Mössbauer spectra of the Illinois #6 and Pittsburgh coals are dominated by contributions from pyrite; only very minor amounts of other iron-bearing species are present in any of the fractions of these coals. The two low-iron coals, Elkhorn/Hazard and Wyodak, exhibit more complex Mössbauer spectra that indicate iron is distributed among a number of phases. In the Elkhorn/

Table 3-6: Mössbauer Data Elkhorn/Hazard Coal

(i)	Raw Coal:					
MK2308	Abs	I.S.	Q.S.	%Fe	Spyr	
	Pyrite	0.31	0.61	57	0.145	
	Fe/clay	1.13	2.61	22		
	Siderite	1.22	1.80	9		
	Jarosite	0.37	1.25	12		
(ii)	Column Float:					
MK2352	Abs	I.S.	Q.S.	%Fe	Spyr	
	Pyrite	0.31	0.61	56	0.115	
	Fe/clay	1.14	2.59	21		
	Siderite	1.23	1.86	9		
	Jarosite	0.34	1.22	14		
(iii)	Column Sink/Bromo Float:					
MK2349	Abs	I.S.	Q.S.	%Fe	Spyr	
	Pyrite	0.32	0.61	58	0.40	
	Fe/clay	1.13	2.62	27		
	Jarosite	0.39	1.32	15		
(iv)	Bromoform Sink:					
	Abs	I.S.	Q.S.	H0	%Fe	Spyr
MK2355	Pyrite	0.31	0.60	—	52	12.6
MK2358*	Siderite	1.23	1.80	—	14	
	Other	0.54	1.38	—	4	
	Hematite?	0.30	-0.01	484	13	
	Goethite?	0.31	-0.12	331	18	

[*Expanded velocity scale to include magnetic phases]

Table 3-7: Mössbauer Data Pittsburgh #8 Coal

(i)	Raw Coal:				
MK2309	Abs	I.S.	Q.S.	%Fe	Spyr
	Pyrite	0.30	0.61	96.5	0.8
	Fe/clay	1.12	2.66	1.5	
	Jarosite	0.44	1.08	2.0	
(ii)	Column Float:				
MK2351	Abs	I.S.	Q.S.	%Fe	Spyr
	Pyrite	0.29	0.61	98	0.7
	Fe/clay	1.08	2.84	2	
(iii)	Column Sink/Bromo Float:				
MK2350	Abs	I.S.	Q.S.	%Fe	Spyr
	Pyrite	0.30	0.61	93	1.60
	Fe/clay	1.14	2.67	7	
(iv)	Bromoform Sink:				
MK2353	Abs	I.S.	Q.S.	%Fe	Spyr
	Pyrite	0.29	0.61	100	15.6

Hazard coal, pyrite, clay, siderite and jarosite have all been identified and similar iron-bearing minerals, although in different relative amounts, are also present in the Wyodak coal. The only unusual iron-bearing mineral observed in any of the four coals was a very minor amount of a magnetic iron oxide which was present in the spectrum of the Elkhorn/Hazard bromoform sink ("HYM") fraction. This phase is a relatively small component in the Mössbauer spectrum and so it can not be identified with any certainty. However, in view of the XAFS data for chromium for this same fraction (see Section 3.5 below), it is likely that this magnetic iron oxide is a complex chromite/magnetite spinel of formula $Fe(Fe,Cr)_2O_4$.

As indicated in Table 3-5, the mineralogy of the Elkhorn/Hazard coal is dominated by clays and mixed silicates (most probably physical mixtures of clays and quartz and/or mixed-layer clays of intermediate compositions). Quartz and pyrite only constitute 12 wt% and 6 wt%, respectively, of the total mineral matter and other minor basic species (e.g. calcite, siderite, sulfates, etc.) are also quite minor. As shown in Figure 3-2, the pyrite in this coal is relatively fine sized; only 14% of the pyrite is coarser than 20 µm, whereas the silicate species are all coarser. This indicates that large pyrite grains are relatively uncommon in this coal.

Table 3-8. Mössbauer Data Illinois #6 Coal

(i)	Raw Coal:				
MK2373	Abs	I.S.	Q.S.	%Fe	Spyr
	Pyr/Marc	0.285	0.59	100	1.40
[Asymmetry in doublet suggests presence of significant (ca. 25%) marcasite.]					
(ii)	1.6 (PCE) Float:				
MK2380	Abs	I.S.	Q.S.	%Fe	Spyr
	Pyrite	0.30	0.58	97	0.71
	Clay	1.10	2.72	3	
(iii)	1.6 Sink/2.875 Float:				
MK2395	Abs	I.S.	Q.S.	%Fe	Spyr
	Pyrite	0.29	0.59	100	9.60
(iv)	2.875 (Bromo) Sink:				
MK2385	Abs	I.S.	Q.S.	%Fe	Spyr
	Pyrite	0.29	0.60	100	34.0
[Less asymmetry in doublet = less marcasite?]					

Table 3-9: Mössbauer Data Wyodak Coal

(i)	Sample As Rec'd Coal:				
MK2460	Abs	I.S.	Q.S.	%Fe	Spyr
	Pyrite	0.29	0.59	38	0.03
	Siderite	1.20	1.85	5	
	Clay	1.16	2.60	13	
	Jar/FeOOH	0.35	0.98	44	

The Pittsburgh coal contains a much higher fraction of basic minerals than the Elkhorn/Hazard coal. Even so, the silicate minerals (clays, quartz, and mixed silicates) still constitute over 60 wt% of the mineral matter. In contrast to the other coals, the pyrite size

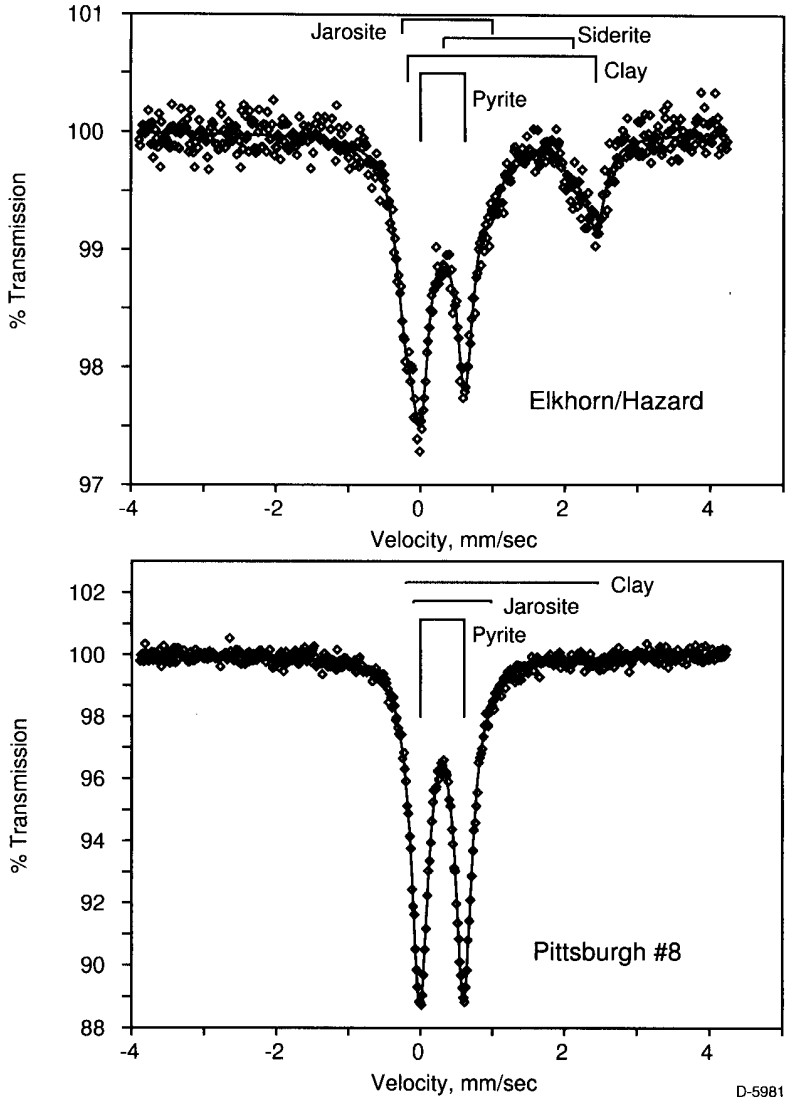

Figure 3-3 Mössbauer spectra for Elkhorn/Hazard and Pittsburgh coals

distribution for this coal is very coarse with almost 75% of the pyrite mass being found in particles larger than 20 µm.

The Illinois #6 coal is the richest of the four coals in pyrite and other basic minerals, but the pyrite size distribution of the pyrite is relatively fine (Figure 3-2), especially in comparison to the Pittsburgh coal. Consequently, of these two coals, it might be anticipated that the Illinois #6 coal should exhibit more fusion between the iron-rich and silicate minerals.

The discrete mineralogy of the Wyodak coal is also presented in Table 3-5. These data are not unlike data we have determined previously (Huffman and Huggins, 1984) for other low-sulfur western U.S. subbituminous coals. The mineral matter is richer in kaolinite than illite, has a low content of basic minerals (calcite, pyrite, siderite), and contains minor amounts of a Ca-Al phosphate mineral, which is most probably crandallite. This coal appears a little unusual in that

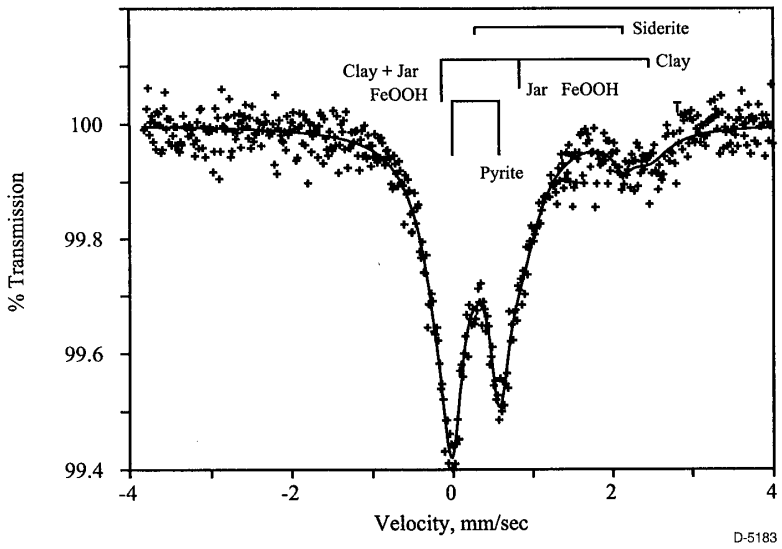

Figure 3-4 Mössbauer spectrum of the Wyodak Coal

the quartz content is quite high and is somewhat coarser in particle size than the other minerals. The illite content is also quite significant. From both the CCSEM data as well as the Mössbauer data, it is clear that iron-bearing minerals are relatively insignificant in this coal. The principal basic element in the coal is likely to be carboxyl-bound calcium, which is not detected using our methods.

Mineral Oxidation

Of the four project coals, the iron minerals in the two high-pyrite coals, Illinois #6 and Pittsburgh, consist almost entirely of pyrite. No oxidized iron form was detected for the Illinois #6 coal and only a very small fraction of jarosite (2 wt% of the total iron) was fit in the Mössbauer spectrum of the as received Pittsburgh coal. However, it should also be noted that no jarosite was observed in any Mössbauer spectra of the derived fractions of the Pittsburgh coal. According to this measurement, these coals would appear not to be significantly oxidized. The other two coals, Elkhorn/Hazard and Wyodak, however, exhibit a sizable fraction of iron as jarosite indicating that the iron minerals in these coals are significantly oxidized.

3.2.4 *Trace Element Analyses*

Raw Coals

Trace element compositions were measured by Neutron Activation Analysis (NAA) at the MIT Nuclear Reactor Laboratory (Table 3-10). It is interesting to note that the concentrations of arsenic and mercury were similar between the Pittsburgh and Elkhorn/Hazard coals. The selenium concentration was higher in the Elkhorn/Hazard coal. As these elements are commonly

Table 3-10. Chemical Analyses of Program Coals by NAA (Whole Coal Basis)

Element	Pittsburgh Concentration (ppm)	Elkhorn/Hazard Concentration (ppm)	Illinois No. 6 Concentration (ppm)	Wyodak Concentration (ppm)
Na	600	340	400	710
Sc	1.8	3.9	2.2	1.8
Cr	13	20	14	7
Fe	8220	2970	13700	2700
Co	2.5	6.2	.6	1.7
Zn	17	18	70	33
As	4.1	4	2.7	1.3
Se	0.62	3.1	2.2	1.6
Br	17	25	3.7	2.4
Rb	8	5.1	13	3.6
Sr	160	120	ND*	ND*
Mo	0.85	4	4.9	1.7
Cd	0.06	0.31	0.15	0.30
Sb	0.26	1	0.38	0.23
Cs	0.55	0.45	0.99	0.26
Ba	110	130	52	370
La	4.5	14	4.7	4.9
Ce	8.8	27	9.3	8.7
Sm	0.78	2.5	0.9	0.71
Eu	0.2	0.37	0.19	0.18
Yb	0.38	1.4	0.032	0.35
Lu	0.063	0.24	0.0054	0.057
Hf	0.44	1.1	0.056	ND*
Au (in ppb)	0.95	0.98	0.51	1.1
Hg	0.11	0.13	0.22	0.19
Th	1.2	4.3	0.095	1.7
U	0.31	1.9	ND*	ND*

* ND=Not determined

associated with pyrite one might expect their concentrations to be higher in the higher pyrite coal. The fact that the concentrations either stay the same or actually increase with decreasing pyrite content suggest that a significant fraction of these elements may be organically associated in the Elkhorn/Hazard coal.

As can be seen from this table, the concentration of arsenic in the Illinois No. 6 coal is lower than was found in the other bituminous coals. Selenium and chromium concentrations were within the range measured in the other coals. Mercury, however, had a much higher concentration in the Illinois No. 6 coal. Most of the trace element concentrations in the Wyodak coal are within the range shown by the bituminous coals. One important exception to this trend is the arsenic. The concentration of this element in the Wyodak is much lower than in the other program coals. The chromium content is also much lower.

The trace element concentrations in the three bituminous coals were also measured by the USGS (Table 3-11). This group utilized a series of techniques, including ICP-MS, that will also be used to characterize the residual solids and the leachate solutions in the leaching test (Section 3.1.3). For most of the elements in common between the MIT analysis and the USGS analysis, there is good to fair agreement. Poor correlation between the two groups is evident for two elements present at low concentrations in coal, Hg and Cd. A more detailed comparison of methods and analytical uncertainties is warranted in Phase II.

Size and Density-Classified Coal

Trace element analysis was also performed using NAA to characterize the size and density-classified coal particles. The classified particles were used for combustion experiments. Examination of the size and density-classified coal particles also provides information on the distribution and association of trace elements in the parent coal.

In the preparation of the coal samples, the coal was first put into seven standard (ASTM) sieves and vibrated for 45 min. Since the fine particles adhere to the large particles, a small vacuum was applied through the bottom of the sieves to separate and remove the fine particles. The homogeneity of the coal size fractions was examined using a microscope. It was found that the coals were separated into well-defined size ranges. In order to study vaporization kinetics, we need to separate coal particles into narrow size ranges. However, we must also choose size ranges such that a reasonably large sample is obtained upon sieving. We chose two size fractions: 45 to 63 μm diameter, and 90 to 106 μm diameter.

The next step was to obtain density-segregated coals using the size segregated samples. An air separator, a small fluidized bed (Figure 3-5), was used to separate the coals into different densities following the procedure developed by Hurt (1995). Samples of coal were placed in the separator up to a height of 27 cm. Compressed argon or helium gas was used as a working fluid. First, a high gas flow rate was used to fluidize the coal particles well, then the flow rates were decreased gradually to the point at which the particles were at the incipient fluidization velocity. The conditions of incipient fluidization were maintained for about 5 min, and then the gas flow was stopped. A small vacuum pump was used to extract the stratified coals. The coals in the top 9 cm were selected as the low density fraction, and the coal in the bottom 9 cm as the high density fraction.

Table 3-11. USGS Chemical Analyses for the Pittsburgh, Elkhorn/Hazard and Illinois No. 6 Feed Coals (concentration in ppmw)

Element	Pittsburgh	Elkhorn/ Hazard	Illinois No. 6	Wyodak	Analytical Technique
Ag	0.15	0.16	0.21	0.16	ICP-MS
As	4.75	5.12	3.09	1.58	
Au	0.73	0.8	1.03	0.79	
Bi	0.15	0.16	0.21	0.16	
Cd	0.06	0.06	0.41	0.08	
Cs	0.59	0.48	1.24	0.24	
Ga	3.58	8	3.81	2.77	
Ge	3.07	3.84	5.36	0.38	
Md	0.88	2.08	6.08	0.95	
Nb	1.46	3.2	2.06	2.37	
Pb	3.14	8.8	13.39	1.58	
Rb	7.15	6.56	15.45	3.16	
Sb	0.29	1.2	0.44	0.32	
Sn	0.73	0.8	1.03	0.79	
Te	0.15	0.16	0.21	0.16	
Tl	0.15	0.32	0.67	0.16	
U	0.41	2.16	1.75	0.66	
Be	0.6	3	1.1	0.4	ICP-AES
Co	2.4	7	3.6	2.4	
Cr	8.8	14.4	18.5	6.3	
Cu	5.3	19.2	8.2	14.2	
Li	5.4	18.4	7.8	6	
Mn	13.1	13.6	37.1	8.7	
Ni	6.6	12	12.4	5.2	
Sc	1.9	3.8	2.7	2.1	
Sr	124.1	136	27.8	268.6	
Th	1.2	3.5	1.5	1.8	
V	11.7	23.2	25.8	17.4	
Y	2.9	12.8	4.5	4.1	
Zn	6.1	6.2	73.1	6.2	
B	29.9	14.4	154.5	0.4	
Ba	116.8	112	43.3	402.9	
Zr	21.2	56	29.9	14.2	
Se	0.96	4.5	2.9	1.3	Hydride method
Hg	0.09	0.05	0.06	0.08	CV

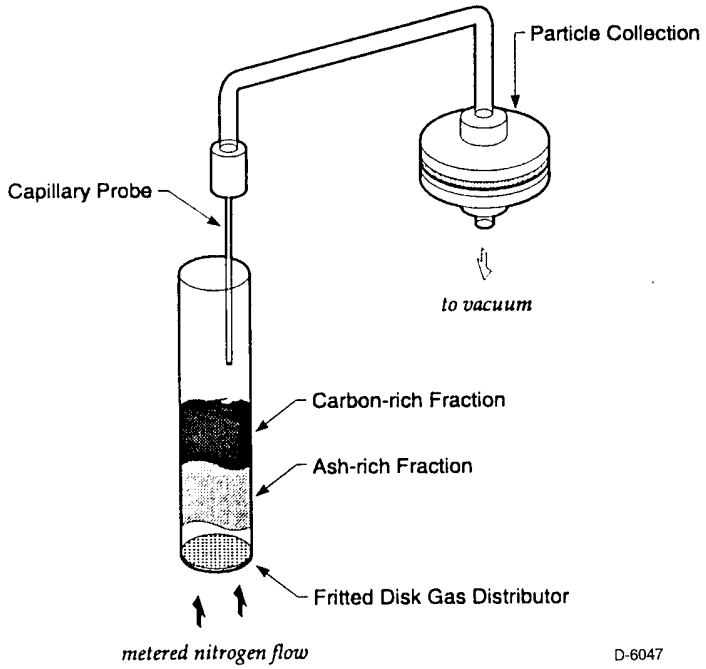

Figure 3-5. Coal separator

The portions with high density and low density were used in this study. The ash yields for the 16 classified coals were analyzed using the ASTM standard procedure (ASTM, 1993). The results are presented in Table 3-12.

Table 3-12. Ash Yield of Classified Coals

	KYH4563	KYL4563	KYH90106	KYL90106	PTH4563	PTL4563	PTH90106	PTL90106
Ash (%)	7.2	6.5	10.3	5.5	7.1	5.9	10.5	5.6
	ILH4563	ILL4563	ILH90106	ILL90106	WYH4563	WYL4563	WYH90106	WYL90106
Ash (%)	9.3	7.4	11.0	6.4	5.8	5.6	7.1	6.6

In the table, KY represents the Elkhorn/Hazard coal, PT is Pittsburgh coal, IL means Illinois coal, WY is Wyodak coal. "H" represents the portion from the high density layer, "L" represents the portion from the low density layer, 4563 means that the coal size is between 45 and 63 µm, and 90106 means that the coal size is between 90 and 106 µm. From the table, it can be seen that except for the Wyodak coal, ash yield for the coal with sizes between 90 and 106 microns in the high density fraction are about twice those in the low density fraction; the difference in ash yield for the different density fractions are not as large for coals with size between 45 and 63 microns. For the Wyodak coal, the differences in ash yields between the different

density fractions are very small. Interestingly, the larger size fraction of the Wyodak coal has a higher ash yield than the smaller one.

The trace elements for the size segregated and density segregated coals were analyzed using Neutron Activation Analysis (NAA) at the MIT Nuclear Reactor Laboratory. The results for the four program coals are tabulated in Appendix B, and are also depicted in Figures 3-6 to 3-12. In those figures the ratios of concentrations in the high-density fraction to that in the low density fraction are presented for several elements in each coal. A ratio greater than one indicates that the element is enriched in one fraction.

As shown in Figure 3-6, arsenic, zinc, mercury, and selenium are concentrated in the high density fraction (45 to 63 microns size cut) of the Pittsburgh and Elkhorn/Hazard coals. For the Illinois No. 6 coal, zinc was greatly enriched in the high density fraction. For Wyodak coal, all the elements are the most uniformly distributed of all the coals. Arsenic and mercury were also enriched in the high density fraction for the 90 to 106 microns size range of the Pittsburgh and Elkhorn/Hazard coals. Fe, a major constituent of the mineral matter, was also found to be enriched in the high density fraction in those samples (Figure 3-7).

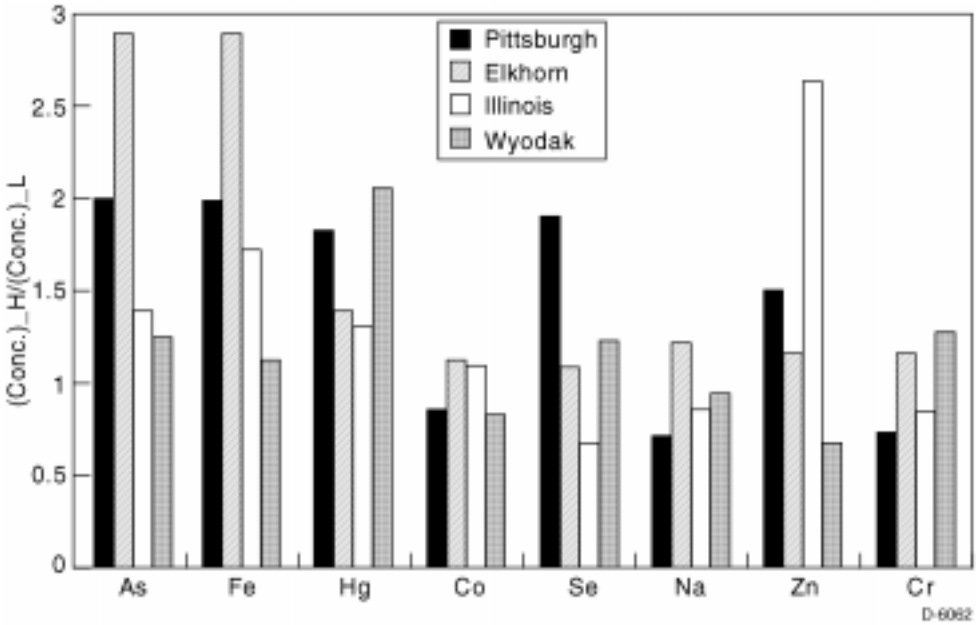

Figure 3-6. Relative element concentrations in two density fractions of the 45 to 63 microns cut of the four program coals

Figure 3-8 illustrates the partitioning of the various elements between two size cuts. As shown in this figure, zinc was enriched in the smaller size fraction for all coals. Arsenic, iron, mercury, sodium, cobalt, chromium, and selenium are more uniformly distributed between these two size cuts.

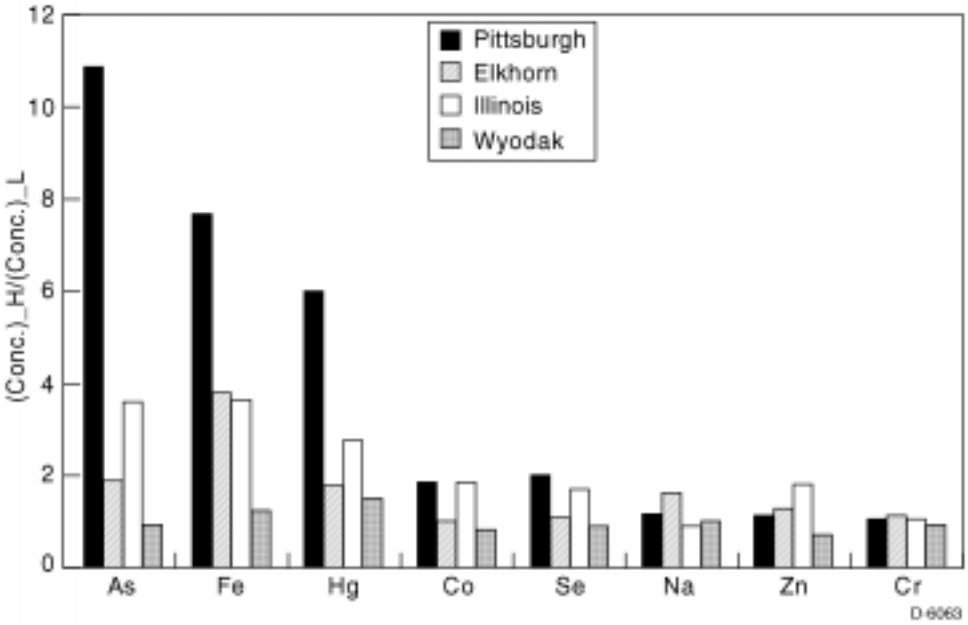

Figure 3-7. Relative element concentrations in two density fractions of the 90 to 106 microns cut of the four program coals

Figures 3-9 and 3-10 show the effect of size on the trace elements concentration in a given density split. Zinc, arsenic, and selenium are enriched in the smaller sizes (low density fraction) in the Pittsburgh coal, while only zinc is enriched in this size range for the Elkhorn/ Hazard coal. Generally, the elements are uniformly distributed between the two size cuts for the low density cuts. For the high density cut, zinc, arsenic, and mercury show significant enrichment in the bituminous coal. For Wyodak coal, most elements are uniformly distributed; only Zn, Hg, As and Se are enriched in the smaller sizes for the high density cut and Zn and Hg for the low density cut.

Figures 3-11 and 3-12 show the distributions of Fe and Na as a function of size in Illinois and Elkhorn/Hazard coals. It is found that, Fe and Na are enriched in the smaller coal particles (smaller than 45 µm), and depleted in bigger coal particles (bigger than 106 µm). However, the differences for the coal particles with size between 45 and 106 µm are not very large.

As has been stated, trace elements are generally considered to be associated with the minerals in coal. The minerals in coal can be determined by using CCSEM (computer controlled scanning electron microscopy). The results from CCSEM are depicted in Figures 3-13 and 3-14, and detailed in Appendix C.

Figure 3-13 shows that most minerals have sizes smaller than 20 microns. It was shown that ash is concentrated in the large dense coal particles, which is consistent with CCSEM observations. Figure 3-14 shows that for Pittsburgh coal, the effect of density segregation on the elemental distribution is mainly due to the concentration of pyrites in the dense and large particle

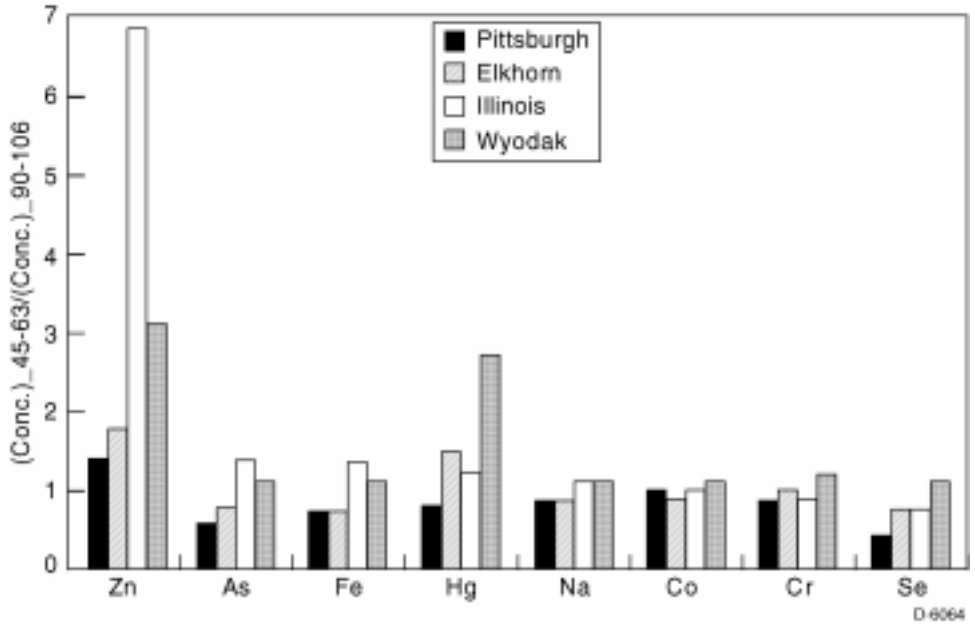

Figure 3-8. Relative element concentrations in two size fractions of the four program coals

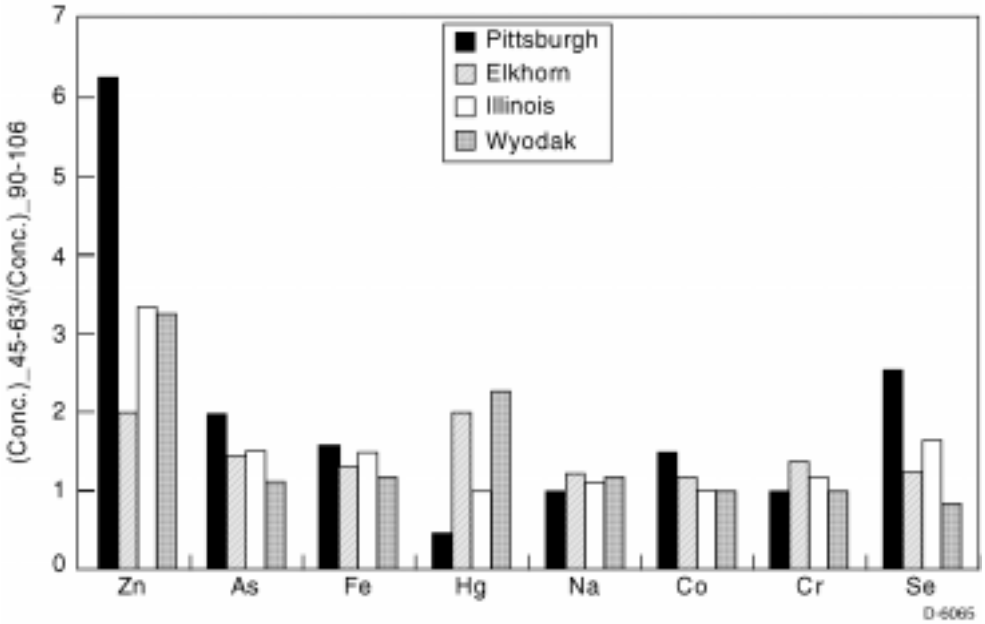

Figure 3-9. Relative element concentrations in the low density fraction of two size cuts of the four program coals.

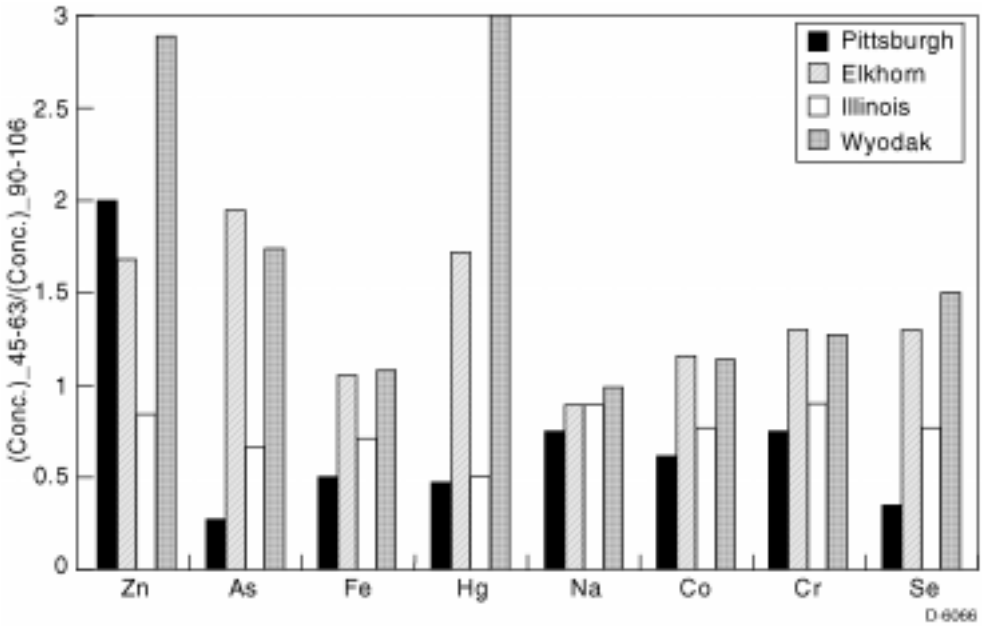

Figure 3-10. Relative element concentrations in the high density fraction of the two size cuts of the four program cuts

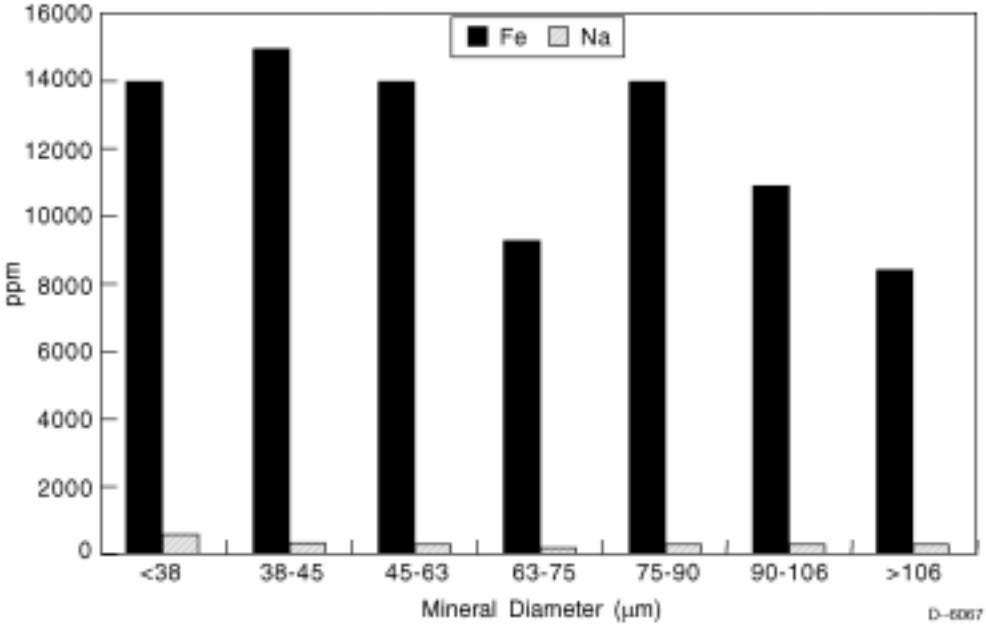

Figure 3-11. Concentrations of Fe and Na in size cuts for Illinois coal

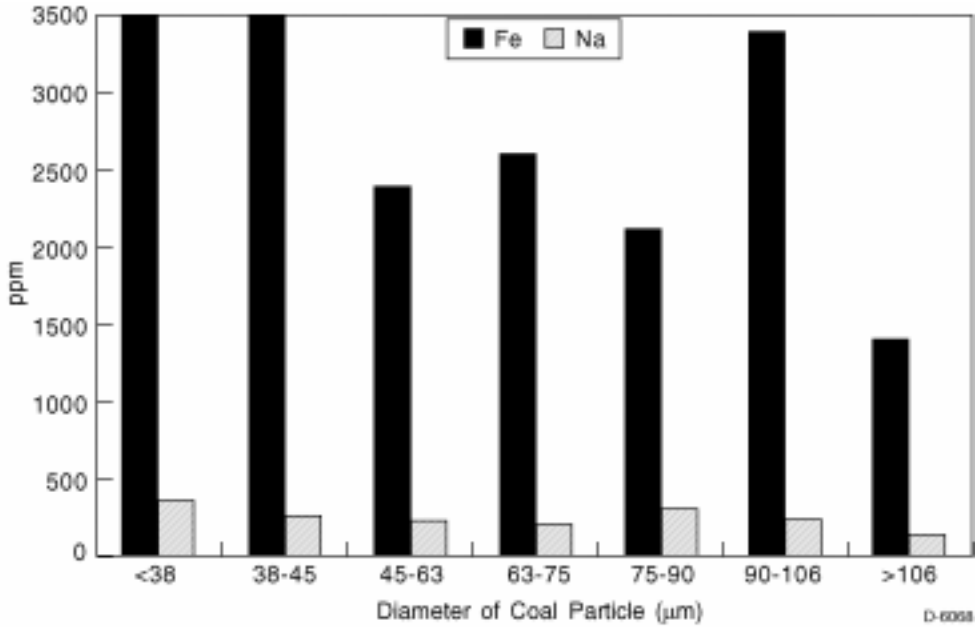

Figure 3-12. Concentrations of Fe and Na in size cuts for Elkhorn/Hazard coal

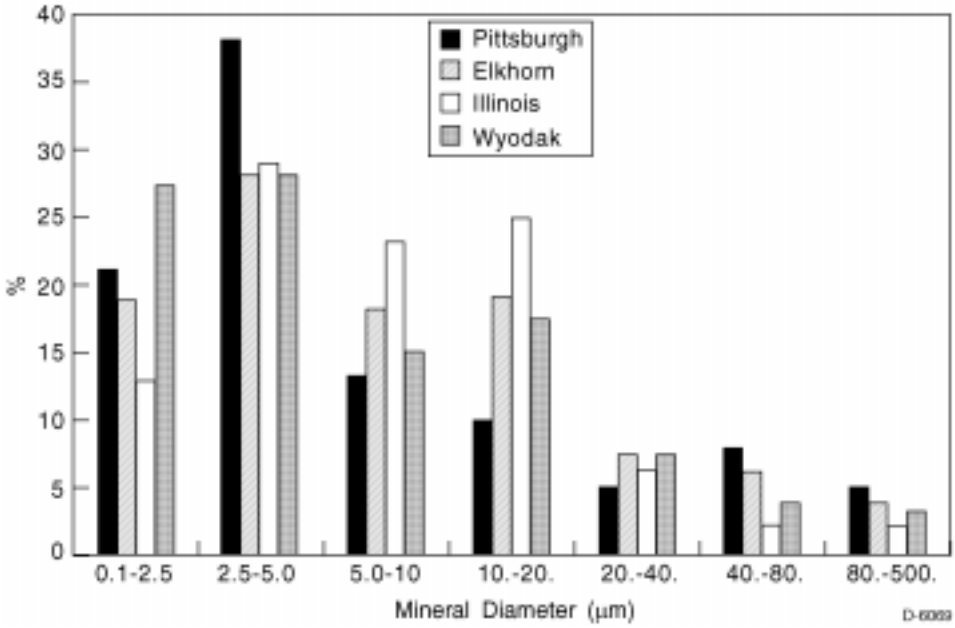

Figure 3-13. Mineral distributions as a function of mineral size (CCSEM results)

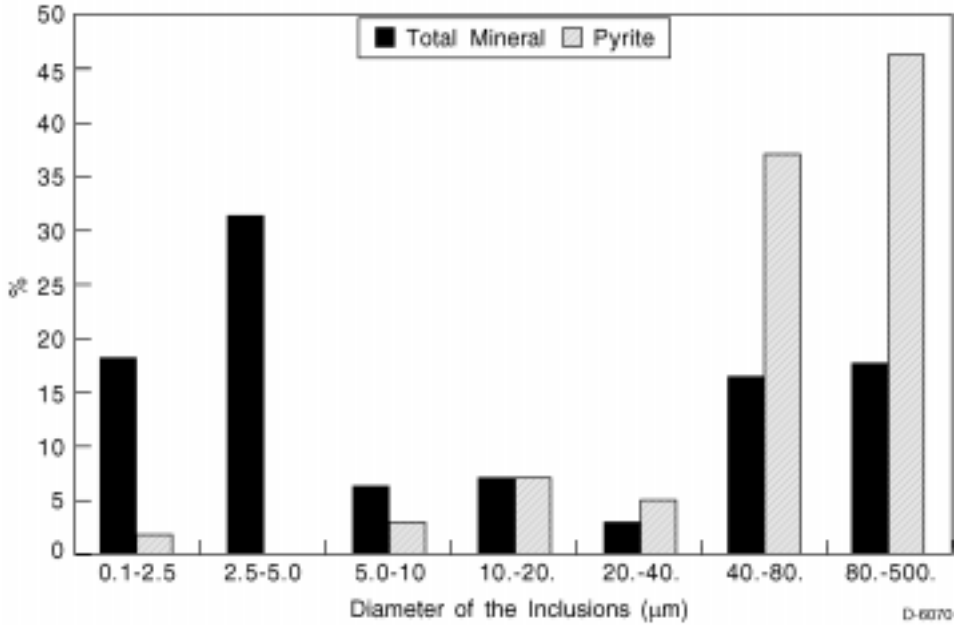

Figure 3-14. Mineral and pyrite distribution for PTH90106 coal

fractions. This can be used to explain why Wyodak coal can not be separated into distinguishable density cuts, because it contains negligible amount of pyrites.

3.3 Trace Element Forms of Occurrence by Microprobe Analysis

3.3.1 *Methods*

Pellets were formed for microprobe analysis as described in Subsection 3.2.3 using the same methods as for SEM analysis. A fully-automated 5-spectrometer instrument (JEOL JXA 8900L Superprobe) was used to quantitatively determine element concentrations in sulfides and clay minerals in program coals by the wavelength-dispersive technique. For sulfides, the following elements were measured: Fe, S, As, Ni, Cu, Zn, Se, Co, and Cd. For clay minerals illite and kaolinite, the elements reported as oxides K_2O, CaO, Na_2O, Al_2O_3, SiO_2, MgO, Cr_2O_3, MnO, FeO, and TiO_2 were measured. Natural and synthetic standards were used. For sulfides, an accelerating potential of 20 KeV was used, at beam currents of 2.0×10^{-8} or 3.0×10^{-8} amps. For clays, an accelerating potential of 15 KeV was used, at a beam current of 2.0×10^{-8} amps. All analyses were done using a focused beam (beam diameter setting = 1 μm), giving an actual working diameter of about 2 to 3 μm.

Detection limits for each of the minor or trace elements determined are estimated to be about 100 ppm in sulfides and 200 ppm in clays. Long counting times, at least 60 s for peak and 30 s for each background, were used to achieve these detection limits. For example, to measure arsenic in pyrite, a peak counting time of 90 s, and a 45 s count for each background were used. Because many of the trace elements of interest are present at levels that are at or near the detection limits of the probe, counting statistics for these elements have large uncertainties.

Microprobe data for pyrite grains (Appendix D) and clays (Appendix E) have been completed. For pyrites, only analyses totaling ≥ 95% were accepted. For clays, most analyses have totals in the 87 to 90% range, reflecting the presence of water in the structures of these phases. In addition to quantitative analyses, wavelength dispersive spectrometry using the JEOL 8900 was used to produce color maps of elemental distribution in project sulfides. This technique was used to delineate arsenic heterogeneity in high-arsenic pyrite of the Elkhorn/Hazard coal (Figure 3-15). In order to obtain additional mode of occurrence information for chromium in the Elhorn/Hazard coal, three density separates (float, middling, and sink fractions) were examined using the SEM.

3.3.2 *Microprobe Analysis of Iron-Sulfides*

Microprobe data for most pyrite grains indicate trace-element concentrations that are at or below the detection limit of ~100 ppm (Appendix D). Of the seven trace elements determined (Se, Cu, Ni, As, Zn, Cd, and Co), only Cu, As, and Ni are commonly present at levels that exceed the detection limit. Concentrations of these three elements were determined for all of the pyrite grains analyzed.

Microprobe data indicate that the arsenic content of pyrite grains in the Illinois No. 6 (< 0.01 to 0.03 wt%) and Pittsburgh (< 0.01 to 0.09 wt%) coals is similar, and that pyrites in these two coals are not distinguishable based on arsenic concentrations. The arsenic concentrations of the pyrite grains in these coals do not appear to vary according to grain size. However, non-framboidal pyrite grains commonly have higher arsenic concentrations than framboidal pyrite grains (Figures 3-16a and 3-16b). Arsenic content of pyrites in the Elkhorn/Hazard coal is much more variable than that in the other program coals, ranging from below the detection limit to greater than 2.0 wt%. As in the Pittsburgh and Illinois No. 6 coals, non-framboidal pyrite grains commonly have higher arsenic concentrations than framboidal pyrite grains and the arsenic concentrations do not appear to vary according to grain size (Figure 3-15c). The presence of scattered high-arsenic pyrite grains in the Elkhorn/Hazard coal makes it difficult to determine a representative arsenic composition for pyrites in this coal (see Mass Balance Calculations in Section 3.4.3). Elemental mapping of one such grain in the Elkhorn/ Hazard coal also reveals fine-scale variation in arsenic content (Figure 3-15).

Overall, the Illinois No. 6 coal has higher concentrations of nickel in pyrite grains (mean = 0.035 wt%) than the Pittsburgh coal (0.01 wt%) or Elkhorn/Hazard coal (0.02 wt%) (Appendix D). In the Pittsburgh and Elkhorn/Hazard coals, the nickel concentrations of pyrite grains do not appear to vary according to the size of grains or according to pyrite morphology (framboidal versus non-framboidal, Figures 3-17a and 3-17c). In the Illinois No. 6, framboidal pyrite grains are more likely to show enrichment in nickel, but there is considerable overlap in values (Figure 3-17b). The highest nickel concentrations determined are 0.26 and 0.40 wt% in two separate Illinois No. 6 framboids.

The concentrations of arsenic in pyrite vs. nickel in pyrite are plotted in Figures 3-18a through 3-18c. These elements appear to show independent enrichment trends, particularly for nickel in the Illinois No. 6 coal (Figure 3-18b) and arsenic in the Elkhorn/Hazard coal (Figure 3-18c).

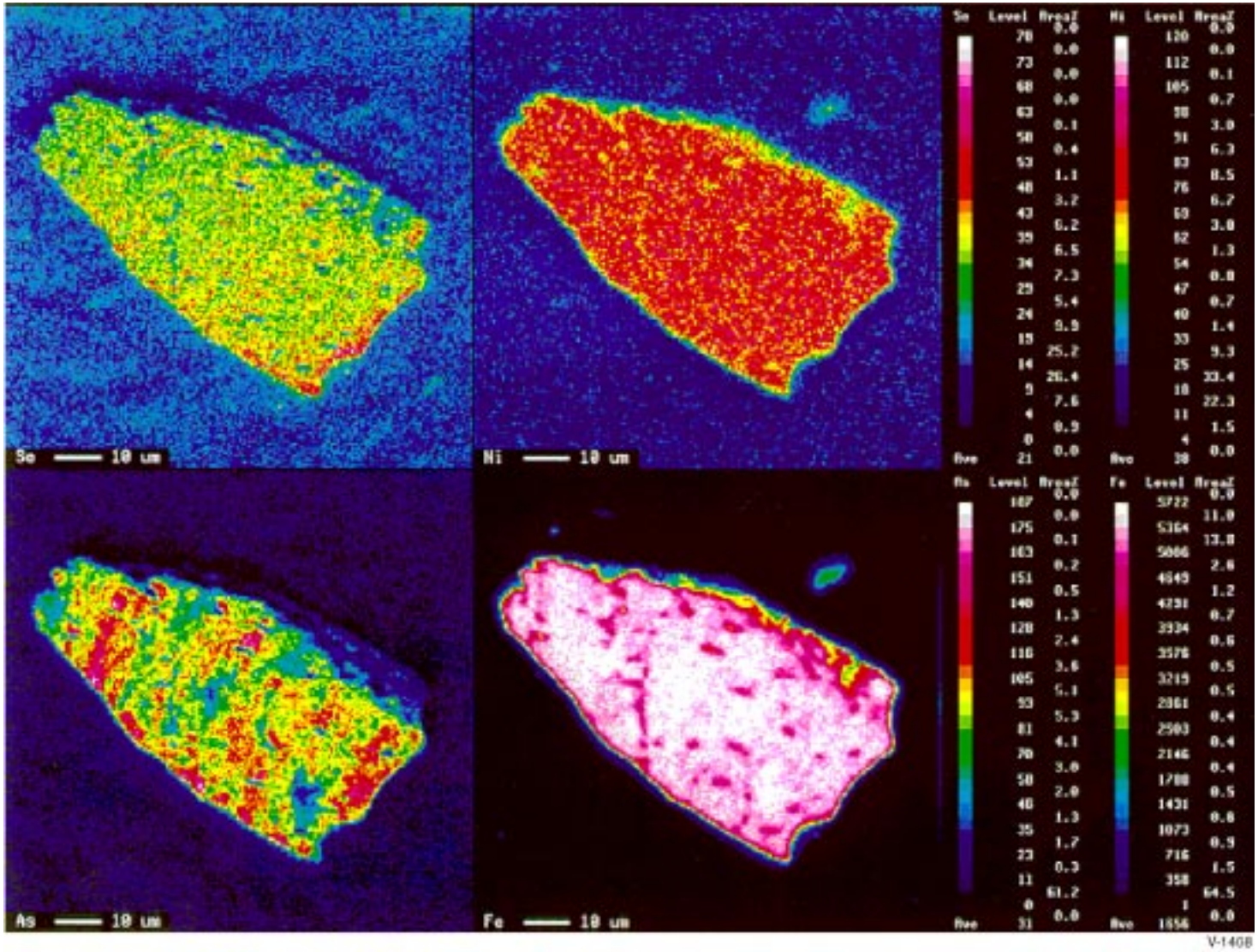

Figure 3-15. Semi-quantitative map of arsenic distribution in a 45 x 85 micron Elkhorn/Hazard pyrite grain. Figure shows heterogeneous arsenic distribution. Maximum arsenic content measured is 0.96 wt.%. Width of field-of-view is 100 microns; pixel size is 0.5 microns. Map is based on raw counts for arsenic obtained at each pixel position.

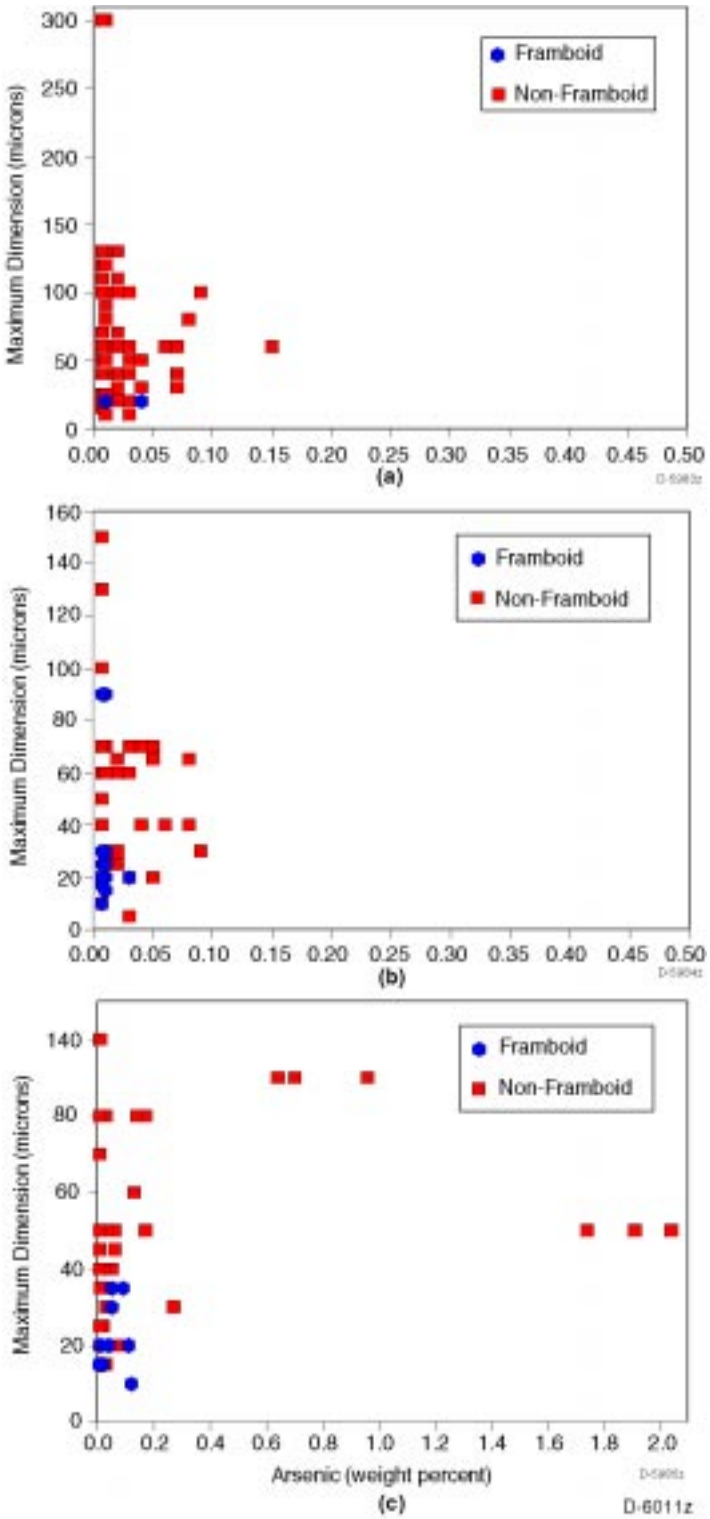

Figure 3-16 Plots of arsenic concentration vs. maximum dimensions for pyrites in the Pittsburgh (a), Illinois #6 (b), and Elkhorn/Hazard (c) coals. Data points represent individual microprobe analyses, and generally include more than one analysis per grain. Arsenic data collected prior to 11-1-96 are adjusted to conform to results obtained with improved analytical technique used thereafter (Appendix D).

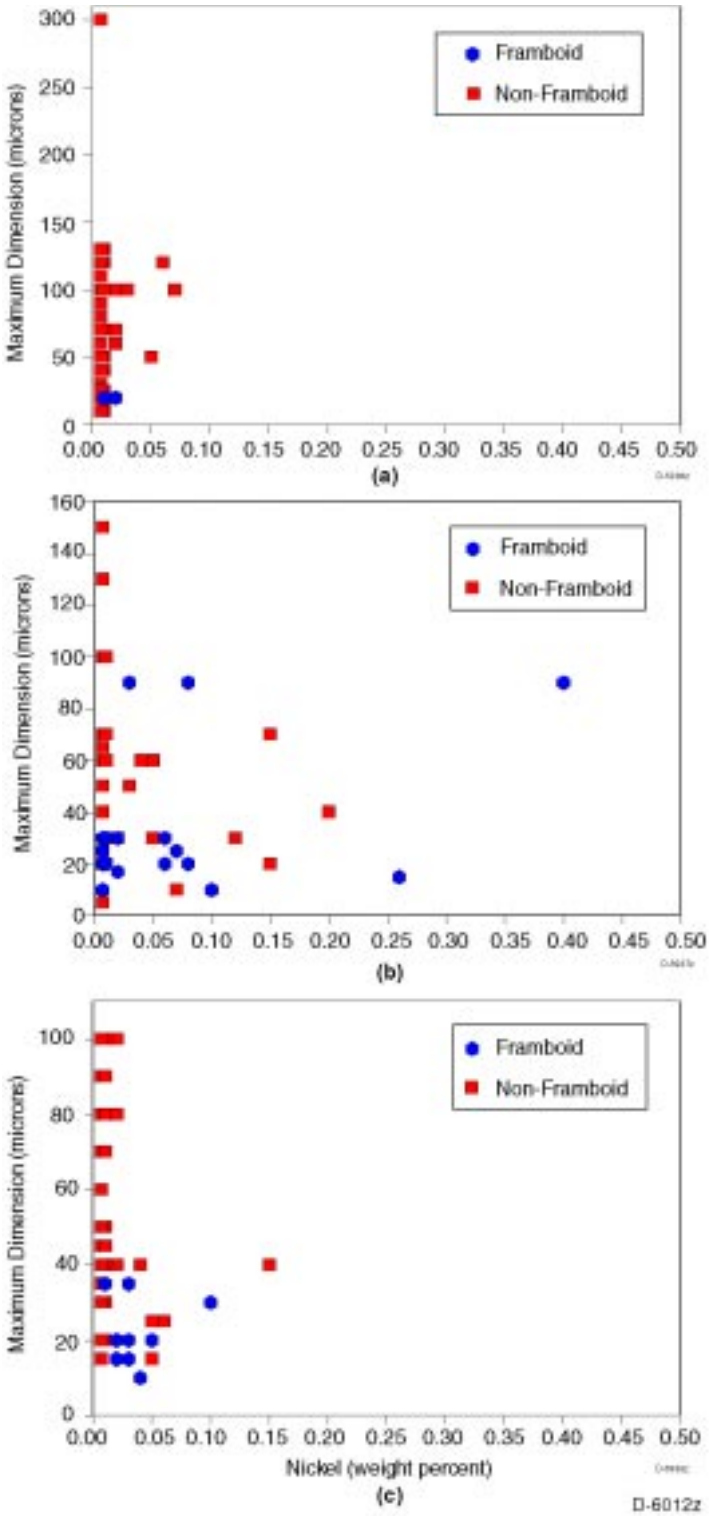

Figure 3-17 Plots of nickel concentration vs. maximum dimensions for pyrites in the Pittsburgh (a), Illinois #6 (b), and Elkhorn/Hazard coals (c). For the Illinois #6 and Elkhorn/Hazard coals, data suggest that smaller pyrites, primarily framboids, are enriched in nickel. Data points represent indivdual microprobe analyses, and generally include more than one analysis per grain.

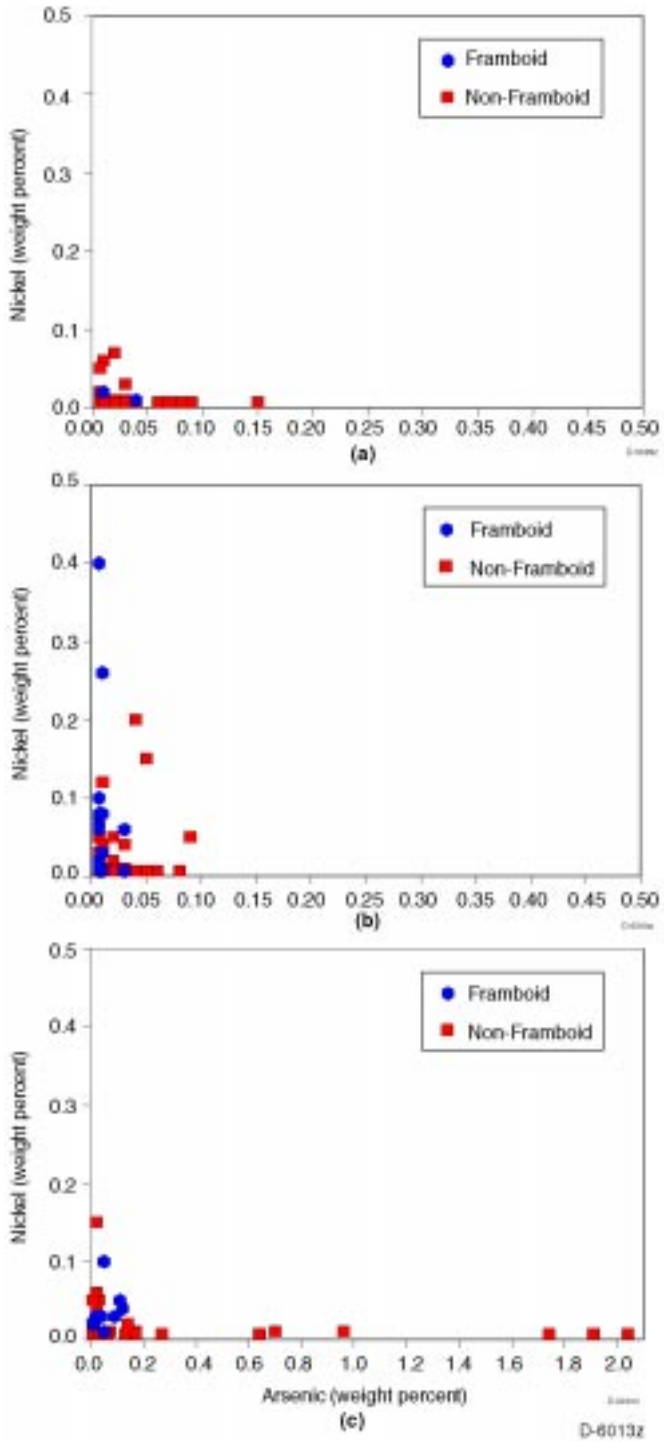

Figure 3-18 Plots of arsenic concentration vs. nickel concentration in pyrites of the Pittsburgh (a), Illinois No. 6 (b), and Elkhorn/Hazard (c) coals. Diagrams show divergent trends towards nickel enrichment in Illinois #6 pyrites (b), and arsenic enrichment in Elkhorn/Hazard pyrites (c). Data points represent individual analyses and generally include more than one analysis per grain. Some data are obscured. Arsenic data collected prior to 11-1-96 are adjusted to conform to results obtained with improved analytical technique used thereafter (Appendix D).

Maximum selenium concentrations of 0.01 to 0.02 wt% were found for pyrite in each coal, but most selenium values were below the detection limit of ~100 ppm (Appendix D).

3.3.3 *Microprobe Analysis of Clay Minerals*

Microprobe analyses of the clay minerals illite and kaolinite are given in Appendix E. For the Elkhorn/Hazard and Illinois No. 6 coals, the average Cr_2O_3 concentration of illites is below the detection limit (about 200 ppm). For the Pittsburgh coal, only one illite gave an acceptable analysis, based on its oxide sum and stoichiometry. This illite (PITTS illite1) has a Cr_2O_3 content (0.02 to 0.03 wt%) that is marginally above the detection limit, and is therefore subject to a large uncertainty.

The grains that we have identified as illites probably also contain mixed-layer clays and finely disseminated quartz, as indicated by the large variations in SiO_2, K_2O and FeO (Appendix E). Unlike the illites, the kaolinites show little chemical variation. The kaolinites are essentially stoichiometric $Al_2Si_2O_5(OH)_4$, with minor substitution by Fe and K, possibly from adjacent illites (Appendix E). Some kaolinites give a response for Cr_2O_3, possibly indicating the presence of a small amount of chromium in this clay mineral as well as illite. Analysis totals for kaolinite and illite are less than 100% because of structural water in these clays.

3.4 Trace Element Forms of Occurrence by Selective Leaching

3.4.1 *Methods*

The sequential selective leaching procedure used in this study is similar to that described by Palmer et al. (1993) and Finkelman et al. (1990). In this procedure, duplicate 5 g samples were sequentially leached in 50 ml polypropylene tubes using 35 ml each of 1N ammonium acetate (CH_3COONH_3), 3N hydrochloric acid (HCl), concentrated hydrofluoric acid (HF; 48%), and 2N (1:7) nitric acid (HNO_3). Each tube was shaken for 18 h on a Burrell wrist action shaker. Because of the formation of gas during some of the leaching procedures, it was necessary to enclose each tube in double polyethylene bags, each closed with plastic coated wire straps. The bags allow gas to escape, but prevent the release of liquid. Approximately 0.5 g of residual solid was removed from each tube for instrumental neutron activation analysis (INAA). The solutions were saved for inductively coupled argon plasma atomic emission spectroscopy (ICP-AES) analysis and inductively-coupled argon plasma mass spectroscopy (ICP-MS) analysis.

Leaching experiments were completed for the four program coals and the resulting leachate solutions and solid residues were submitted for chemical analysis. Leachate solutions were analyzed by ICP-AES and ICP-MS; solid residues were analyzed by INAA. For each analytical method, chemical data were processed to derive the mean percentages of each element leached by each of the four leaching agents, as compared to the original concentration of each element in the unleached coal. A single value for the percent leached for each element was then determined, based on the potential uncertainty of each technique (Table 3-13) and reproducibility of analytical results. The resulting calculated percentages were used as an indirect estimate of the mode of occurrence of specific trace elements in the coals. We estimate an error of up to ±25% for these data.

Table 3-13. Percentages of Elements Leached by Ammonium Acetate, Hydrochloric Acid, Hydrofluoric Acid, and Nitric Acid as Compared to the Total Concentration of the Element in the Unleached Coal

	CH_3COONH_3	HCl	HF	HNO_3	Total
Arsenic					
Pittsburgh	0%	10%	0%	80%	90%
Elkhorn/Hazard	0%	30%	5%	25%	60%
Illinois No. 6	0%	20%	0%	60%	80%
Wyodak	0%	35%	15%	0%	50%
Iron					
Pittsburgh	0%	0%	5%	90%	95%
Elkhorn/Hazard	5%	40%	15%	15%	75%
Illinois No. 6	5%	5%	5%	85%	100%
Wyodak	0%	65%	25%	0%	90%
Chromium					
Pittsburgh	0%	20%	25%	30%	75%
Elkhorn/Hazard	0%	15%	20%	10%	45%
Illinois No. 6	0%	10%	20%	15%	45%
Wyodak	5%	10%	45%	10%	70%
Mercury					
Pittsburgh	5%	25%	0%	10%	40%
Elkhorn/Hazard	10%	40%	0%	0%	50%
Illinois No. 6	0%	0%	5%	0%	5%
Wyodak	0%	0%	0%	0%	0%
Selenium					
Pittsburgh	0%	5%	0%	90%	95%
Elkhorn/Hazard	10%	15%	0%	20%	45%
Illinois No. 6	10%	0%	0%	50%	60%
Wyodak	20%	5%	0%	5%	30%
Nickel					
Pittsburgh	20%	35%	20%	20%	95%
Elkhorn/Hazard	10%	15%	5%	5%	35%
Illinois No. 6	10%	25%	20%	30%	85%
Wyodak	10%	15%	15%	15%	55%

3.4.2 *Results of Leaching Experiments and Comparison to Other Data*

In the following section, the leaching behavior of arsenic, selenium, chromium, mercury, and nickel (Table 3-13, Figure 3-19) are discussed and compared to the results from microprobe and SEM analysis. Final modes of occurrence (Figure 3-20) are determined for each element based on integration of data from leaching experiments, SEM analysis, electron microprobe analysis, and XRD data.

Arsenic

Pittsburgh and Illinois No. 6 coals: The bulk of the arsenic in the Pittsburgh and Illinois No. 6 coals is in pyrite, as indicated by high percentages of arsenic leached by HNO_3 (60 to 80%, Figure 3-19a). Microprobe data confirms the presence of arsenic in pyrite and shows typical concentration ranges to be from < 0.01 to 0.09 wt% in the Pittsburgh coal and from < 0.01 to 0.03 wt% in the Illinois No. 6 coal. The high total percentage of arsenic leached in the Pittsburgh and Illinois No. 6 coals (80 to 90%) suggests little or no organic association. Minor amounts of arsenic (10 to 20%) were leached by HCl, which may indicate an association with mono-sulfides such as sphalerite or galena. However, these mono-sulfides were not observed with SEM analysis. Percentages for the mode of occurrence diagram (Figure 3-20a) were derived directly from the leaching percentages (Figure 3-19a).

Elkhorn/Hazard Coal: The Elkhorn/Hazard coal may have several modes of occurrence for arsenic. In contrast to the Pittsburgh and Illinois No. 6 coals, 30% of arsenic in the Elkhorn/ Hazard coal was leached by HCl and 25% of arsenic was leached by HNO_3. A minor amount of arsenic was leached by HF (5%). Leaching of arsenic by HCl may indicate the presence of arsenates that were formed by the oxidation of pyrite. It is also possible that HCl-soluble arsenic-bearing sulfides (such as sphalerite or galena) are present, but these were not observed with SEM analysis.

Because only 60% of the total arsenic in the Elkhorn/Hazard coal was leached, an organic association for arsenic or the presence of organically encapsulated (shielded) arsenic-bearing pyrite might be suggested. However, petrographic and SEM analysis of solid residues from the nitric acid leach have identified the presence of both shielded and unshielded pyrite grains in the solid residues. The amount of unleached pyrite observed may be sufficient to account for the low percentage of leachable arsenic in the Elkhorn/Hazard coal. To estimate the total amount of arsenic present in pyrite, we adjusted the amount of nitric acid leached arsenic (25%) by adding the amount of unleached arsenic (40%), to obtain the total arsenic in pyrite (60%, Figure 3-20a). Work in Phase II will include examination of unleached pyrite grains in Elkhorn/Hazard residue to determine why they were not dissolved in nitric acid.

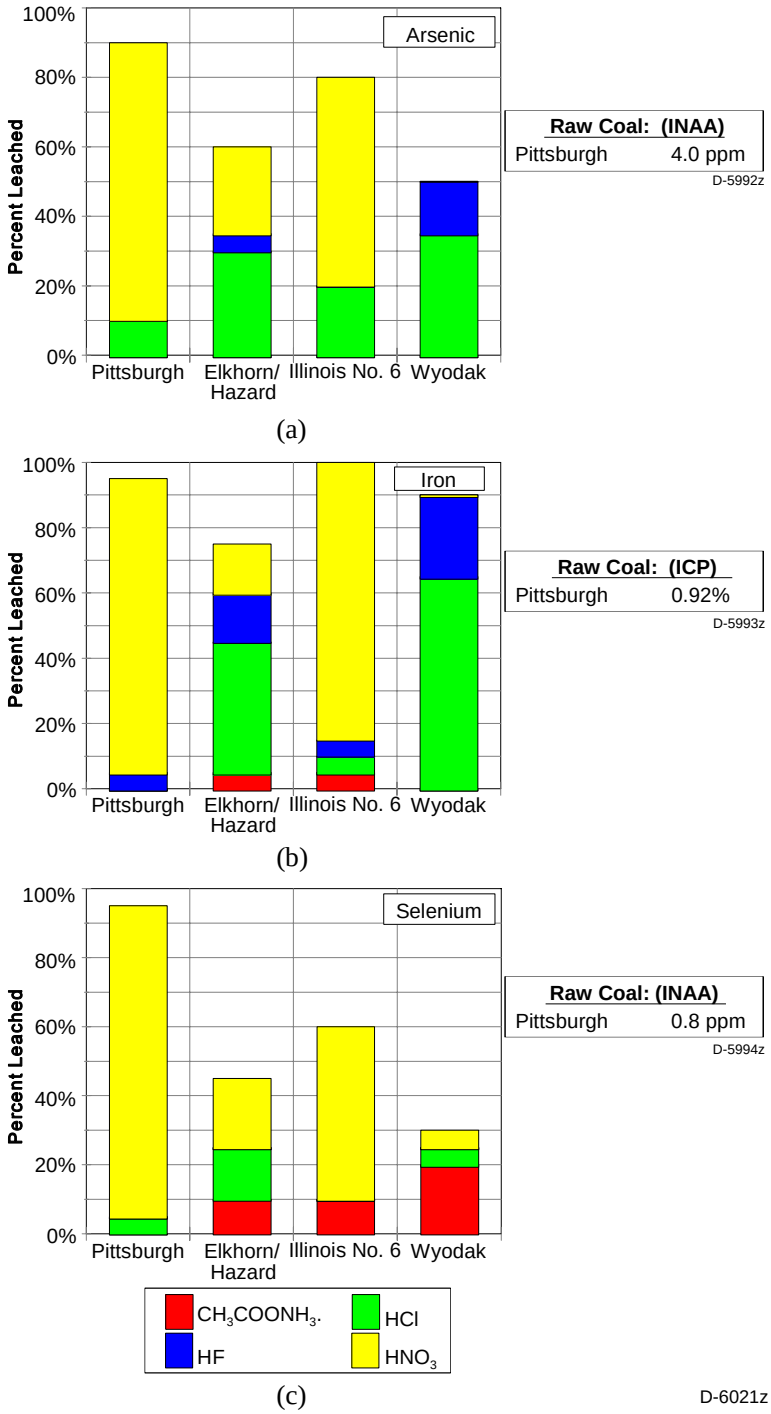

Figure 3-19 Bar charts showing the percentage of each trace element leached arsenic (a), iron (b), selenium (c), chromium (d), nickel (e), and mercury (f) by each leaching agent (ammonium acetate, hydrochloric acid, hydrofluoric acid, and nitric acid) compared to the concentration of the element in the raw coal

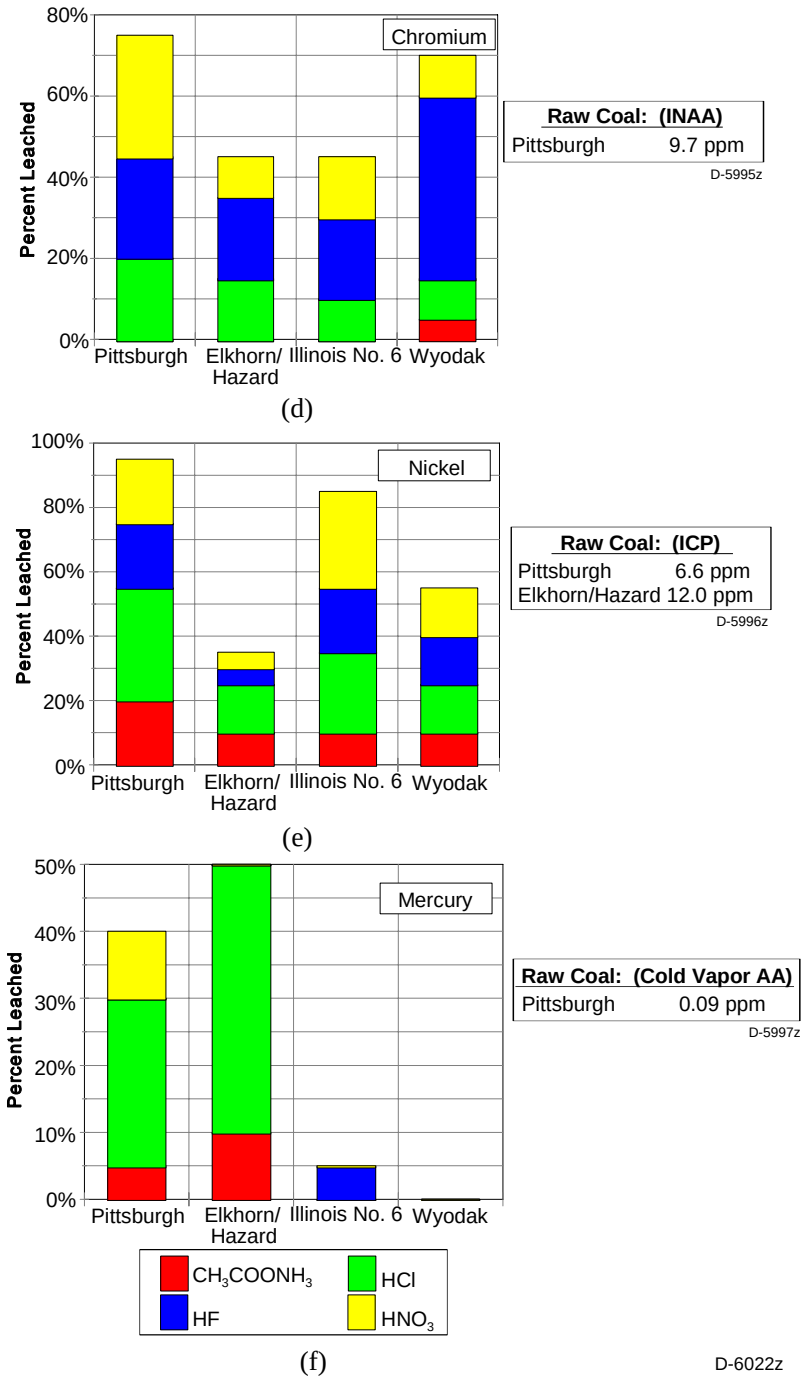

Figure 3-19 (continued) Bar charts showing the percentage of each trace element leached arsenic (a), iron (b), selenium (c), chromium (d), nickel (e), and mercury (f) by each leaching agent (ammonium acetate, hydrochloric acid, hydrofluoric acid, and nitric acid) compared to the concentration of the element in the raw coal

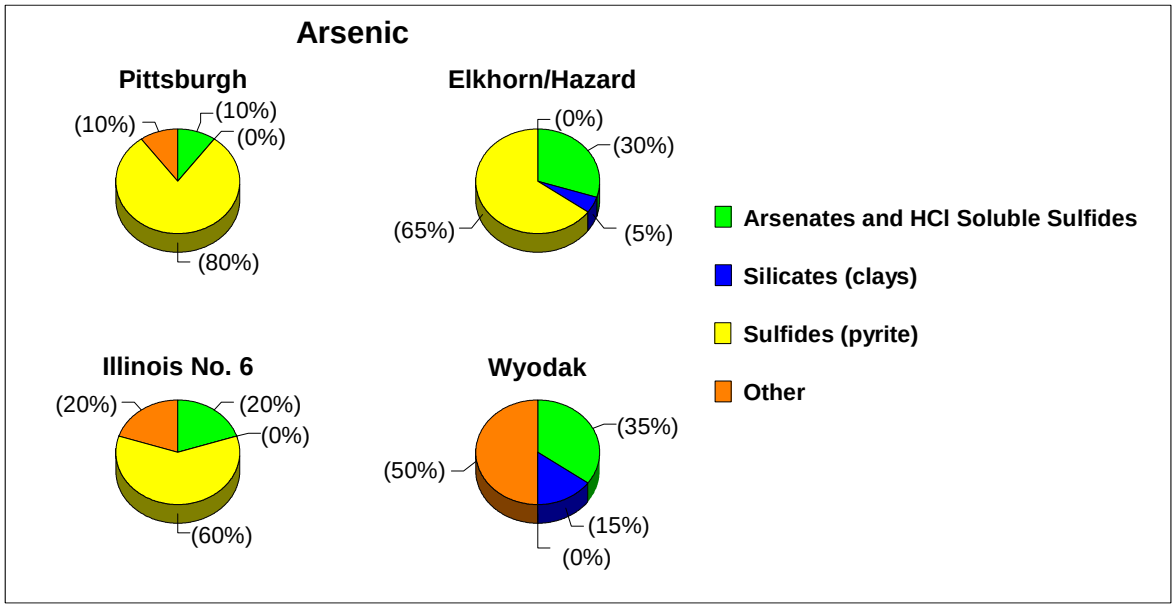

(a)

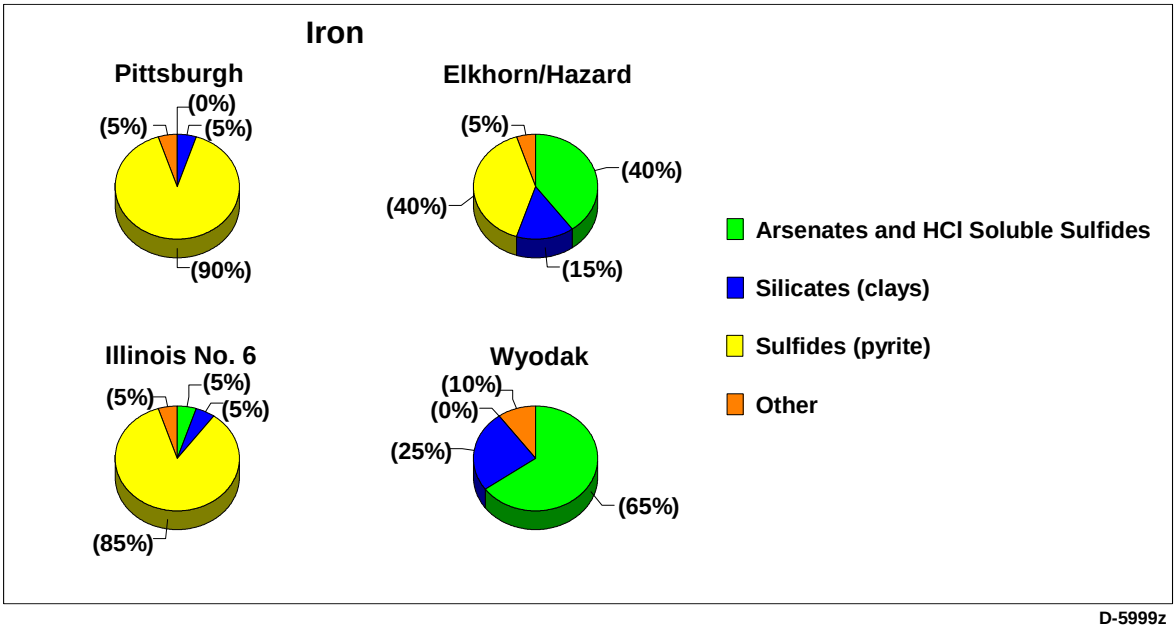

(b)

Figure 3-20 Mode of occurrence diagrams for arsenic (a), iron (b), selenium (c), and nickel (d) in the Pittsburgh, Elkhorn/Hazard, Illinois No. 6, and Wyodak coals

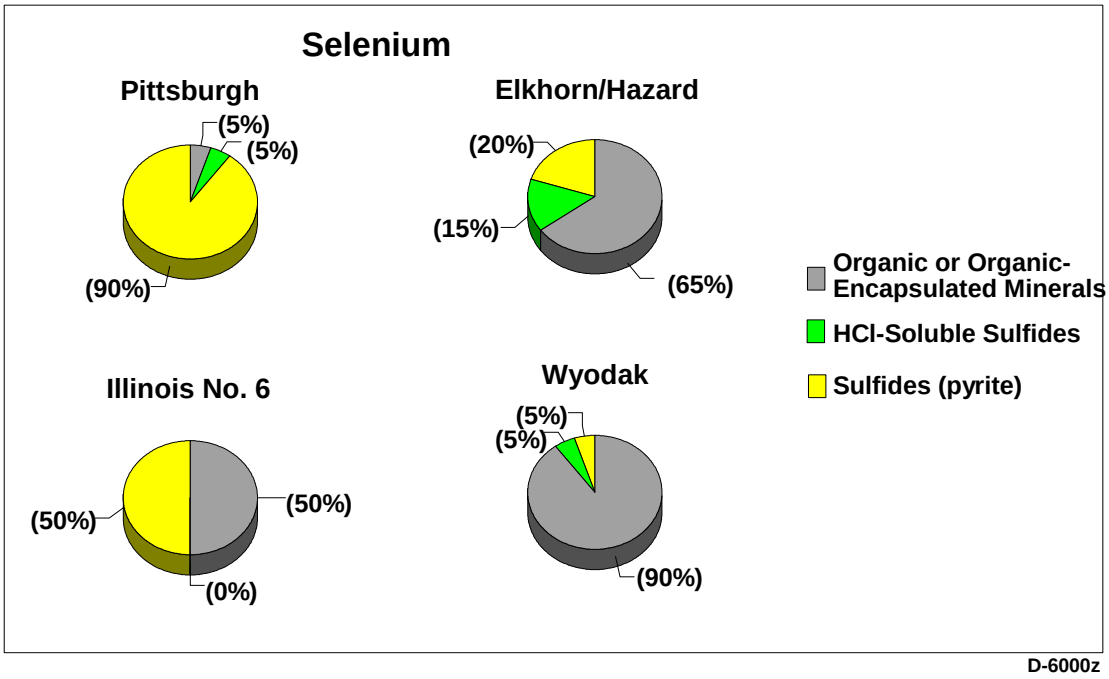

(c)

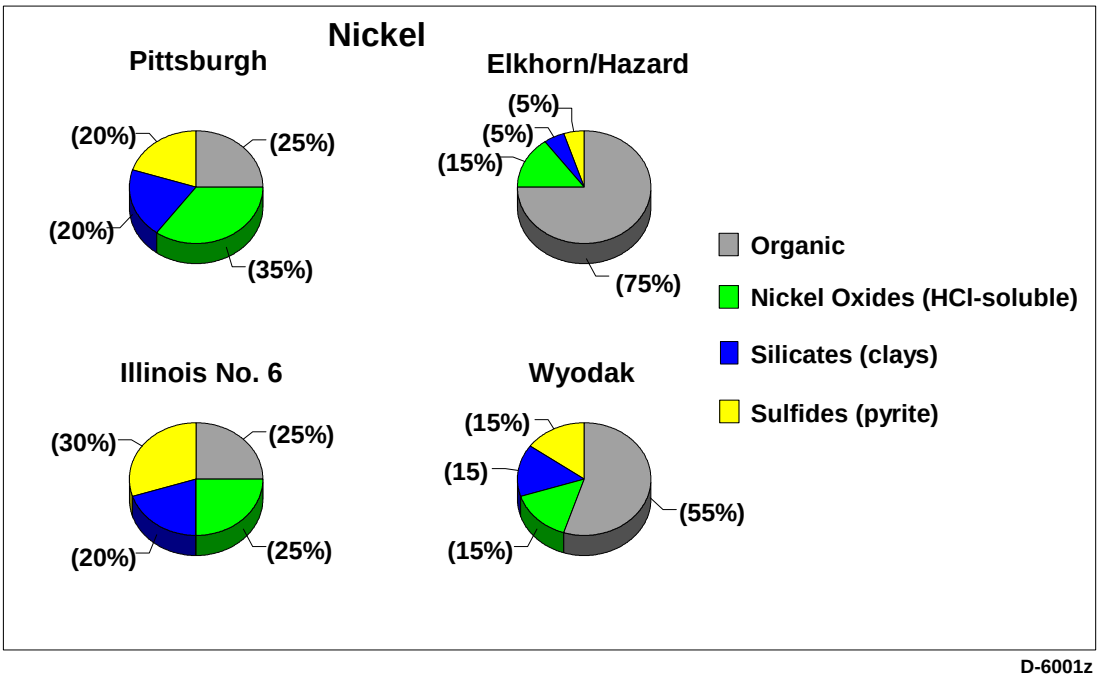

(d)

Figure 3-20 (continued) Mode of occurrence diagrams for arsenic (a), iron (b), selenium (c), and nickel (d) in the Pittsburgh, Elkhorn/Hazard, Illinois No. 6, and Wyodak coals

Similar to the Elkhorn/Hazard coal, the Wyodak coal has more than one mode of occurrence for arsenic. Thirty-five percent of arsenic in the Wyodak coal was leached by HCl; 15% of the arsenic was leached by HF. Leaching by HCl may indicate an association of arsenic with iron oxides; leaching by HF probably indicates an association with clays (possibly illite). Fifty percent of the total arsenic was not leached in the Wyodak coal. Because most of the iron was leached (see next section), some of the arsenic may be associated with organics. Percentages for the mode of occurrence diagram (Figure 3-20a) were derived directly from the leaching percentages (Figure 3-19a).

Iron

The leaching behavior of arsenic was also compared to that of iron in the Pittsburgh, Elkhorn/Hazard, and Illinois No. 6 coals. In the Pittsburgh and Illinois No. 6 coals, the leaching behavior of iron is similar to that of arsenic (Figure 3-14b). Iron was leached primarily by HNO_3 (85 to 90%). Percentages given in the iron mode of occurrence diagram (Figure 3-20b) were derived directly from the leaching data. For the Illinois No. 6 coal, we assume that there is little or no organic iron, because the cumulative amount of iron leached by the four solvents is 100%.

In the Elkhorn/Hazard coal, only 75% of the total iron was leached, and only a small portion of iron (15%) was leached by HNO_3 (Figure 3-19b). Based on our observations of unleached pyrite grains in the nitric acid solid residue, we have estimated that the sum of leachable iron in pyrite (15%) and unleached iron (25%) is approximately equivalent to the total amount of iron in pyrite (40%) (Figure 3-20b). The assumption that the Elkhorn/Hazard coal contains little or no organically-bound iron is inherent in this estimate. The ratio of leachable iron in pyrite to total iron in pyrite (15/40) is approximately 38%. Because the ratio of leachable arsenic in pyrite to total arsenic in pyrite (25/65=38%) is equal to the ratio found for iron (38%), we infer that the leaching behavior of iron is similar to the leaching behavior of arsenic.

In the Wyodak coal, 65% of the iron was leached by HCl and 25% was leached by HF. In contrast to arsenic, nearly all of the iron was leached (90%). We infer that the iron is primarily associated with iron oxides or carbonates (as indicated by leaching with HCl) and clays (as indicated by leaching with HF).

Selenium

In the Pittsburgh coal, selenium was leached to a large degree by nitric acid (90%), suggesting an association with pyrite (Figure 3-19c). An association of selenium with pyrite is also evident in the Elkhorn/Hazard coal, where selenium was leached primarily by nitric acid (50%). In the Elkhorn Hazard coal and Illinois No. 6 coals, because the total amount of selenium leached is fairly low (45% and 60%, respectively), we infer an association with the organics. In the Pittsburgh and Elkhorn/Hazard coals, selenium was leached to some degree (5% and 15%, respectively) by HCl. The HCl-soluble selenium may be in accessory mono-sulfides such as sphalerite (ZnS) and galena (PbS).

Selenium concentrations in pyrite grains were generally below the microprobe detection limit (~100 ppm) in the Pittsburgh, Illinois No. 6, and Elkhorn/Hazard coals. Isolated values of 100 or 200 ppm were obtained for selenium in pyrite in each of these coals. Microprobe data for the Wyodak coal are not sufficient to estimate selenium content in pyrite (Appendix D). In the Elkhorn/Hazard coal, concentrations of selenium in pyrite were near the detection limit of selenium (100 ppm). To estimate the total organic selenium in these coals (Figure 3-20c), we have added the ammonium acetate-leached selenium to the unleached selenium.

In the Wyodak coal, selenium was leached primarily by ammonium acetate (20%). Only 30% of the total selenium was leached, suggesting an association with organics. To estimate the total organic selenium in the Wyodak coal (Figure 3-20c), we have added the ammonium acetate-leached selenium to the unleached selenium.

Chromium

The leaching behavior of chromium is varied (Figure 3-19d). Chromium is leached to some extent by HF (20 to 25%) in the Pittsburgh, Elkhorn/Hazard, and Illinois No. 6 coals. In the Wyodak coal, 45% of the chromium is leached by HF. Leaching by HF suggests an association with silicates (possibly illite). In the Elkhorn/Hazard and Illinois No. 6 coals, totals for leaching of chromium are low (45%). In the Wyodak coal, the total leached chromium is fairly low (70%). The low leaching totals possibly suggest an organic association for chromium. It is also possible that the unleached chromium is due to the presence of shielded (organically encapsulated) illite grains. In the Pittsburgh coal, chromium is leached to some degree by HCl (20%), suggesting an association with carbonates or HCl-soluble sulfides. Chromium is also leached by HNO_3 (30%) in the Pittsburgh coal, indicating an association with pyrite. Because the leaching data for chromium are inconclusive, we did not make a final determination for its forms of occurrence.

Huggins and Huffman (University of Kentucky) have identified the mode of occurrence of chromium in density separates of the program coals, based on XAFS data to be discussed in Section 3.5. Their results indicate the presence of CrOOH in the float fractions of the coals, chromium in silicates of the middling fractions, and chromite in the sink fractions of the coals. We examined float, middling, and sink density fractions of the Elkhorn/Hazard coal with the SEM to determine the forms of occurrence of chromium. Overall, our findings present no evidence to conflict with the observations of Huggins and Huffman. In the sink fraction, we detected chromite in 2 out of 21 grains analyzed, a relatively high proportion of chromite. Although we did not observe any species of chromium in the float fraction of the coal, identification of the amorphous CrOOH grains by SEM is difficult and concentrations may have been below detection limits. We also did not observe any species of chromium in the middling fraction of the coal. However, as discussed earlier, our microprobe analysis of the raw coal indicates the presence of chromium in illite, at concentrations that are near the detection limits of the microprobe.

Nickel

The leaching behavior of nickel is also varied (Figure 3-19e). In the Pittsburgh, Elkhorn/ Hazard, and Illinois No. 6 coals, nickel is leached to some degree by each of the four leaching agents (ammonium acetate, HCl, HF, and HNO_3). In the Elkhorn/Hazard coal, total leaching levels are low (35%). In each of the coals, nickel leached by HNO_3 is probably associated with pyrite. The presence of nickel in pyrite in these coals is confirmed by microprobe data. Nickel leached by HCl may possibly be in nickel-oxides, however, nickel-oxides were not observed with the SEM. Modes of occurrence for nickel, as indicated by leaching data, are shown in Figure 3-20d.

Mercury

The leaching behavior of mercury is highly varied (Figure 3-19f). In the Pittsburgh and Elkhorn/Hazard coal, mercury is leached primarily by HCl (25 to 40%). HCl-leachable mercury in these coals may be associated with oxidized pyrite or HCl-soluble sulfides. Overall, a total of 40% to 50% of mercury is leached in the Pittsburgh and Elkhorn Hazard beds. In the Illinois No. 6 coal, a total of only 5% of the mercury is leached. In the Wyodak coal, leaching data for mercury are also highly varied. Work planned for Phase II will allow us to gain a better understanding of the behavior of mercury in the program coals. Because the leaching data for mercury are inconclusive, we did not make a final determination of its forms of occurrence.

3.4.3 *Mass Balance Calculations*

Using the mean arsenic and nickel concentrations obtained for pyrite by electron microprobe analysis, mass-balance calculations were done for the Pittsburgh, Elkhorn/Hazard, and Illinois No. 6 coals. The contribution of pyrite to the mass balance of arsenic and nickel was calculated by multiplying the concentration of each element in pyrite by the amount of pyrite (Appendix F). The amount of pyrite (in weight percent) was calculated from pyritic sulfur values (Table 3-2). The calculated concentration of each element is expressed as a percentage of the whole-coal value. Results for arsenic and nickel are shown in Figures 3-21 and 3-22, in which mass-balance fractions obtained by microprobe are compared with the mode of occurrence percentages based primarily on leaching data with an estimated error of ± 25% (Figure 3-20).

Mass-balance calculations based on our microprobe data indicate that 60% of arsenic in the Pittsburgh coal can be accounted for by pyrite, comparing well (within the leaching data error of ±25%) with our final mode of occurrence determination, which indicates that 80% of arsenic is associated with pyrite (Figure 3-21). In the Illinois No. 6 coal, microprobe data indicate a higher proportion of arsenic associated with pyrite (over 100%) than our final mode of occurrence determinations (60%, Figure 3-21). This result is also within uncertainty, because the 70% of the detection limit (70 ppm) in the calculation.

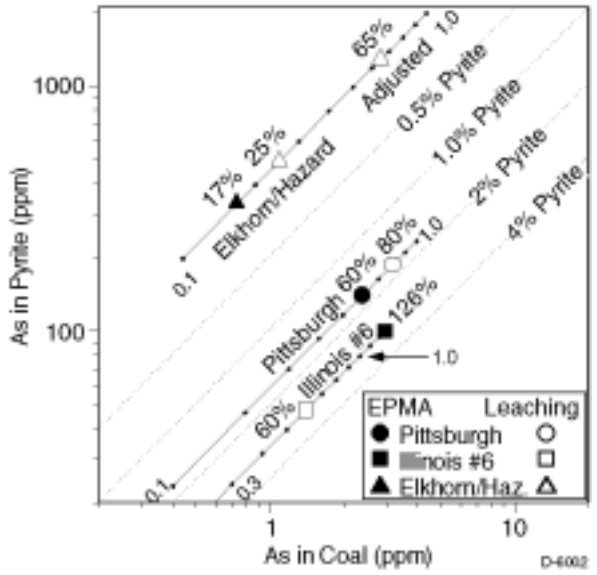

Figure 3-21 Arsenic-in-pyrite mass-balance diagram. For each coal, diagram shows a sliding scale of fractions of whole-coal arsenic accounted for by pyrite, in increments of 10% (0.1). Diagram also shows arsenic-in-pyrite fractions indicated by selective leaching (HNO_3 fraction; open symbols), and mass-balances obtained by electron microprobe (EPMA; filled symbols).

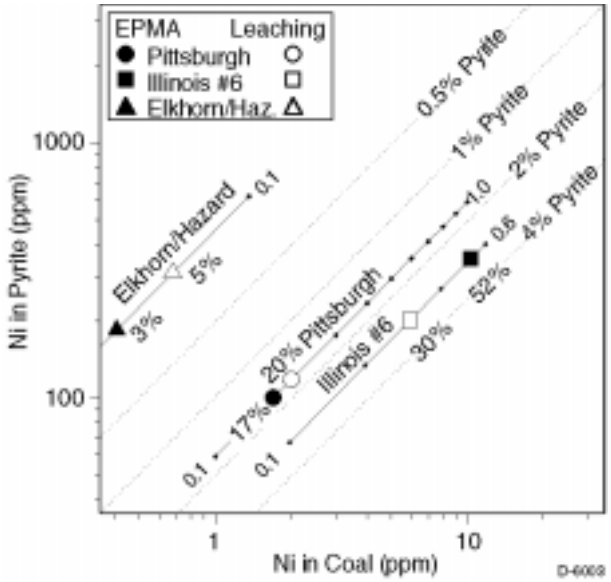

Figure 3-22 Nickel-in-pyrite mass-balance diagram. For each coal, diagram shows a sliding scale of fractions of whole-coal nickel accounted for by pyrite, in increments of 10% (0.1).

Microprobe data for the Elkhorn/Hazard coal indicate that only about 20% of arsenic is associated with the pyrite. These data do not compare well to our final mode of occurrence estimates (65% of total arsenic associated with pyrite), as derived from the sum of arsenic leached by nitric acid (25%) and the fraction of unleached arsenic (40%). However, because arsenic has a heterogeneous distribution in pyrites of the Elkhorn/Hazard coal, it is difficult to obtain an accurate mean value for arsenic and the mass balance estimate based on microprobe data may be low.

Mass-balance for nickel calculated from microprobe analyses of pyrite is in fairly good agreement (within the leaching data error of ±25%) with leaching data for the Pittsburgh, Illinois No. 6, and Elkhorn/Hazard coals (Figure 3-20). Microprobe data indicate the following percentages of nickel associated with pyrite: Pittsburgh (17%), Elkhorn/Hazard (3%), and Illinois No. 6 (50%). These data compare fairly well with final values based primarily on leaching: Pittsburgh (20%), Elkhorn/Hazard (5%), and Illinois No. 6 (30%).

The number of illite analyses was not sufficient to calculate mean values for chromium concentrations in illite based on microprobe data. If an average Cr_2O_3 value of 0.025 wt% (equivalent to about 170 ppm Cr) in illite is assumed, mass balance calculations indicate that about 10% of the chromium in the Pittsburgh, Illinois No. 6, and Elkhorn/Hazard coals can be accounted for by illite. This compares well to values of 20% to 25% obtained in the HF stage of leaching.

Selenium concentrations in pyrite are generally below the microprobe detection limit (Appendix D) for the Pittsburgh or Illinois No. 6 coals. Based on mass-balance calculations, if all selenium is assumed to be in pyrite in the Pittsburgh and Illinois No. 6 coals, concentration levels in pyrite would still be lower than the detection limit (100 ppm). For the Elkhorn/Hazard coal, the mean selenium concentration in pyrite is marginally above the detection limit (about 110 ppm, based on 11 pyrite grains, Appendix D). A mass-balance calculation based on these data indicates that only about 8% of the selenium in the Elkhorn/Hazard coal is in pyrite. The rest of the selenium may be associated with the organics.

3.4.4 *Experiments to Determine the Volatility of Trace Elements*

Experiments were conducted to determine the volatility of trace elements by heating the coal samples to 473 K, 823 K, and 1273 K in air. Analytical data indicate that the concentrations of arsenic, chromium, and nickel are not affected by heating samples to temperatures of up to 1273 K within the analytical errors of the experiment.

3.5 Trace Element Forms of Occurrence by X-ray Absorption Fine Structure Spectroscopy (XAFS)

3.5.1 *Methods*

The principal technique that is being utilized by University of Kentucky personnel for characterization of trace elements is X-ray absorption fine structure (XAFS) spectroscopy. Our initial studies (Huggins et al., 1993a; Huffman et al., 1994) demonstrated that this technique has an unparalleled ability to probe a complex material such as coal or ash and obtain information about the local structure and bonding of a specific element at concentrations as little as 5 ppm. From this information, the mode of occurrence of the element in the coal or ash can often be deduced. Such information is basically a description of how an element occurs in coal or ash and is complementary to information on the concentration of the element or how much of an element is present in the coal or ash. Information on both the concentration and the mode of occurrence is necessary to understand fully the behavior of an element during combustion and for assessing the potential threat to human health posed by the "air-toxic" group of trace elements.

In this work, XAFS spectroscopy has been carried out at two of the three major synchrotron facilities in the U.S.: viz., the National Synchrotron Light Source (NSLS) at Brookhaven National Laboratory, New York, and the Stanford Synchrotron Radiation Laboratory (SSRL), Stanford University, California. At NSLS, beam-lines X-19A and X-18B were used in this investigation, whereas at SSRL most of the research was carried out at beam-line IV-3. For the most part, similar experimental procedures were carried out at both facilities.

XAFS spectroscopy is basically a measurement of the variation (or fine structure) of the X-ray absorption coefficient with energy associated with one of the characteristic absorption edges of the absorbing element. The XAFS spectrum is normally divided into two distinct regions for analysis: the X-ray absorption near-edge structure (XANES) region and the extended X-ray absorption fine structure (EXAFS) region. As these names imply, these regions incorporate the fine structure in the vicinity of the edge itself and further away from the edge, respectively (Figure 3-23). Quite different analysis is done for each region of the spectrum. The XANES spectrum is used, without significant modification, as a "fingerprint" for the element in the material under investigation, whereas the EXAFS region can be extensively mathematically manipulated to obtain information on the short-range local structure around the absorbing atom or ion.

Synchrotron radiation is produced by electron (or positron) storage rings in which highly energetic particle beams are "stored" in a stable orbit in an ultrahigh vacuum (10^{-9} torr). The particle beam in the storage ring emits synchrotron radiation as a consequence of the principle of conservation of momentum when the charged particles, moving at velocities very near to that of

light, are forced to change direction through the application of a magnetic field normal to the path of the particle beam. This synchrotron radiation is a broad "white" radiation that is emitted tangentially to the orbit of the charged particles. It is then collimated by a series of slits and/or mirrors and delivered to an experimental beam-line station. For XAFS experiments, a monochromatic beam is required rather than white radiation, so a monochromator or grating is inserted into the white beam to select a specific energy that is determined by the spacing of the reflection planes of the monochromator crystal or grating, the angle of the monochromator with respect to the beam, and application of Bragg's law. There are usually additional slits and focussing mirrors between the monochromator and the exit of the beam in the experimental hutch. The intensity of the monochromatic X-ray beam at the sample is typically 6 to 9 orders of magnitude greater than that which can be achieved with a conventional X-ray tube.

To generate an XAFS spectrum, the absorption by the sample is measured as a function of the monochromator angle or, equivalently, the energy of the incident X-ray beam. Most XAFS spectra are still recorded in a discrete manner by stepping across an energy interval that includes an X-ray absorption edge of the element of interest. Typically, the energy interval may start as much as 100 to 200 eV below the edge and extend as much as 1000 to 1500 eV above the edge. However, the stepping will not be uniform across the energy interval but will be subdivided into at least three regions (the pre-edge, XANES, and EXAFS regions; q.v. Figure 3-23) so as to maximize the information quality and thereby facilitate the data analysis. For the pre-edge region (from -200 eV to around -20 eV below the edge), which contains no spectral information but has to be measured in order to determine the pre-edge slope, the stepping is generally coarse with a short time/step. The edge or XANES region, which for trace elements often contains much, if not all, of the useful information, is then measured very carefully and slowly (0.1 to 0.25 eV/step with a longer time/step) from about -20 eV below the edge to as much as +50 eV above the edge. The EXAFS region is then measured out to at least +250 eV up to as much as +1500 eV above the edge, depending on the strength of the EXAFS oscillations or chi signal. The stepping across the EXAFS region is usually now done in terms of reciprocal-space inverse distance (e.g. 0.05 $Å^{-1}$/step) with the time per step determined by the actual interval in real space. This procedure gives a more uniform appearance to the χ versus k spectrum, which, after application of a Fourier transform, results in a better quality radial structure function (RSF) spectrum (Figure 3-23).

The XAFS spectrum can be acquired by one of three different methods, depending on the concentration of the element under investigation. For standard samples or for samples in which the element of interest comprises more than about 5 wt% of a reasonably X-ray transparent

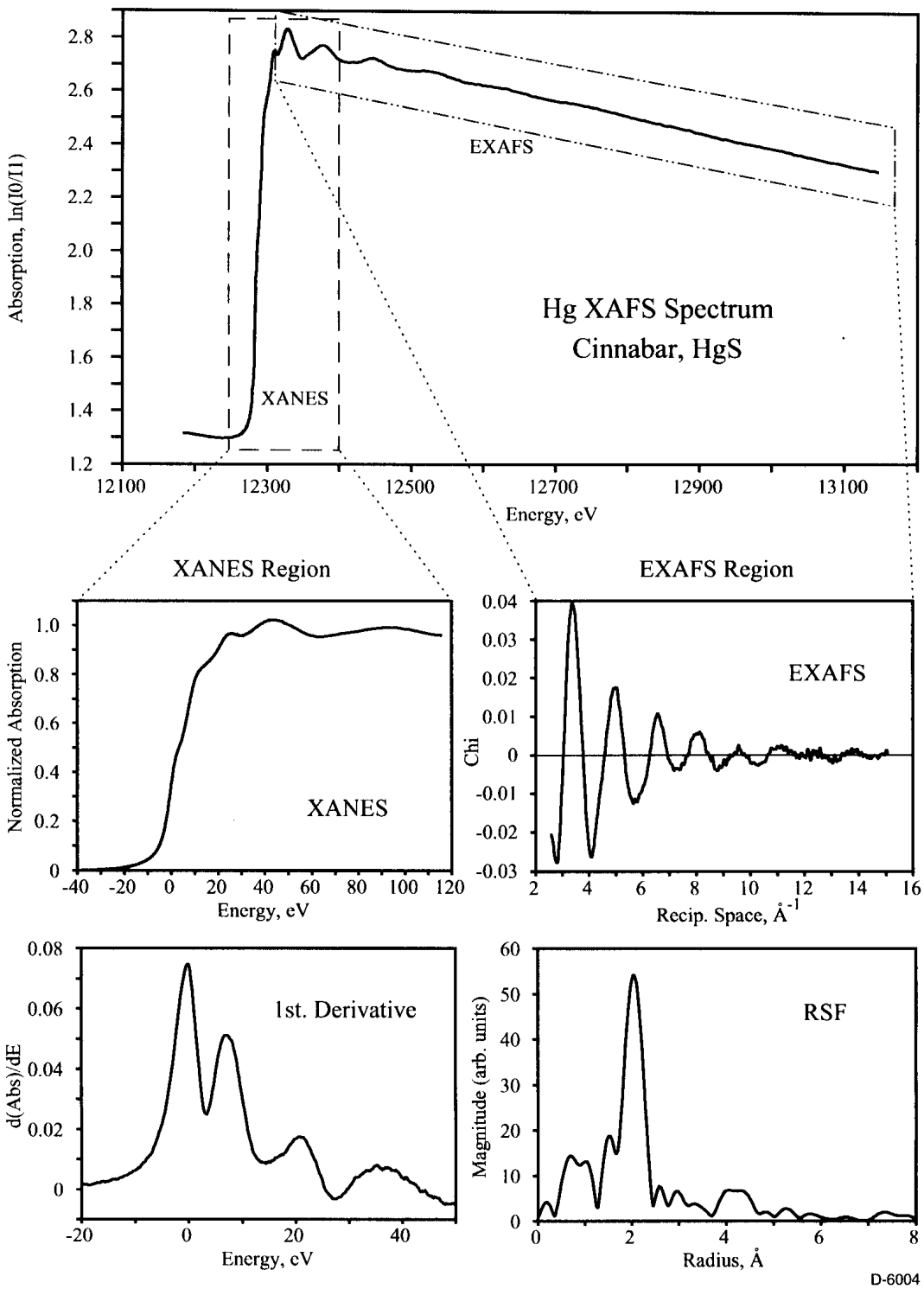

Figure 3-23 XAFS spectrum of HgS (red, cinnabar) showing how spectrum is first divided into XANES and EXAFS spectral regions and then mathematically processed further to give derivative spectra and radial structure functions (RSF), respectively.

material such as coal, the XAFS spectrum is best measured in absorption geometry by measurement of the X-ray intensity before and after absorption by the sample. Such measurements are made with simple ion chambers. The relationship between the X-ray intensity and the absorption coefficient ($\mu(E)$) is as follows:

$$I_t = I_0 \exp(-\mu t) \quad (1)$$

where I_0 is the intensity of the X-ray beam incident on the sample, I_t is the intensity of the X-ray beam after transmittance through the sample, and t is the thickness of the sample. The thickness of the sample is invariant; hence, any variation in $\ln(I_0/I_t)$ with energy is directly equivalent to variation in the absorption coefficient. For samples with elements of interest with concentrations ranging from 0.1 to 5 wt%, it is better practice to measure the spectrum in fluorescence geometry. In this experiment, the intensity of the X-rays fluoresced by the sample in response to the absorption process is measured. Typically, a large solid angle ion chamber fluorescence detector (Stern and Heald, 1979; Lytle et al., 1984) is located at 90 deg to the incident X-ray beam with the sample turned to 45 deg with respect to both the detector and the incident beam. In this case, the relationship between the fluorescent X-ray intensity (I_f) and the absorption coefficient is as follows:

$$I_f = I_0 \mu(E) \quad (2)$$

It should be noted that this equation is only exact in the limit that the sample is thin and/or the element of interest is sufficiently dilute not to give rise to self-absorption phenomena. However, if the element of interest is of trace abundance (5 to 500 ppm), the background fluorescent X-ray intensity from other elements will overwhelm the fluorescence signal from the desired element. At this point, the ion chamber should be replaced by a thirteen-element, solid-state germanium detector that has been optimized for the measurement of the XAFS spectra of dilute elements in materials (Cramer et al., 1988). This type of detector counts X-rays only in a narrow energy window set specifically for the X-rays fluoresced by the element of interest and thereby rejects most of the X-rays fluoresced by other elements. This signal selection process can greatly enhance the signal/noise ratio. However, care must be taken to avoid count-rate saturation effects with this type of detector when the signal is reasonably strong. This can be achieved by simply moving the detector away from the sample or by increasing the filter thickness. Use of the appropriate filters and Soller slits (Stern and Heald, 1979) will also enhance the signal/noise ratio with either fluorescent detection method. Finally, for exceedingly dilute concentrations (< 100 ppm), the spectra can be repetitively scanned and added together to obtain a composite spectrum of better quality.

Analysis of experimental XAFS data consists of the following steps (Figure 3-23): (i) isolation of the EXAFS from the edge step, (ii) conversion of the energy scale to reciprocal space (k-space) inverse dimensions, generating the "chi vs. k" spectrum, and (iii) application of a Fourier transform to the chi spectrum to create a radial structure function (RSF) that describes the position and coordination number of atomic shells that surround the absorbing atom or ion. These techniques and procedures are well described in reviews and textbooks on XAFS spectroscopy (Eisenberger and Kincaid, 1978; Lee et al., 1981; Koningsberger and Prins, 1988; Brown

et al., 1988). Unfortunately, analysis of the EXAFS region for trace elements in coal generally becomes uninformative as the element's concentration decreases below about 50 ppm because the relatively weak EXAFS oscillations get lost in the background noise. Hence, much reliance is placed on interpretation of the XANES region for elements in coal that are in the concentration range 5 to 50 ppm. Generally, the interpretation of elemental modes of occurrence from just the XANES spectrum relies primarily upon comparison with standards. However, more creative measures are often needed if the element occurs in two or more distinct forms. Such measures may also have to be applied because of natural-world phenomena such as diadochy (solid solution), polymorphism in mineral systems, small-particle phenomena, *etc.*, that can cause the appearance of the XANES spectrum to vary from that of a particular bulk standard. Specific measures may include (i) comparison of derivative XANES spectra; (ii) comparison with XANES spectra from different but chemically similar elements; (iii) subdivision of the coal into different fractions to separate or concentrate different forms of occurrence; (iv) simulation of spectra from weighted additions of XANES spectra of standards and/or coals or coal fractions. Examples of these procedures applied to the interpretation of XANES spectra of minor and trace elements in coal are described elsewhere (Huggins et al., 1993a; Huffman et al., 1994; Huggins and Huffman, 1996a; Huggins et al., 1997a; Huggins and Huffman, 1996b).

In addition to the XANES and EXAFS spectral data, the analysis of the XAFS spectra also provides data on the step-height, which can be used as an approximate estimate of the concentration of the absorbing element. Provided the samples are similar in bulk composition and measured under more or less identical conditions, the step-height is a reasonably precise measure of the relative concentration of the element in the different samples. In this investigation, limited use of this parameter is made to compare and contrast the concentrations of elements in different fractions of a single coal.

3.5.2 *XAFS Investigation of Phase I Coals*

XAFS spectroscopy was used to examine the form of occurrence of arsenic, chromium, selenium, chlorine, and zinc in most coals and fractions. Less complete investigation has been made of a number of other elements including manganese, nickel, and sulfur. Owing to their sub-ppm levels of abundance in the project coals, no investigation has been attempted of other important HAPs elements, such as antimony, cadmium, or mercury. However, with assistance from R. B. Finkelman, of the USGS, a coal of unusually high mercury content was made available for this study in order to augment the XAFS database for this important HAPs element. The XAFS data will be presented on an element by element basis in order to emphasize the differences in occurrences among the project coals.

Arsenic

Arsenic is present in all project coals at concentration levels (Table 3-10) that are significantly less than the "average" arsenic concentrations in U.S. coals, which is about 16 ppm (Huggins and Huffman, 1996b; Bragg et al., 1994). Such observations apply to the Wyodak coal as well, even though the "average" arsenic content of subbituminous coals in the U.S. is only about 3.2 ppm (Bragg et al., 1994). Despite these low concentrations, a complete identification

of the mode of occurrence of arsenic in all coals proved possible from XAFS spectroscopy. Furthermore, quantification of the different forms of occurrence of arsenic in these coals was also achieved (Table 3-14) using the spectral fitting method described elsewhere (Huffman et al., 1994; Huggins et al., 1997b).

Table 3-14. Arsenic Forms of Occurrence by XAFS for Phase I coals

Coal Sample Fraction	Relative Step-Hgt	%As (pyrite)	%As (carboxyl)	%As (arsenate)
Elkhorn/Hazard RAW	1.0	61		39
ORG	0.6	55		45
CLAY	2.1	64		36
HYM	4.0	94		6
Pittsburgh RAW	1.0	88		12
ORG	0.9	83		17
CLAY	2.8	86		14
HYM	5.0	93		7
Illinois #6 RAW	1.0	86		14
ORG	0.75	**		**
CLAY	4.0	83		17
HYM	6.0	92		8
Wyodak RAW	1.0		50±10	50±10

** Data too weak for adequate fitting.
Estimated errors ±5% for As/pyrite, As/arsenate distribution

The arsenic XANES spectra for the Elkhorn/Hazard and Pittsburgh coal fractions are shown in Figures 3-24 and 3-25, and for the Wyodak coal in Figure 3-26. The arsenic XANES spectra for the Illinois coal fractions are similar, but weaker, to those for the Pittsburgh coal samples and are not shown. The spectra for the three bituminous coals and fractions indicate the presence of two distinct arsenic forms: (i) an arsenical pyrite, in which arsenic substitutes for

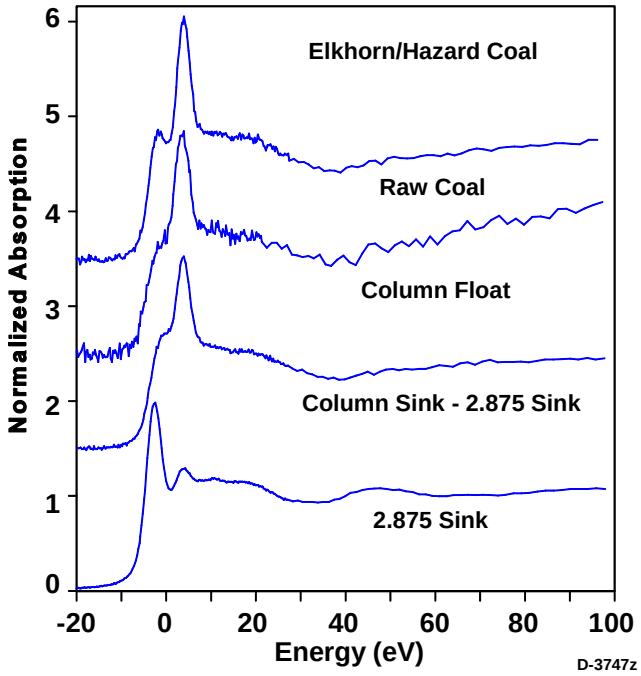

Figure 3-24. Arsenic XANES spectra for Elkhorn/Hazard coal and fractions

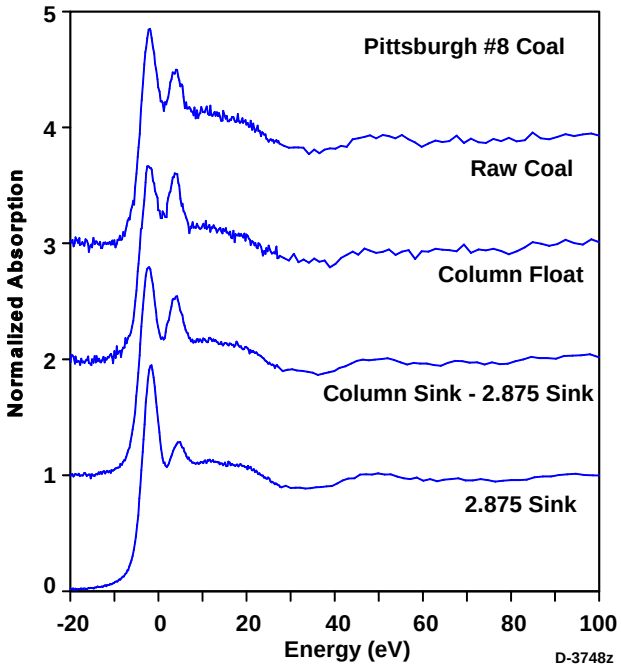

Figure 3-25 Arsenic XANES spectra for Pittsburgh coal and fractions

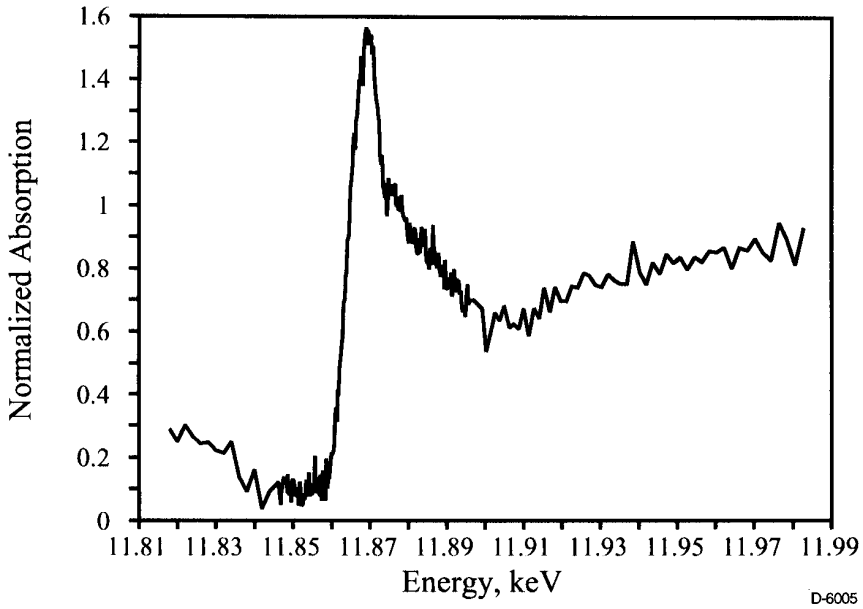

Figure 3-26 Arsenic XANES spectra for the Wyodak coal

sulfur in the pyrite structure, and (ii) an arsenate (AsO_4^{3-}) form, that most likely has been formed from the arsenical pyrite upon exposure to air. These forms are unoxidized and oxidized arsenic forms, respectively. Discrimination between arsenical pyrite and arsenopyrite (FeAsS) was based on the observation of a weak peak in the arsenic XANES spectra at about 65 to 70 eV (Huggins et al., 1993a; Huggins and Huffman, 1996b) above the arsenic K-edge.

The arsenic XANES spectrum of the Wyodak coal (Figure 3-26) is quite different to those of the bituminous coals and indicates a quite different form of occurrence of arsenic. In this coal, the arsenic oxidation states are As^{3+} and As^{5+}, and there is no evidence for any arsenical pyrite. These observations are similar to those reported for other subbituminous coals from the western U.S. and Canada (Huggins et al., 1996). The main form of occurrence of arsenic in such coals is believed to be an organically associated As^{3+} form coordinated by oxygen that oxidizes to arsenate upon exposure to air. Such an interpretation is consistent with arsenic bound to macerals via carboxyl groups, an occurrence for arsenic in low-rank coals that has been postulated previously (Miller and Given, 1986; Given and Miller, 1987).

All three bituminous coals show a similar pattern of behavior of arsenic distribution among the different fractions (Table 3-14). The arsenic is always least oxidized in the "HYM" fraction, most oxidized in the "ORG" fraction, and intermediate in the "RAW" and "CLAY" fractions. However, whereas arsenic in the Pittsburgh and Illinois #6 coals appears to be only slightly oxidized, the arsenic in the Elkhorn/Hazard coal is significantly oxidized. This observation is consistent with the data from Mössbauer spectroscopy shown in Tables 3-6 to 3-8, in which oxidized and unoxidized forms of iron show a similar behavior.

A comparison of the concentrations of arsenic (using the arsenic step-height) and pyritic iron (using Mössbauer data) is shown in Figure 3-27 for the bituminous coal fractions. Although

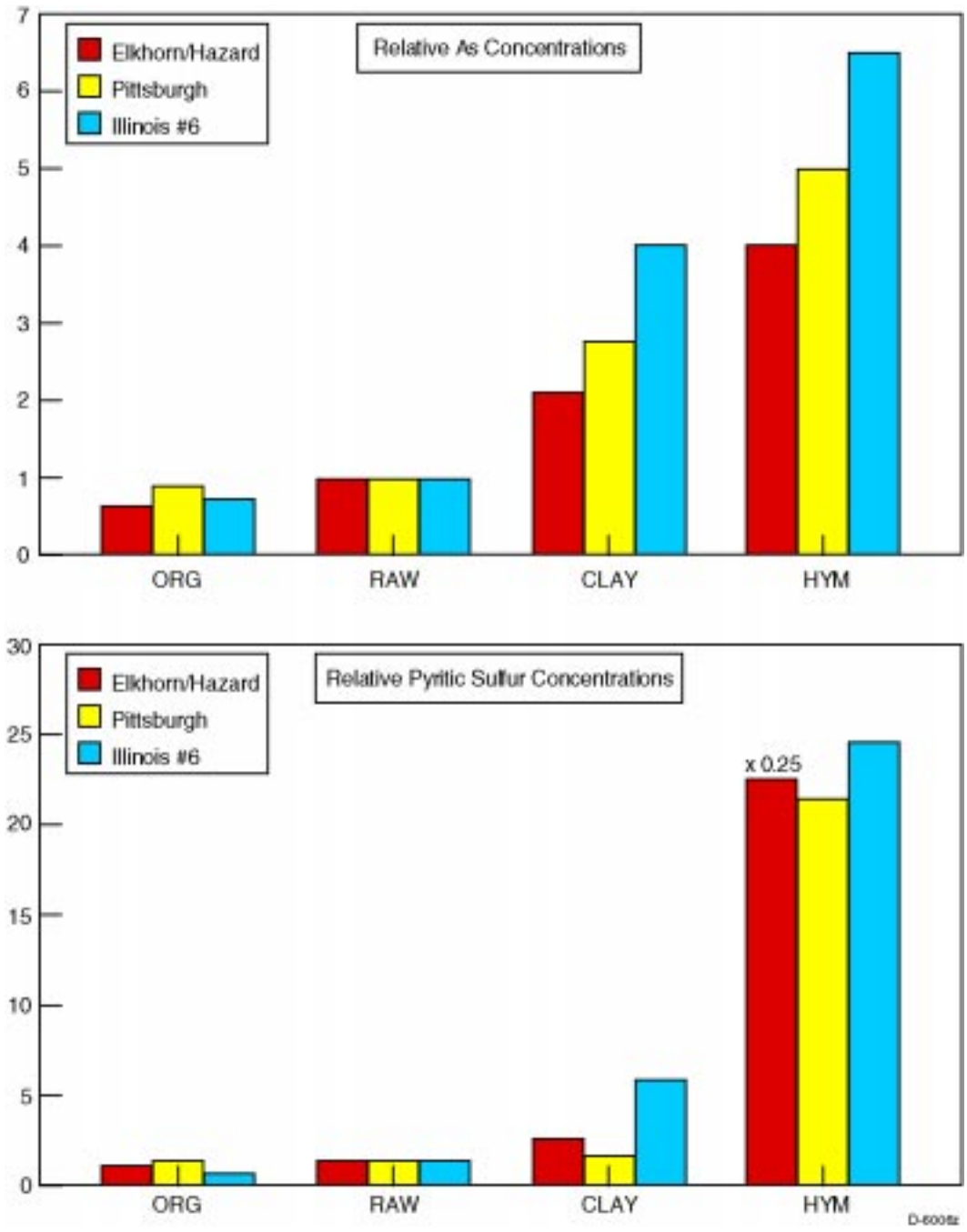

Figure 3-27. Comparison of relative arsenic concentrations and pyritic sulfur concentrations

both elements exhibit parallel increases in concentration from the low-density "ORG" fraction to the high-density "HYM" fraction, it is clear that the pyritic iron concentration increases more steeply across the fractions than the arsenic concentration. The implications of this observation are as follows: (i) the average arsenic concentration in the fine-grained pyrite trapped in the "ORG" fraction must be *higher* than that in other fractions; and (ii) conversely, the average arsenic concentration present in the coarse pyrite in the "HYM" fraction must be significantly *lower* than in the other fractions. This would imply that there are relationships between the

average arsenic concentration of a fraction, the size of the pyrite grains, and the degree of oxidation of both the arsenic and iron in pyrite. As has been postulated previously, the substitutional mismatch of arsenic for sulfur in pyrite may result in a structural weakness where oxidation can initiate and occur at an accelerated rate.

It is also of interest to compare the data for arsenic forms of occurrence from XAFS spectroscopy with that from the leaching experiments carried out by USGS personnel. As shown in Table 3-15, it would appear that the sum of the arsenic removed by leaching in nitric acid and the remnant, non-leachable arsenic more or less corresponds to the arsenical pyrite form determined by XAFS spectroscopy. Conversely, the arsenic leached by HCl and by ammonium acetate corresponds to the arsenate forms determined by XAFS spectroscopy. Such oxidized arsenic forms are most likely to be found in jarosite and other oxidation products of pyrite weathering (Huggins et al., 1997a).

Table 3-15 Comparison of Arsenic Forms by Leaching and XAFS Methods

	XAFS Spectroscopy		USGS Leaching Method		
Coal	As(pyr)	AsO_4^{3-}	As(HNO_3, Resid.)	As(HF)	As(HCl, Amm)
Elkhorn/Hazard	61	39	65	5	30
Illinois #6	86	14	80		20
Pittsburgh	88	12	90		10

Considering all the possible sources of error in both determinative methods and the fact that the coal oxidation is an on-going dynamic process (hence, the relative proportions of the arsenic forms change with time and there was no agreement to make the determinations on or near a specific date), the agreement between the two methods shown in Table 3-15 is surprisingly good. Such joint XAFS and leaching studies should be carried out for all critical elements as this would appear to be the best use of valuable synchrotron time: viz., to use the direct spectroscopic method to validate or refute assumptions inherent in the indirect laboratory method so that the information obtained by the latter method is as reliable as possible.

In summary, arsenic is present in the project coals as follows:

- Elkhorn/Hazard: 60% As/pyrite, 40% arsenate
- Pittsburgh: 88% As/pyrite, 12% arsenate
- Illinois #6: 85% As/pyrite, 15% arsenate
- Wyodak: 40-60% As^{3+}(carboxyl?), 40-60% arsenate

It should be emphasized that the probable mode of occurrence for arsenic in the *unmined* bituminous coals would consist of 100% arsenical pyrite, as the XAFS data strongly imply that

the formation of the arsenate is an artifact due to oxidation of the arsenical pyrite subsequent to mining of the coal.

Chromium

Chromium was examined in all project coals. The concentration levels of chromium in the three bituminous coals (Table 3-10) are similar to or somewhat higher than the "average" chromium content of U.S. coals of about 13 ppm. The chromium content of the Wyodak coal is significantly lower than that found in the bituminous coals, but is in line with the typical concentration level of chromium in low-rank U.S. coals. As for arsenic, it was found useful to examine float and tailings fractions of the coals in addition to the as-received coal in order to interpret the chromium XANES spectra better.

Figure 3-28 shows the chromium K-edge XAFS spectra for the as-received Elkhorn/Hazard coal and the fractions generated according to the scheme shown in Figure 3-1. The corresponding XANES spectra prepared from the XAFS spectra are shown in Figure 3-29. Two interesting observations should be made regarding these figures. First, the rare-earth elements, cerium and neodymium, are indicated by the presence of their L-edges in the chromium XAFS spectrum at approximately 175 and 220 eV, respectively, above the chromium edge at 5,989 eV. Although these lines are well removed from the XANES region, they were usually strong enough to render the EXAFS region for chromium uninformative in most instances. However, note that in the chromium XAFS spectrum of the "HYM" fraction, both rare-earth edges are more or less
.

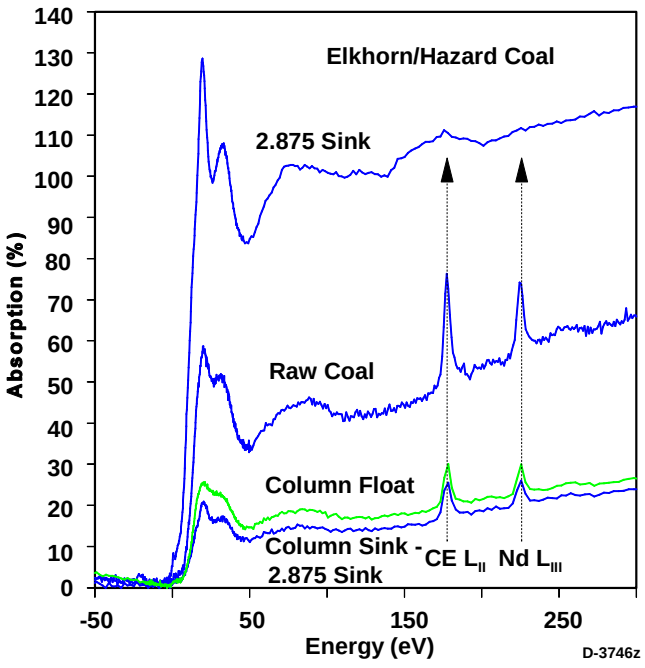

Figure 3-28 Chromium XAFS spectra for Elkhorn/Hazard coal and fractions

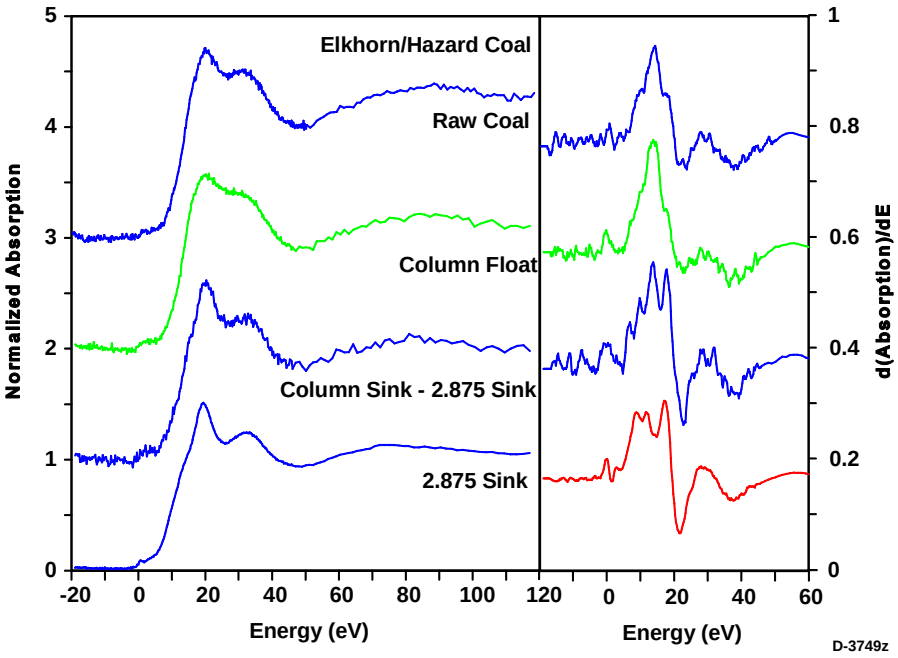

Figure 3-29 Chromium XANES spectra for Elkhorn/Hazard coal and fractions

absent. Second, the XANES and derivative XANES spectra of each fraction is different, indicating that there is a different form of chromium that dominates each float/tailings fraction

For the Elkhorn/Hazard coal, there are at least three distinct forms of chromium present in the coal. For the "CLAY" fraction, there is reasonable agreement between the observed spectrum and that exhibited by chromium-bearing illite. In particular, the three-pronged appearance of the derivative XANES spectrum is fairly diagnostic. The spectrum of the "HYM" fraction is quite similar to that of chromite ($FeCr_2O_4$), but, in view of the Mössbauer data for Elkhorn/Hazard coal (Table 3-6), which indicated the presence of a magnetic iron oxide in the "HYM" fraction, it is likely that the composition of the spinel is closer to a chromium-substituted magnetite. Data on the chromium K-edge step-heights (Table 3-16) indicate that the chromium concentration of the "HYM" fraction is about 5 times that of the other fractions. However, the "HYM" fraction constituted less than 1 wt% of the total mass of the Elkhorn/Hazard coal; hence, only a relatively minor fraction (no more than 5%) of the total chromium in this coal can actually be present as chromite/magnetite. The remaining 95% of the chromium is distributed among the

Table 3-16 Step-Height Data for Chromium K-edge Spectra

Coal	ORG	RAW	CLAY	HYM
Elkhorn/Hazard	1.0	1.0	0.7	5.1
Pittsburgh	0.8	1.0	1.6	0.6
Illinois #6	1.1	1.0	0.4	0.4

chromium forms in the "CLAY" and "ORG" fractions. Since the chromium concentration levels in these two fractions are quite similar, most of the chromium in this coal is associated with the larger "ORG" fraction. The chromium form that dominates the "ORG" fraction is believed to be an amorphous CrOOH phase, most probably of extremely small particle size. As discussed elsewhere (Huggins et al., 1993a; Huggins and Huffman, 1996a), the spectrum of the "ORG" fraction is most similar, but not exactly identical, to a CrOOH phase made by heating a fine-grained precipitate of $Cr(OH)_3$ to 423 K for 18 h. This CrOOH phase exhibited a few very broad peaks in its X-ray diffraction (XRD) pattern that matched in position, but not sharpness, with the strongest lines in the XRD pattern of grimaldiite, a crystalline CrOOH phase. From a geochemical and petrological viewpoint, a CrOOH occurrence would be compatible with the low-grade metamorphism experienced during coalification, even though occurrences of CrOOH phases in the natural world are extremely rare.

Both the Pittsburgh and Illinois #6 coals appear to contain the same two major chromium forms as the Elkhorn/Hazard coal: amorphous CrOOH and Cr-bearing illite. In both of these coals, there was no evidence for chromite/magnetite in either the chromium XAFS spectra or the Mössbauer spectra of the "HYM" fractions. Indeed in contrast to the Elkhorn/Hazard coal, the chromium edge-step for the "HYM" fractions in these two coals was less than or similar to that for the "ORG" fractions. Furthermore, for the Pittsburgh coal, the dominant chromium phase in the "HYM" fraction was identified as Cr-bearing illite. For the Illinois coal, the amorphous CrOOH phase is the dominant chromium form and accounts for at least 80% of the chromium. For the Pittsburgh coal, the Cr-bearing illite is more abundant and may approach 50% of the chromium occurrence.

The chromium XANES spectra for the Wyodak coal is shown in Figure 3-30. This spectrum is different from those observed for the fractions of the bituminous coals, and moreover, can not be simulated by any combination of the spectra for Cr-illite and amorphous CrOOH. The data suggest a quite different form, and using the systematics present in the XANES of chromium standards, it would appear that the chromium is surrounded predominantly by water molecules, as the spectrum closely matches hydrated chromium standards such as $Cr_2(SO_4)_3.xH_2O$. However, as indicated in Figure 3-30, a better match still is with the chromium XANES spectrum of a western Kentucky lignite ion-exchanged with Cr^{3+}. The slight differences that can be noted between the spectra in Figure 3-30 may indicate the presence of a minor second chromium phase in the Wyodak coal. This observation implies that chromium in low-rank coals is probably present at ion-exchange (carboxyl) sites in the maceral matrix. Further, it provides evidence that the chromium XANES spectra for the "ORG" fractions in bituminous coals do *not* arise from carboxyl-bound Cr^{3+} and gives added strength to the interpretation of such spectra in terms of an amorphous, fine particle CrOOH.

None of the XANES spectra measured for the project coals and fractions indicate the presence of detectable amounts of the Cr(VI) oxidation state in any sample. Hence, it can be safely concluded that the oxidation state of chromium in these three coals is entirely Cr^{3+}.

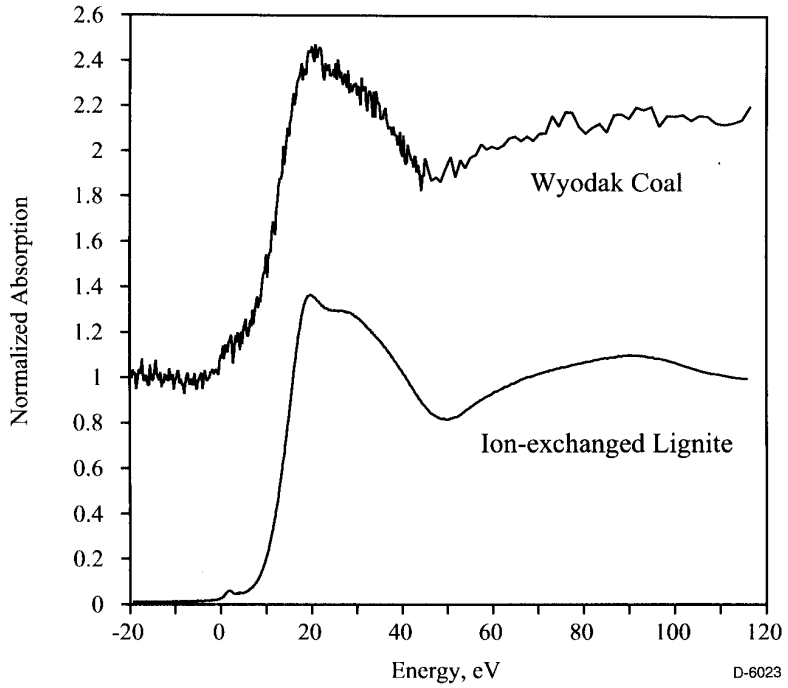

Figure 3-30. Chromium XANES spectra of Wyodak coal and of a western Kentucky lignite ion-exchanged with Cr^{3+}.

In summary, chromium in the four project coals is estimated to occurs as follows:

- Elkhorn/Hazard: 70 to 85% amorph. CrOOH, 10 to 20% Cr^{3+}/illite, 5% Cr^{3+}/Fe spinel
- Pittsburgh: 50 to 70% amorph. CrOOH, 30-50% Cr^{3+}/illite
- Illinois #6: 80 to 90% amorph. CrOOH, 10-20% Cr^{3+}/illite
- Wyodak: > 80% carboxyl-bound Cr^{3+}

Selenium

In comparison to arsenic and chromium, a less detailed study of the modes of occurrence of selenium was carried out. The selenium contents of the Elkhorn/Hazard and Illinois #6 coals were sufficient for examination, whereas the selenium content of the Pittsburgh coal was too low and that of the Wyodak coal was borderline. Float/tailings fractions of both the Illinois #6 and Elkhorn/Hazard coals were examined, but only the as received Wyodak coal was examined. The data for the two bituminous coals are summarized in Figure 3-31. As shown in Figure 3-32, there is a very strong correspondence of the selenium XAFS spectrum for the Elkhorn/Hazard coal "HYM" fraction with that for arsenical pyrite. The same relationship was also noted for the Illinois #6 coal. This similarity can only arise from the fact that selenium and arsenic both substitute for sulfur in the pyrite structure in the bituminous coals and hence have very similar

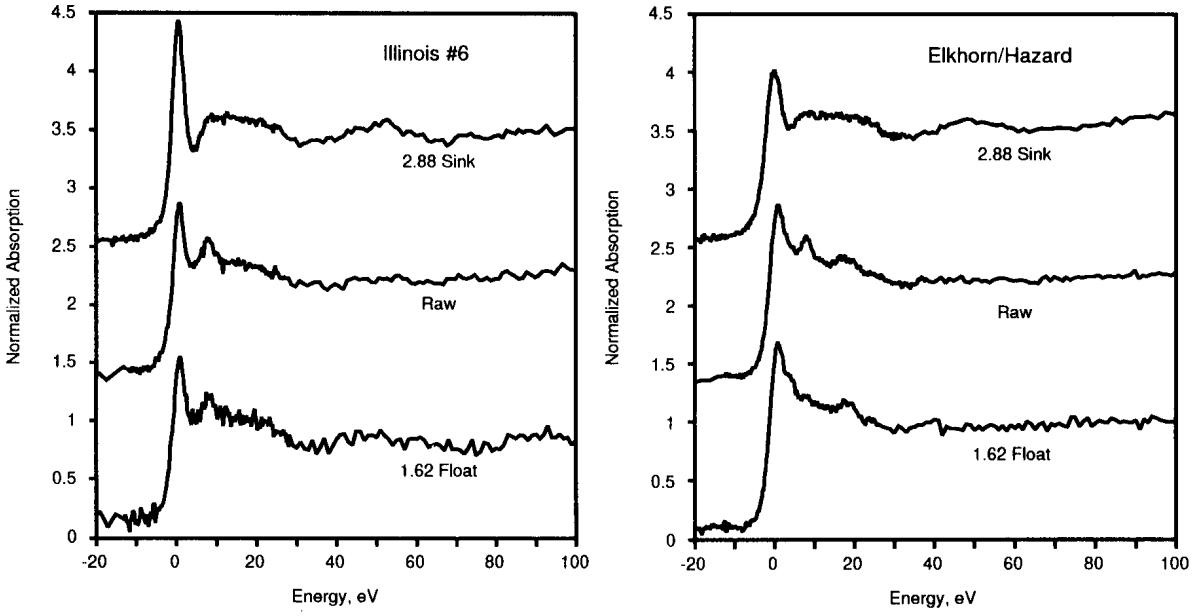

Illinois #6

	Se	Pyrite
1.62 Float	0.8	0.5
Raw Coal	1.0	1.0
1.62 Sk/2.88 Fl		6.9
2.88 Sink	5.0	24.0

Elkhorn/Hazard

	Se	Pyrite
1.62 Float	0.9	0.8
Raw Coal	1.0	1.0
1.62 Sk/2.88 Fl		2.8
2.88 Sink	2.0	87.0

D-6007

Figure 3-31 Selenium XANES spectra for Elkhorn/Hazard and Illinois #6 coals and fractions. Tables list relative step-height and pyritic sulfur variation.

local structures. The other fractions for the Illinois #6 coal exhibit similar, but weaker selenium XANES spectra, suggesting that the main occurrence of selenium in the Illinois #6 coal is as selenical pyrite (Se/pyrite). In addition, the "RAW" and "ORG" fractions show a weak peak at about 8 ev above the selenium K-edge; this peak indicates the presence of a small fraction of selenate, (SeO_4^{3-}). In similar fashion to the formation of arsenate, it is likely that selenate is formed from Se/pyrite due to oxidation. However, the selenate peak is not nearly so strong as the arsenate peak, suggesting that the oxidation of Se/pyrite to selenate occurs significantly more slowly than As/pyrite to arsenate. For the Elkhorn/Hazard coal, the selenium XANES spectrum from the "ORG" spectrum is different from that for Se/pyrite and must arise predominantly from a different selenium form, most likely an organoselenium form. Note also that the selenium concentration, as measured by the step-height (Figure 3-33), shows a relatively weak correlation with pyritic sulfur for the Elkhorn/Hazard coal, but a much stronger one for the Illinois #6 coal. Again, this difference would be consistent with a significant organoselenium occurrence for the Elkhorn/Hazard coal.

The selenium XANES spectrum for the Wyodak coal is shown in Figure 3-34. This spectrum appears different from any of those of the bituminous coals and fractions discussed

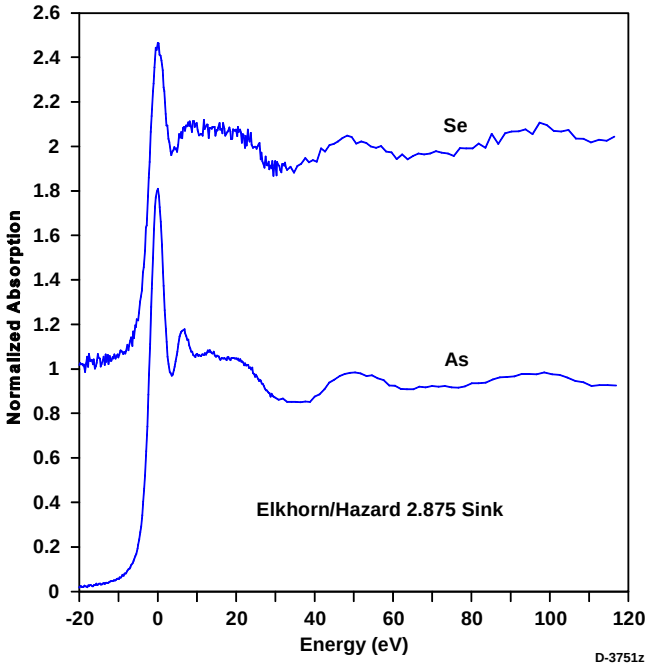

Figure 3-32 Comparison of arsenic and selenium XANES spectra for the Elkhorn/Hazard "HYM" fraction

above, although the peak position and the overall shape does resemble that for the "ORG" fraction of the Elkhorn/Hazard coal. In view of the fact that virtually all the sulfur in the Wyodak coal is organic, it might be anticipated that the principal selenium form will also be organic.

In summary, selenium in the four project coals is estimated to occur as follows:

- Elkhorn/Hazard: 20 to 40% Se/pyrite, 60-80% organic selenium, 5% selenate
- Pittsburgh: no data
- Illinois #6: 60 to 80% Se/pyrite, 20 to 40% organic selenium, 10% selenate
- Wyodak: 100% organic selenium?

Chlorine

Chlorine XANES of the three bituminous coals are shown in Figure 3-35. Except for the Illinois #6 coal, the spectra are identical to those reported previously for other U.S. bituminous coals (Huggins and Huffman, 1995). The Illinois #6 coal, although similar to the other two coals, exhibits a split main peak that may well be related to the unusually low level (340 ppm) of chlorine present in this coal. It would appear that chlorine occurs in the bituminous coals as chloride anions with some degree of attachment to the maceral surface, as has been concluded in previous studies (Huggins and Huffman, 1995).

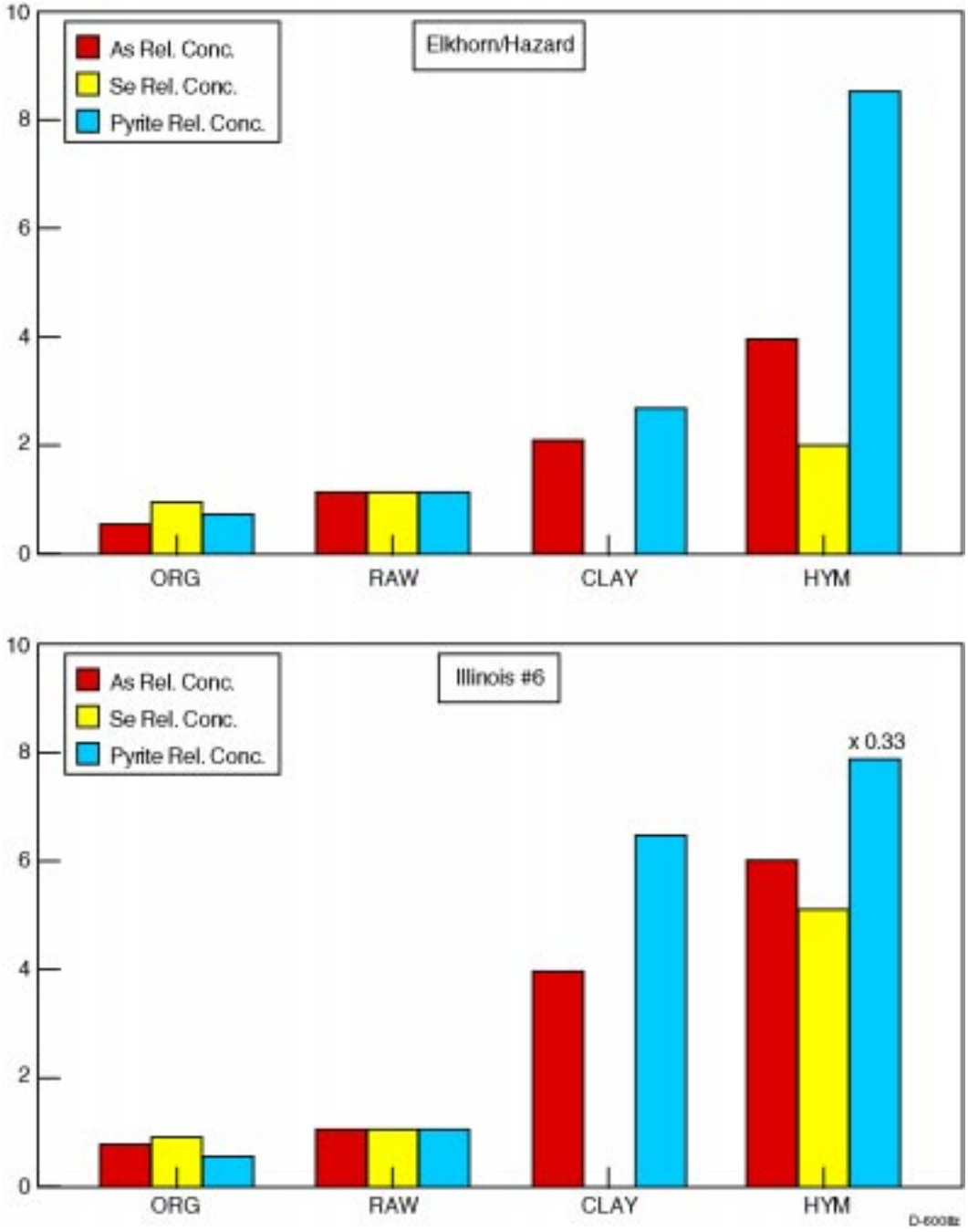

Figure 3-33 Comparison of As and Se step-heights and wt% pyritic sulfur for Elkhorn/Hazard and Illinois #6 coals

An attempt was made to record the chlorine XAFS spectrum of the Wyodak coal. However, the edge step was so weak that no fine structure could be discerned. The chlorine content of this coal is estimated to be at least an order of magnitude less than that for the Illinois #6 coal or no more than about 30 ppm.

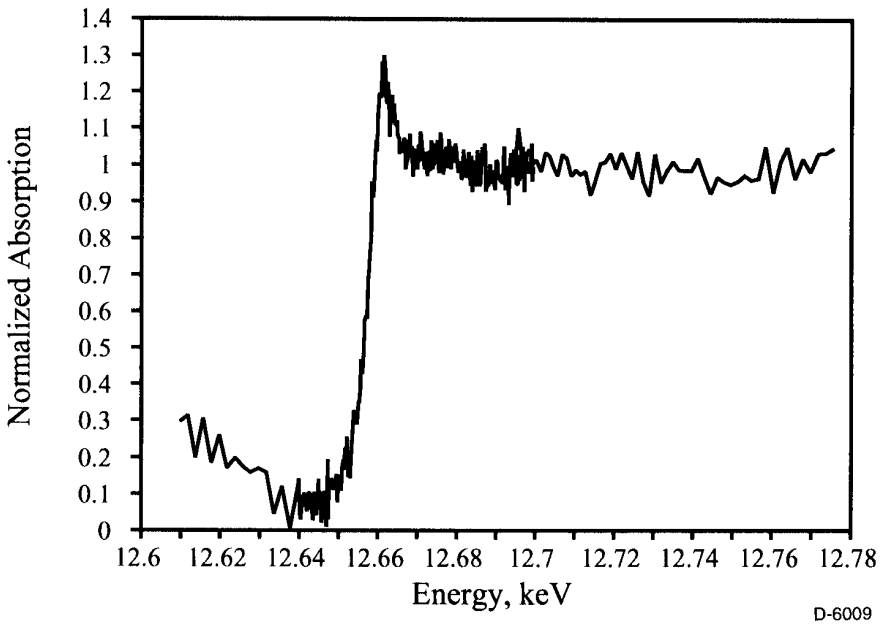

Figure 3-34 Selenium XANES spectrum for the Wyodak coal

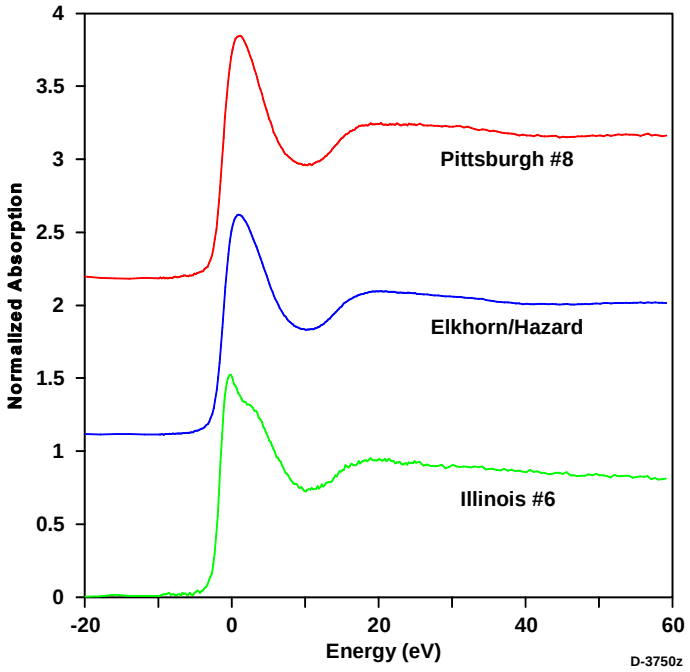

Figure 3-35 Chlorine XANES spectra for the three project bituminous coals.

In summary, chlorine occurs in the project coals as follows:

- Elkhorn/Hazard: 100% chloride anions in maceral moisture
- Pittsburgh: 100% chloride anions in maceral moisture
- Illinois #6: 100% chloride anions in maceral moisture
- Wyodak: insufficient concentration

Zinc

Zinc XAFS spectra were recorded from the Illinois #6 coal and its fractions because of the unusually high concentration of zinc (70 ppm) reported for this coal in comparison to the other bituminous coals, which have zinc concentrations close to the "average" value of 17 ppm for U.S. coals (Table 3-10). The zinc XANES spectra for the three bituminous coals are shown in Figure 3-36 and the zinc XANES for fractions of Illinois #6 coal are shown in Figure 3-37. The zinc XANES spectrum of the "HYM" fraction can be identified as arising from zinc sulfide (sphalerite, ZnS) and this spectrum is clearly a major component in the spectra of the "CLAY" and "RAW" fractions as well. However, the spectrum of the "ORG" fraction is clearly dominated by some other form of zinc. For the Elkhorn/Hazard and Pittsburgh coals, there is little or no evidence for the presence of any sphalerite in either coal based on the spectra shown in Figure 3-36. At this time, we are unable to identify the zinc form or forms that give rise to the spectra of the Pittsburgh and Elkhorn/Hazard coals or to the spectrum of the "ORG" fraction derived from the Illinois #6 coal. No examination of the zinc edge in the Wyodak coal has been performed.

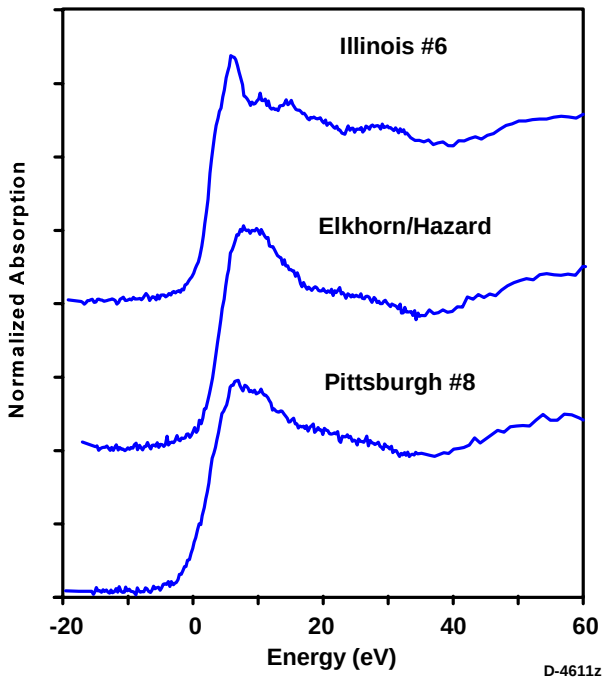

Figure 3-36 Zinc XANES spectra of the three project bituminous coals.

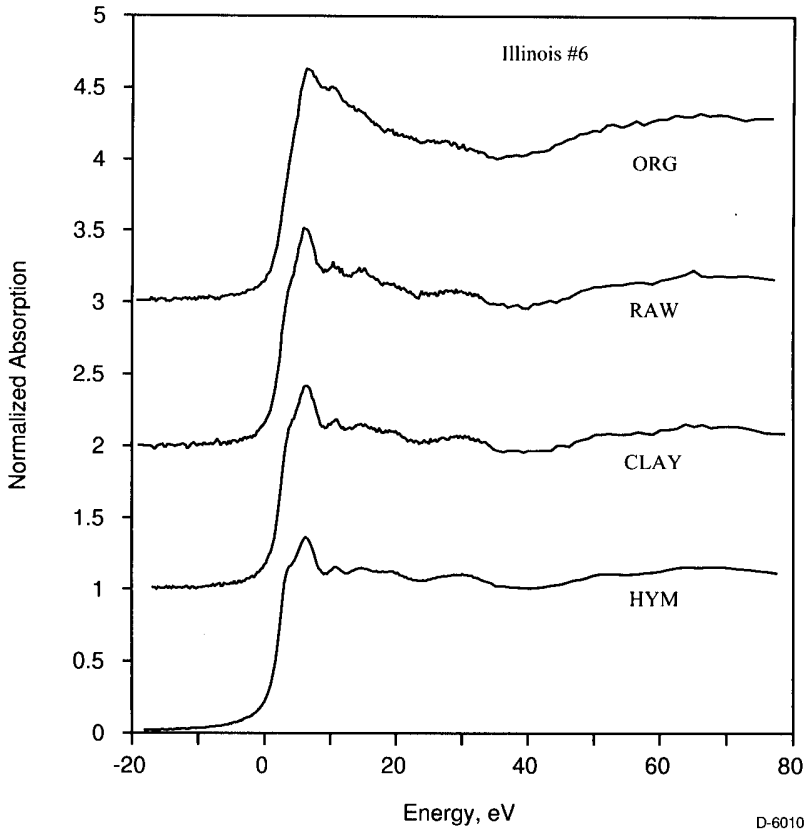

Figure 3-37 Zinc XANES spectra of Illinois #6 coal and fractions

In summary, zinc occurs in the project coals as follows:

- Elkhorn/Hazard: Unidentified form(s)
- Pittsburgh: Unidentified form(s)
- Illinois #6: Mainly ZnS, minor unidentified form(s)
- Wyodak: Not examined

Other Elements

Some preliminary data have been obtained on manganese and nickel. Figure 3-38 shows the manganese XANES spectra of the as received Elkhorn/Hazard and Pittsburgh coals. It would appear that manganese probably occurs in a number of forms in these two coals because the spectra do not resemble any individual manganese mineral or standard that we have examined previously (Huggins and Huffman, 1996a; Huggins and Huffman, 1996b). It is possible that a carbonate form is a major form of manganese in the Pittsburgh coal, as its spectrum has some features in common with that obtained from manganese in calcite.

Some testing of "HYM" fractions at the nickel K-edge was done for the three bituminous coals to see if the nickel was enriched in the "HYM" fractions in order to establish whether or not

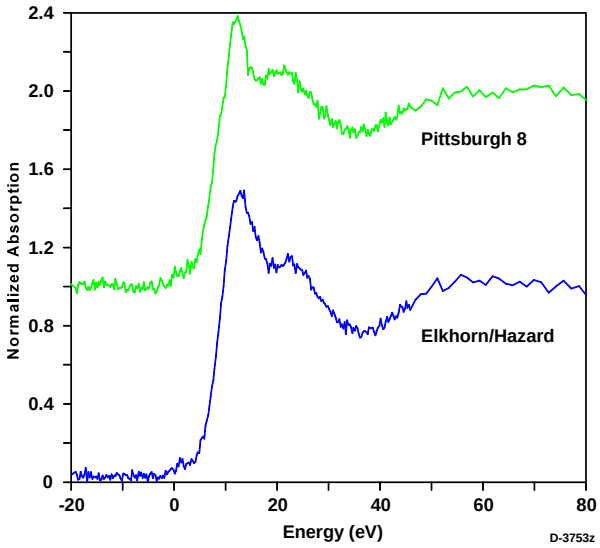

Figure 3-38 Manganese XANES spectra for the Elkhorn/Hazard and Pittsburgh coals

there was an association of nickel with pyrite. In actual fact, the spectra were not very strong at all, indicating if anything, the lack of an association between nickel and pyrite.

Sulfur

Sulfur XANES spectra of all four coals were obtained in the course of the investigation and fitted according to the procedure described elsewhere (Huffman et al., 1991). An example of a fitted sulfur K-edge spectrum is shown in Figure 3-39 for the Wyodak coal. The different sulfur forms derived from this analysis are listed in Table 3-17. This information was obtained in order to interpret the sulfur XANES spectra of chars derived from the project coals that were used for mercury sorption experiments (see Section 3.3.4).

3.5.3 *XAFS Spectroscopy of High Mercury Coal*

One element for which virtually no XAFS data exists is mercury. To rectify this situation, XAFS data were obtained in the course of this study on mercury standard compounds and minerals, and also on high-mercury coals. We were able to complete an XAFS investigation of a coal that contains almost 10 ppm of mercury and we acknowledge the cooperation of M. Brownfield and R. Finkelman, U.S. Geological Survey, who were able to supply us with this particular sample from Washington State. As was done for the program coals, "ORG", "CLAY", and "HYM" fractions were prepared for XAFS analysis from the raw coal using float/sink procedures. The coal and related fractions were examined at the Stanford Synchrotron Radiation Laboratory at the L_{III} edge of mercury, which occurs at about 12,284 eV.

The mercury XANES spectra of the "RAW" coal and of a number of mercury standard compounds measured in transmission are shown in Figure 3-40. As is common with most

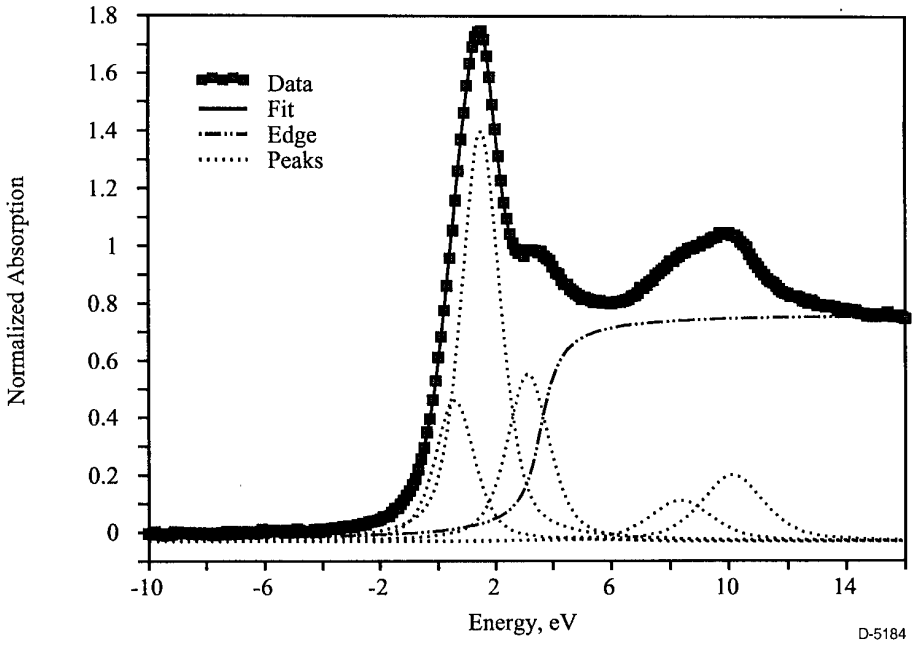

Figure 3-39 Least-squares fitted sulfur XANES spectrum of the as-received Wyodak coal

Table 3-17 Wt% Sulfur Forms in Project Coals from Sulfur XANES data

	Elk./Hazard	Pittsburgh	Illinois #6	Wyodak
Pyr. sulfur*	0.14	0.80	1.40	0.03
Org. sulfide	0.20	0.21	0.91	0.11
Thiophene	0.51	0.98	1.28	0.3
Oxid. Organic	0.01	0.01	0.04	0.00
Sulfate	0.04	0.00	0.04	0.02
Total (wt%)	0.91	2.01	3.67	0.46

*from Mössbauer spectroscopy (Tables 3-6 to 3-9)

mercury compounds, the fine structure associated with the absorption edge is rather weak and to accentuate the differences, the first derivatives of the spectra are also shown. None of the spectra of the standards is an exact match for the spectrum of the coal. The closest standard would appear to be the red form of HgS (cinnabar); however, some of the fine structure present in the spectrum of HgS (red) is definitely not present in the coal spectrum. The spectra of the coal and the three fractions are compared in Figure 3-41. As can be seen from this figure, the spectra of all four samples are virtually the same, implying that mercury exists predominantly in a single form in this coal.

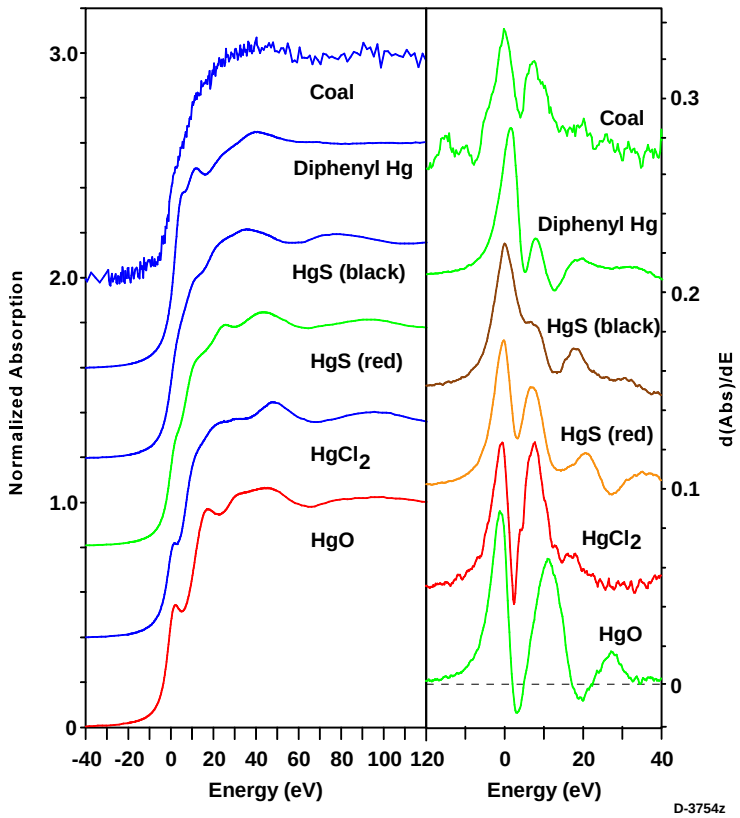

Figure 3-40. Comparison of the mercury L_{III} XANES spectra and their 1st derivatives for a high mercury coal from near Seattle, WA, and for various mercury standards

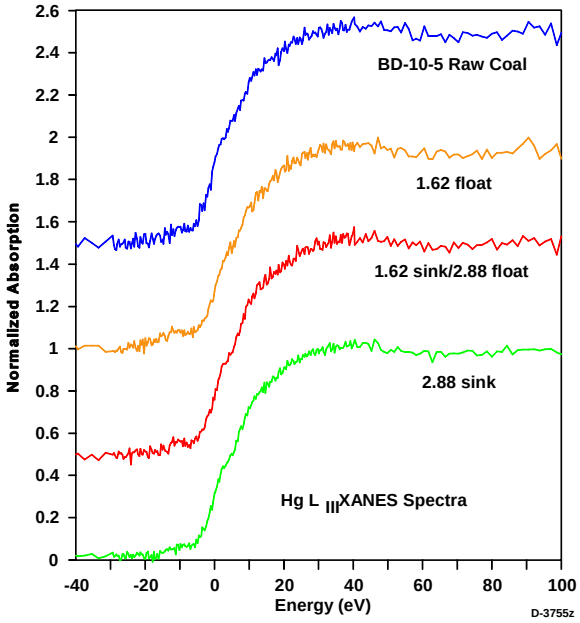

Figure 3-41. Mercury L_{III} XANES spectra for high mercury coal from Washington and fractions

Mössbauer studies of the high-mercury coal and fractions have also been obtained for comparison with the mercury XAFS data. These results are summarized in Table 3-18. It would appear that the iron is found exclusively in this sample of coal in the form of pyrite and its oxidation products. Both ferrous (szomolnokite, $FeSO_4.H_2O$) and ferric (jarosite) sulfates are present in minor amounts (< 10% of the total iron) in all samples. Figure 3-42 shows a

Table 3-18. Mössbauer Data for Sample BD-10-5 and Fractions from John Henry Mine No. 1, near Seattle, WA

(i)	Sample BD-10-5 As Rec'd Coal:				
MK2319	Abs	I.S.	Q.S.	%Fe	Spyr
MK2360	Pyrite	0.30	0.60	83	1.95
	Szomol.	1.26	2.71	9	
	Jarosite	0.36	1.09	8	
(ii)	BD-10-5 1.6 (PCE) float:				
MK2361	Abs	I.S.	Q.S.	%Fe	Spyr
	Pyrite	0.29	0.61	85	1.47
	Szomol.	1.27	2.71	9	
	Jarosite	0.34	1.15	6	
(iii)	BD-10-5 1.6 Sink/2.875 Float:				
MK2389	Abs	I.S.	Q.S.	%Fe	Spyr
	Pyrite	0.29	0.61	86	6.65
	Szomol.	1.25	2.77	9	
	Jarosite	0.38	1.05	5	
(iv)	BD-10-5 2.875 (Bromo) Sink:				
MK2386	Abs	I.S.	Q.S.	%Fe	Spyr
	Pyrite	0.31	0.62	91	22.0
	Szomol.	1.26	2.70	4	
	Melant.	1.25	3.20	5	

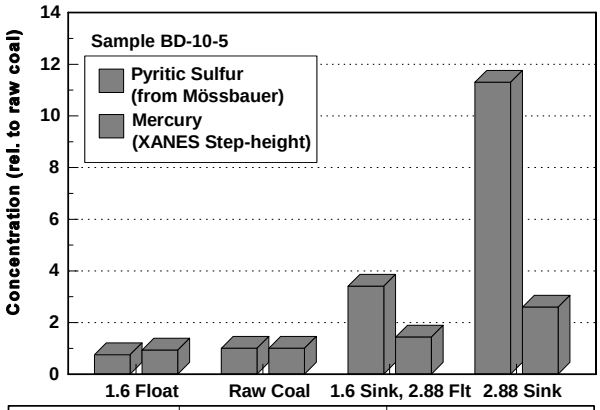

Sample BD-10-5	Wt% Pyritic Sulfur (from Mössbauer)	Mercury (XANES Step-height)
1.6 Float	1.47	0.93
Raw Coal	1.95	1.00
1.6 Sink, 2.88 Flt	6.65	1.43
2.88 Sink	22.00	2.59

Figure 3-42. Comparison of relative mercury concentration (estimated from XAFS step-height) and pyrite concentrations (from Mössbauer data, Table 3-18)

comparison of the mercury edge-step, a rough measure of the mercury concentration, and the wt% pyritic sulfur in the coal and fractions. Although both the mercury and pyrite concentrations vary in the same order in the suite of samples, the change in pyrite concentration is much larger, by about a factor of 5, than the change in mercury concentration. One interpretation of this trend is that the mercury is no more than 20% associated with the pyrite. A second alternative, as was suggested above for arsenic in the program coals, is that there may be two distinct generations of pyrite in the coal: one that does not contain any mercury, and one that is significantly enriched in mercury. Of these two generations, the mercury-bearing generation is only poorly separated by the float/sink processing, whereas the mercury-free generation is efficiently separated by the same processes. Thirdly, of course, there may be no relationship between mercury and pyrite at all.

In summary, this work shows that in this particular coal, mercury appears to exist in a single, sulfide-like form but that the form is NOT cinnabar (red HgS) nor meta-cinnabar (black HgS), nor any of the other common mercury forms shown in Figure 3-40. In addition, there is only a relatively weak association between mercury and pyrite. One possible explanation is that mercury exists only in a certain type of pyrite that does not separate well in float/sink tests, whereas the pyrite that does separate well in float/sink tests is basically free of mercury. Alternatively, mercury is not associated with pyrite but exists in an as yet unidentified form.

SECTION 4

CONCLUSIONS

4. CONCLUSIONS

This work represents the most comprehensive attempt to determine forms of occurrence of trace metals in coal to date, using diverse analytical methods: XAFS, Mössbauer, electron microprobe and selective leaching analyses. As Table 4-1 indicates, there was remarkably good agreement between the methods used by the University of Kentucky and the USGS in identification of forms of occurrence. Se, As, and Hg are commonly associated with pyrite grains in the coal, although not exclusively. Other mineral associations or organic associations were also observed as described below.

Table 4-1. Forms of Occurrence of Selected Trace Elements in Phase I Coals

		Elkhorn-Hazard	Pittsburgh	Illinois No. 6	Wyodak
Arsenic	UKy	60% pyrite 40% arsenate	88% pyrite 12% arsenate	85% pyrite 15% arsenate	50% carboxyl 50% arsenate
	USGS	65% pyrite 30% arsenate 5% clay	80% pyrite 10% arsenate 10% clay	60% pyrite 20% arsenate 20% clay	35% arsenate 15% silicate 50% other
Chromium	UKy	70-85% CrOOH 10-20% illite 5% spinel	50-70% CrOOH 30-50% illite	80-90% CrOOH 10-20% illite	>80% carboxyl
	USGS	some detected in silicate clays (20-25%)	silicate clays carbonate/ sulfide pyrite?	some detected in silicate clays (20-25%)	N.D.*
Selenium	UKy	20-40% pyrite 60-80% organic 5% selenate	N.D.*	60-80% pyrite 20-40% organic 10% selenate	100% organic
	USGS	20% pyrite 65% organic 15% sulfide	90% pyrite 5% organic 5% sulfide	50% pyrite 50% organic	90% organic
Mercury	UKy	N.D.*	N.D.*	N.D.*	N.D.*
	USGS	oxidized pyrite or soluble sulfide?	oxidized pyrite or soluble sulfide?	N.D.*	N.D.*

* N.D. = Not determined

Arsenic was almost entirely associated with pyrite in the three bituminous coals, although a significant amount of the pyrite (and arsenic) in the Elkhorn/Hazard coal appears to have been oxidized. Excellent agreement between the University of Kentucky and the USGS was obtained. Arsenic in the Wyodak coal appeared to be split between mineral (iron oxides or clays) and organic associations.

Selenium was entirely associated with pyrite in the Pittsburgh coal, but split between pyrite and an organic form in the Illinois 6 and Elkhorn/Hazard coals. Selenium appeared to be

organically associated in the Wyodak coal. Determination of mercury proved difficult for the USGS. Poor mass balance closure in the leaching analysis precluded a definite conclusion,

SECTION 5

REFERENCES

5. REFERENCES

ASTM (American Society for Testing and Minerals), 1993, Annual Book of ASTM Standards.Vol. 5.05 Gaseous Fuels, Coal and Coke. Philadelphia, PA, 526 pp.

Bool, L.E., III, and Helble, J.J., "A laboratory study of the partitioning of the trace elements during pulverized coal combustion", Energy and Fuels, 9, p. 880-997 (1995).

Bragg, L.J., Oman, J.K., Tewalt, S., Oman, C.L., Rega, N.H., Washington, P.M., and Finkelman, R.B., U. S. Geological Survey Open-File Report, 94-205, 35Mb CD-ROM, (1994).

Brown, G.E., Calas, G., Waychunas, G.A., and Petiau, J., in: Spectroscopic Methods in Mineralogy and Geology, Mineralogical Society of America, Reviews in Mineralogy Series, Vol. 18, Chapter 11, 431-512, (1988).

Cramer, S.P, Tench, O., Yocum, N., and George, G.N., Nucl. Instrum. Meth**.**, A266, p.586-591, (1988).

Eisenberger, P., and Kincaid, B.M., Science, 200, p.1441-1447, (1978).

Finkelman, R.B., Fuel Proc. Technol**.**, 39, p.21-34, (1994).

Finkelman, R.B. Palmer, C.A., Krasnow, M.R., Aruscavage, P.J. Sellers, G.A., and Dulong, F.T., "Combustion and leaching behavior of elements in Argonne Premium Coal Samples", Energy and Fuels 4(5), p.755-766 (1990).

Given. P.H. and Miller, R.N., Geochim. et Cosmochim**. Acta**, 51, p.1843-1853, (1987).

Huffman, G.P., and Huggins, F.E., Fuel, 57, p.592-604, (1978).

Huffman, G.P., and Huggins, F.E., in Chemistry of Low-Rank Coals, (ed. H. H. Schobert), American Chemical Society, Symposium Series, Vol. 264, 159-174, (1984).

Huffman, G.P., Huggins, F.E., Shah, N., and Zhao, J., Fuel Proc. Technol**.**, 39, p.47-62, (1994).

Huggins, F.E., and Huffman, G.P., Analytical Methods for Coal and Coal Products, Vol. III, (ed. C. Karr, Jr.), Academic Press, Chapter 50, 371-423, (1979).

Huggins, F.E., and Huffman, G.P., Coal and Coal Products: Analytical Characterization Techniques, (ed. E. L. Fuller, Jr.), ACS Symposium Series, Vol. 205, American Chemical Society, 239-258, (1982).

Huggins, F.E., and Huffman, G.P., Fuel, 74, p.556-569, (1995).

Huggins, F.E., and Huffman, G.P., Int. J. Coal Geol**.**, 32, p.31-53, (1996a).

Huggins, F.E., and Huffman, G.P., in Mineral Spectroscopy: A Tribute to Roger G. Burns, (eds. M. D. Dyar, C. A. McCammon, and M. W. Schaefer), The Geochemical Society, Special Publication No. 5, 133-151, (1996b).

Huggins, F.E., Shah, N.,. Zhao, J., Lu, F., and Huffman, G.P., Energy & Fuels, 7(4), p.482-489, (1993).

Huggins, F.E., Sri Kantapura, S., Parekh, B.K., Blanchard, L., and Robertson, J.D., Energy and Fuels 10, p. 691-701 (1997a).

Huggins, F.E., Zhao, J., Shah, N., Lu, F., Huffman, G.P., Bool, L.E. III, and Senior, C.L., in Proceedings 9th International Conference on Coal Science, Elsevier, in press (1997b).

Hurt, R., Davis, K., Yang, N., and Hardesty, D., "The origin and properties of unburned carbon from pulverized coal combustion", Report to EPRI, EPRI TR-105743, Project 8005, 1995

Koningsberger, D.C. and Prins, R., X-ray Absorption. Principles, Applications, Techniques of EXAFS, SEXAFS, and XANES, J. Wiley & Sons, (1988).

Lee, P.A., Citrin, P.H., Eisenberger, P.A., and Kincaid, B.M., Rev. Mod. Phys., 53, p.769-808, (1981).

Lee, R.J., Huggins, F.E., and Huffman, G.P., Scanning Electron Microscopy/1978/I, (ed. O. Johari), SEM Inc., 561-568, (1978).

Lytle, F.W., Greegor, R.B., Sandstrom, D.R., Marques, E.C., Wong, J.,. Spiro, C.L., . Huffman, G.P., and Huggins, F.E., Nucl. Instrum. Meth., 226, p.542-548, (1984).

Miller, R.N. and Given, P.H., Geochim. et Cosmochim. Acta, 50, p. 2033-2043, (1986)

Palmer, C.A., Krasnow, M.R., Finkelman, R.B., and D'Angelo, W.M., "An evaluation of leaching to determine modes of occurrence of selected toxic elements in coal", Journal of Coal Quality 12 (4) 135-141 (1993).

Shah, A., *Ph. D. Thesis*, University of Kentucky, (1996)

Shah, N., G. P. Huffman, F. E. Huggins, and A. Shah, in Inorganic Transformations and Ash Deposition During Combustion, (Proceedings, Engineering Foundation Conference, Palm Coast, FL), (ed. S. A. Benson), American Society of Mechanical Engineers, 179-190, (1992).

Stern, E.A., and S. M. Heald, Rev. Sci. Instrum., 50, p.1579-1582, (1979).

Swaine,D.J. Trace Elements in Coal, Butterworths, London, 1990.

APPENDIX A
CCSEM Data for Raw Coals

SAMPLE PSI PITT#8 COAL 3 2
RUN 1 DATE 25-JUN-96 SUMMARY 104 TOTAL 1199

AVERAGE SPECIES COMPOSITION

#	MINERAL SPECIES	Na	Mg	Al	Si	P	S	Cl	K	Ca	Ti	Fe	Weight %
142	Quartz	0.	0.	0.	98.	0.	1.	0.	1.	0.	0.	0.	11.1
133	Kaolinite	0.	0.	46.	53.	0.	1.	0.	1.	0.	0.	0.	9.2
122	Illite	0.	0.	30.	53.	0.	4.	0.	11.	0.	1.	1.	12.8
7	K-Feldspar	0.	0.	20.	52.	0.	2.	0.	23.	0.	1.	2.	1.4
1	Chlorite	0.	9.	20.	32.	0.	0.	0.	0.	3.	0.	36.	0.0
8	Montmorillonite	10.	0.	19.	67.	0.	0.	1.	0.	2.	0.	0.	0.4
291	Misc. Silicates	0.	0.	30.	58.	0.	5.	0.	4.	1.	0.	0.	28.8
152	Pyrite	0.	0.	0.	0.	0.	64.	0.	0.	0.	0.	36.	18.0
11	Misc. sulf.	0.	0.	1.	4.	0.	50.	0.	0.	22.	0.	23.	0.2
1	Apatite	0.	0.	0.	0.	26.	5.	3.	0.	61.	5.	0.	0.1
1	Misc. Phosphate	0.	0.	44.	0.	37.	5.	0.	0.	14.	0.	0.	0.0
2	Fe-rich	0.	0.	0.	0.	0.	0.	0.	0.	0.	0.	100.	0.6
51	Calcite	0.	1.	0.	0.	0.	0.	0.	0.	98.	0.	0.	6.0
28	Mixed Carbonate	0.	4.	0.	2.	17.	2.	0.	0.	72.	0.	2.	2.3
3	Ti oxide	0.	0.	0.	0.	1.	0.	0.	0.	2.	97.	0.	0.1
1	Ti-rich	0.	0.	0.	11.	0.	0.	0.	3.	0.	86.	0.	0.0
1	Trace-comp	10.	0.	0.	8.	0.	22.	0.	0.	33.	0.	0.	0.1
9	Quartz-Sulfate	0.	0.	4.	56.	0.	32.	2.	5.	0.	0.	0.	0.2
3	Quartz-Pyrite	0.	0.	0.	47.	0.	36.	0.	0.	0.	0.	17.	0.0
62	Sil-sulf	0.	0.	26.	41.	0.	26.	1.	3.	1.	1.	0.	2.2
4	Silicate-Pyrite	0.	0.	16.	28.	0.	32.	0.	5.	1.	0.	16.	0.3
1	Alumina-rich	0.	0.	100.	0.	0.	0.	0.	0.	0.	0.	0.	0.1
127	Misc. Mixed	1.	0.	18.	35.	2.	17.	2.	5.	17.	1.	2.	5.9
1161	GRAND TOTALS	0.	0.	19.	44.	1.	16.	0.	3.	9.	0.	8.	100.0

WEIGHT DISTRIBUTION

Size Ranges (Microns)

0 MINERAL SPECIES	WT. %	0.1 2.5	2.5 5.0	5.0 10.0	10. 20.	20. 40.	40. 80.	80. 500.
Quartz	11.1	10.	38.	21.	19.	3.	3.	7.
Kaolinite	9.2	3.	38.	23.	30.	5.	1.	0.
Illite	12.8	30.	51.	10.	6.	1.	1.	0.
Misc. Silicates	28.8	28.	53.	10.	5.	2.	1.	0.
Pyrite	18.0	3.	0.	14.	10.	16.	34.	23.
Calcite	6.0	2.	65.	13.	8.	5.	8.	0.
Misc. Mixed	5.9	62.	29.	5.	1.	2.	0.	0.
MINOR MINERALS	8.1	47.	34.	9.	6.	2.	1.	0.
GRAND TOTALS	100.0	21.	38.	13.	10.	5.	8.	5.

SAMPLE PSI ILLINOIS #6 COAL 3 2
RUN 1 DATE 28-JUN-96 SUMMARY 112 TOTAL 1199

AVERAGE SPECIES COMPOSITION

#	MINERAL SPECIES	Na	Mg	Al	Si	P	S	Cl	K	Ca	Ti	Fe	Weight %
144	Quartz	0.	0.	0.	99.	0.	1.	0.	0.	0.	0.	0.	12.8
68	Kaolinite	0.	0.	46.	53.	0.	1.	0.	0.	0.	0.	0.	5.4
97	Illite	0.	0.	27.	53.	0.	5.	0.	11.	0.	0.	2.	11.1
4	K-Feldspar	0.	0.	16.	51.	0.	12.	2.	17.	2.	0.	0.	0.1
2	Chlorite	0.	0.	19.	30.	0.	5.	0.	1.	0.	0.	45.	0.2
1	Montmorillonite	0.	0.	20.	77.	0.	0.	0.	0.	3.	0.	0.	0.0
273	Misc. Silicates	0.	0.	19.	64.	0.	9.	0.	6.	0.	0.	1.	22.9
3	Elem. Sulfur	0.	0.	0.	0.	0.	73.	10.	8.	0.	0.	0.	0.0
260	Pyrite	0.	0.	0.	0.	0.	65.	0.	0.	0.	0.	35.	29.8
2	Ferrous Sulfate	0.	0.	0.	0.	0.	49.	0.	0.	0.	0.	51.	0.2
1	Gypsum	0.	0.	0.	0.	0.	47.	0.	0.	53.	0.	0.	0.0
24	Misc. sulf.	0.	0.	1.	8.	0.	67.	0.	1.	0.	0.	24.	1.5
3	Fe-rich	0.	0.	0.	0.	0.	0.	0.	0.	0.	0.	100.	0.3
53	Calcite	0.	0.	0.	0.	0.	0.	0.	0.	100.	0.	0.	3.2
7	Mixed Carbonate	0.	0.	0.	5.	7.	5.	0.	0.	68.	0.	14.	0.7
1	Ti oxide	0.	0.	0.	0.	0.	0.	0.	0.	0.	100.	0.	0.1
1	Ti-rich	0.	0.	0.	0.	0.	36.	0.	0.	0.	64.	0.	0.1
73	Quartz-Sulfate	0.	0.	4.	58.	0.	33.	0.	3.	1.	1.	0.	3.7
4	Quartz-Pyrite	0.	0.	0.	39.	0.	39.	0.	0.	2.	0.	20.	0.7
109	Sil-sulf	0.	0.	18.	40.	0.	30.	0.	8.	1.	1.	2.	4.1
4	Silicate-Pyrite	0.	0.	16.	44.	0.	21.	0.	9.	0.	0.	9.	0.3
56	Misc. Mixed	0.	0.	18.	38.	2.	23.	1.	8.	4.	0.	5.	2.7
1190	GRAND TOTALS	0.	0.	11.	42.	0.	27.	0.	3.	4.	0.	12.	100.0

WEIGHT DISTRIBUTION

0 MINERAL SPECIES	WT. %	Size Ranges (Microns) 0.1 2.5	2.5 5.0	5.0 10.0	10. 20.	20. 40.	40. 80.	80. 500.
Quartz	12.8	3.	29.	34.	24.	1.	0.	7.
Kaolinite	5.4	2.	15.	31.	43.	6.	3.	0.
Illite	11.1	8.	48.	19.	21.	1.	2.	0.
Misc. Silicates	22.9	18.	41.	26.	13.	2.	0.	0.
Pyrite	29.8	2.	17.	20.	40.	13.	4.	3.
MINOR MINERALS	18.0	38.	23.	14.	14.	5.	4.	1.
GRAND TOTALS	100.0	13.	29.	23.	25.	6.	2.	2.

SAMPLE PSI ELKHORN/HAZARD 3 2
RUN 1 DATE 26-JUN-96 SUMMARY 108 TOTAL 1199

AVERAGE SPECIES COMPOSITION

#	MINERAL SPECIES	Na	Mg	Al	Si	P	S	Cl	K	Ca	Ti	Fe	Weight %
122	Quartz	0.	0.	0.	99.	0.	1.	0.	0.	0.	0.	0.	12.0
281	Kaolinite	0.	0.	45.	52.	0.	1.	0.	1.	0.	0.	0.	25.8
195	Illite	0.	0.	31.	52.	0.	2.	0.	11.	0.	1.	2.	14.5
3	K-Feldspar	0.	0.	17.	58.	0.	1.	0.	18.	0.	2.	5.	0.3
1	Montmorillonite	0.	0.	27.	61.	0.	8.	0.	0.	4.	0.	0.	0.0
383	Misc. Silicates	0.	0.	34.	55.	0.	4.	0.	4.	1.	1.	1.	29.2
31	Pyrite	0.	0.	1.	1.	0.	64.	0.	0.	0.	0.	35.	6.1
2	Chalcopyrite	0.	0.	0.	0.	0.	52.	0.	0.	0.	0.	25.	0.5
8	Misc. sulf.	0.	0.	4.	8.	1.	50.	0.	3.	6.	0.	28.	0.4
2	Apatite	0.	0.	2.	0.	27.	0.	1.	0.	70.	0.	0.	0.3
7	Misc. Phosphate	0.	1.	1.	46.	30.	0.	3.	0.	17.	2.	0.	1.5
7	Fe-rich	0.	0.	0.	0.	0.	0.	0.	0.	4.	0.	96.	1.1
4	Calcite	0.	0.	0.	3.	0.	0.	0.	0.	97.	0.	0.	0.8
9	Mixed Carbonate	0.	0.	0.	0.	16.	4.	0.	0.	55.	0.	24.	1.6
1	Ti oxide	0.	0.	0.	0.	0.	0.	0.	0.	0.	100.	0.	0.2
7	Ti-rich	0.	0.	1.	9.	0.	7.	0.	0.	0.	67.	13.	0.9
3	Quartz-Sulfate	0.	0.	0.	39.	0.	31.	19.	11.	0.	0.	0.	0.1
1	Quartz-Pyrite	0.	0.	7.	24.	0.	45.	0.	0.	0.	0.	23.	0.6
29	Sil-sulf	0.	0.	26.	40.	0.	26.	4.	1.	0.	1.	0.	0.5
6	Silicate-Pyrite	0.	0.	16.	23.	0.	28.	1.	4.	1.	0.	26.	0.2
1	Alumina-rich	0.	0.	93.	0.	0.	5.	0.	0.	0.	0.	0.	0.1
81	Misc. Mixed	0.	0.	24.	34.	2.	13.	3.	2.	9.	1.	10.	3.4
1184	GRAND TOTALS	0.	0.	27.	51.	1.	7.	0.	3.	3.	1.	5.	100.0

WEIGHT DISTRIBUTION

0 MINERAL SPECIES	WT. %	Size Ranges (Microns) 0.1 2.5	2.5 5.0	5.0 10.0	10. 20.	20. 40.	40. 80.	80. 500.
Quartz	12.0	10.	24.	16.	12.	10.	5.	24.
Kaolinite	25.8	6.	30.	15.	29.	10.	7.	1.
Illite	14.5	16.	24.	28.	14.	8.	10.	0.
Misc. Silicates	29.2	31.	26.	20.	15.	3.	4.	0.
Pyrite	6.1	8.	22.	15.	41.	7.	7.	0.
MINOR MINERALS	12.4	31.	39.	12.	6.	4.	2.	5.
GRAND TOTALS	100.0	19.	28.	18.	19.	7.	6.	4.

Wyodak Coal

AVERAGE SPECIES COMPOSITION

#	MINERAL SPECIES	Na	Mg	Al	Si	P	S	Cl	K	Ca	Ti	Fe	Weight %
300	Quartz	0.	0.	0.	99.	0.	0.	0.	0.	0.	0.	0.	26.7
192	Kaolinite	0.	0.	47.	51.	0.	0.	0.	0.	1.	0.	0.	19.1
110	Illite	0.	0.	30.	54.	0.	0.	0.	10.	2.	1.	1.	8.0
3	K-Feldspar	0.	0.	15.	62.	0.	0.	0.	18.	2.	0.	2.	1.5
27	Montmorillonite	0.	0.	26.	62.	0.	2.	0.	0.	6.	2.	0.	2.2
301	Misc. Silicates	0.	0.	27.	61.	0.	2.	0.	3.	3.	1.	1.	29.0
4	Pyrite	0.	0.	0.	0.	0.	63.	0.	0.	0.	0.	35.	0.9
3	Ferrous Sulfate	0.	0.	0.	1.	0.	52.	0.	0.	2.	1.	43.	0.1
1	Chalcopyrite	0.	0.	0.	0.	0.	55.	0.	0.	0.	0.	22.	0.2
7	Misc. sulf.	0.	0.	0.	3.	0.	49.	0.	1.	6.	8.	31.	0.7
23	Misc. Phosphate	0.	0.	33.	2.	28.	0.	0.	0.	34.	1.	1.	2.5
5	Fe-rich	0.	0.	0.	0.	0.	1.	0.	0.	1.	0.	98.	0.4
1	Calcite	0.	0.	0.	0.	0.	0.	0.	0.	100.	0.	0.	0.1
5	Mixed Carbonate	0.	0.	2.	3.	6.	1.	1.	0.	32.	2.	53.	0.3
4	Ti oxide	0.	0.	0.	0.	0.	0.	0.	0.	6.	93.	0.	0.4
4	Ti-rich	0.	0.	4.	17.	0.	5.	0.	0.	13.	60.	0.	0.3
1	Sil-sulf	0.	0.	18.	44.	0.	20.	0.	0.	17.	0.	0.	0.1
1	Silicate-Pyrite	0.	0.	28.	28.	0.	23.	0.	0.	11.	0.	10.	0.1
1	Alumina-rich	0.	0.	100.	0.	0.	0.	0.	0.	0.	0.	0.	0.1
129	Misc. Mixed	0.	0.	29.	28.	7.	7.	1.	1.	23.	2.	0.	7.4
1122	GRAND TOTALS	0.	0.	23.	63.	1.	2.	0.	2.	4.	1.	2.	100.0

WEIGHT DISTRIBUTION

Size Ranges (Microns)

MINERAL SPECIES	WT. %	0.1	2.5	5.0	10.	20.	40.	80.
		2.5	5.0	10.0	20.	40.	80.	500.
Quartz	26.7	8.	21.	16.	23.	12.	10.	10.
Kaolinite	19.1	24.	33.	16.	21.	4.	1.	0.
Illite	8.0	11.	17.	23.	36.	8.	5.	0.
Misc. Silicates	29.0	38.	35.	12.	9.	5.	2.	0.
Misc. Mixed	7.4	56.	27.	12.	5.	0.	0.	0.
MINOR MINERALS	9.9	42.	29.	14.	9.	5.	1.	0.
GRAND TOTALS	100.0	27.	28.	15.	17.	7.	4.	3.

APPENDIX B
Chemical Analysis by NAA for Coal Size and Density Fractions

	COAL1		COAL2		COAL3	
Element	ILH90106 heavy(bottom)	+/-	ILL90106 light(top)	+/-	PittL4563 light(top 4563)	+/-
ppm						
Na	310	20	290	20	460	30
Sc	2.1	0.1	1.9	0.1	1.7	0.1
Cr	14	1	13	1	8.5	0.4
Fe	23000	1000	6700	300	6900	300
Co	3.7	0.2	2.7	0.2	3	0.2
Zn	130	20	7.7	1.9	9.3	1.9
As	4.1	0.4	1.2	0.1	3	0.3
Se	1.7	0.4	1.1	0.3	0.45	0.16
Br	3.5	0.9	3.8	1	17	5
Rb	11	2	8.5	1.6	4.8	1.3
Mo	5.4	1.2	4.7	1	0.85	0.21
Cd	0.17	0.14	0.11	0	0.19	0
Sb	0.45	0.04	0.35	0.03	0.28	0.02
Cs	0.64	0.11	0.76	0.12	0.45	0.09
Ba	26	10	30	9	84	12
La	3.7	0.2	3.2	0.2	4.3	0.3
Ce	7.6	0.4	6.4	0.3	7.5	0.37
Sm	0.79	0.07	0.69	0.06	0.72	0.06
Eu	0.23	0.05	0.17	0.05	0.15	0.05
Yb	0.48	0.08	0.42	0.07	0.36	0.06
Lu	0.072	0.016	0.079	0.017	0.053	0.012
Au*	0.29	0	0.1	0.06	0.2	0.09
Hg	0.18	0.01	0.068	0.01	0.071	0.019
Th	1.4	0.1	1.4	0.1	1.2	0.1
U	1.5	0.1	1.7	0.1	0.23	0.02

* ng/g

	COAL4		COAL5		COAL6	
Element	PittM4563 medium(middle)	+/-	PittM90106 medium(middle)	+/-	PittL90106 light(top)	+/-
ppm						
Na	450	30	480	30	490	30
Sc	1.7	0.1	1.7	0.1	1.6	0.1
Cr	8.3	0.3	7.8	0.3	8.4	0.4
Fe	7200	300	4400	200	3900	200
Co	2.5	0.1	1.9	0.1	2.2	0.2
Zn	6.7	1.1	8.7	2.5	5.6	2.9
As	3.3	0.4	1.8	0.2	1.5	0.2
Se	0.41	0.12	0.96	0.56	1.1	0.6
Br	17	5	18	5	18	5
Rb	4.6	0.8	5.3	1.3	3.5	1.3
Mo	1	0.2	0.91	0.22	0.71	0.17
Cd	0.19	0	0.057	0.035	0.055	0.033
Sb	0.25	0.02	0.21	0.02	0.2	0.02
Cs	0.35	0.06	0.42	0.1	0.38	0.09
Ba	92	10	90	12	83	12
La	4.4	0.3	4.5	0.3	4.5	0.3
Ce	7.4	0.4	8.2	0.4	7.8	0.4
Sm	0.72	0.06	0.71	0.06	0.71	0.06
Eu	0.24	0.04	0.14	0.04	0.12	0.04
Yb	0.34	0.06	0.4	0.07	0.34	0.06
Lu	0.06	0.013	0.055	0.012	0.054	0.012
Au*	0.33	0	0.17	0.07	0.13	0.09
Hg	0.09	0.02	0.061	0.019	0.045	0.013
Th	1.1	0.1	1.2	0.1	1.1	0.1
U	0.25	0.02	0.31	0.02	0.3	0.02

* ng/g

	COAL7		COAL8		COAL9	
Element	ILM4563 medium(middle)	+/-	PittH4563 heavy(bottom)	+/-	ILH4563 heavy(bottom)	+/-
ppm						
Na	320	20	380	20	290	19
Sc	2.1	0.1	1.4	0.1	1.9	0.1
Cr	14	1	6.6	0.3	13	1
Fe	11000	1000	14000	1000	14000	1000
Co	2.8	0.2	2.3	0.2	2.9	0.2
Zn	67	9	14	3	71	10
As	1.9	0.2	6.1	0.6	2.5	0.2
Se	1.8	0.6	0.87	0.33	1.2	0.4
Br	3.8	1	13	3	3	0.8
Rb	7.7	1.5	3.8	1.3	8.4	1.7
Mo	4.3	0.9	0.63	0.15	3.9	0.9
Cd	0.098	0.075	0.45	0.21	0.29	0.16
Sb	0.36	0.03	0.31	0.02	0.35	0.03
Cs	0.87	0.14	0.43	0.1	0.85	0.14
Ba	29	9	98	11	23	9
La	3.4	0.2	3.7	0.2	3.2	0.2
Ce	7.3	0.4	6.6	0.3	6.4	0.3
Sm	0.74	0.06	0.62	0.05	0.69	0.06
Eu	0.23	0.05	0.17	0.03	0.19	0.04
Yb	0.46	0.08	0.28	0.05	0.42	0.07
Lu	0.085	0.019	0.047	0.01	0.078	0.017
Au*	0.42	0.15	0.36	0.14	0.55	0.21
Hg	0.073	0.018	0.13	0.01	0.085	0.012
Th	1.5	0.1	0.99	0.06	1.3	0.1
U	1.9	0.1	0.15	0.01	0.94	0.03

* ng/g

	COAL10		COAL11		COAL12	
Element	PittH90106 heavy(bottom)	+/-	ILL4563 light(top)	+/-	IL106 (d>106)	+/-
ppm						
Na	540	30	320	20	300	20
Sc	1.8	1.1	2	0.1	2	0.1
Cr	9.4	0.4	15	1	15	1
Fe	30000	1000	10000	1000	8300	300
Co	3.8	0.2	2.6	0.2	2.5	0.2
Zn	6.3	2.1	27	4	45	7
As	16	2	1.8	0.2	1.6	0.2
Se	2.1	0.6	1.7	0.5	1.1	0.3
Br	15	4	3.6	1	3.4	0.9
Rb	6	1.7	10	2	11	2
Mo	1.3	0.3	3.7	0.8	5.3	1.2
Cd	0.031	0	0.066	0	0.12	0.09
Sb	0.47	0.04	0.34	0.03	0.43	0.03
Cs	0.65	0.15	0.68	0.12	0.74	0.12
Ba	76	14	43	9	50	8
La	5.2	0.3	3.3	0.2	3.7	0.2
Ce	9.9	0.5	6.9	0.4	8.4	0.4
Sm	0.86	0.07	0.74	0.06	0.77	0.07
Eu	0.23	0.05	0.21	0.04	0.12	0.03
Yb	0.47	0.08	0.46	0.08	0.47	0.08
Lu	0.067	0.015	0.089	0.019	0.13	0.03
Au*	0.23	0.19	0.9	0.37	0.35	0.19
Hg	0.28	0.02	0.065	0.016	0.048	0.011
Th	1.3	0.1	1.5	0.1	1.6	0.1
U	0.18	0.02	1.4	0.1	2	0.1

* ng/g

	COAL13		COAL14		COAL15	
Element	ILM90106 medium(middle)	+/-	KY53 (45<d<63)	+/-	KY85 (38<d<45)	+/-
ppm						
Na	320	20	220	10	280	20
Sc	2.1	0.1	3.6	0.2	3.8	0.2
Cr	16	1	15	1	16	1
Fe	7500	300	2400	100	3500	100
Co	2.7	0.2	6.7	0.4	5.2	0.3
Zn	13	3	17	2	16	2
As	1.3	0.1	3.4	0.3	3.7	0.4
Se	1.3	0.4	2.2	0.5	3	0.7
Br	3.8	1	28	7	30	8
Rb	10	2	4.2	0.8	4.1	1.1
Mo	5	1.1	3.8	0.8	3.9	0.9
Cd	0.049	0	0.32	0.2	0.46	0.26
Sb	0.41	0.03	0.94	0.07	0.96	0.07
Cs	0.75	0.13	0.36	0.07	0.16	0.06
Ba	44	11	85	9	130	10
La	3.5	0.2	12	1	13	1
Ce	7.5	0.4	24	1	25	1
Sm	0.78	0.07	2.3	0.2	2.4	0.2
Eu	0.19	0.04	0.35	0.05	0.46	0.07
Yb	0.48	0.08	1.5	0.2	1.4	0.2
Lu	0.11	0.02	0.21	0.04	0.22	0.05
Au*	0.51	0.28	0.6	0.2	0.51	0.22
Hg	0.048	0.012	0.1	0.02	0.15	0.03
Th	1.6	0.1	3.9	0.2	4.3	0.3
U	1.8	0.1	1.5	0.1	3.6	0.1

* ng/g

	COAL16		COAL17		COAL19	
Element	KY35 (63<d<75)	+/-	KY8 (d<38)	+/-	KY6 (d>106)	+/-
ppm						
Na	210	20	380	30	170	10
Sc	3.6	0.2	3.8	0.2	3.1	0.2
Cr	15	1	24	1	12	1
Fe	2600	100	3500	100	1400	100
Co	6.6	0.4	6.1	0.3	6.1	0.3
Zn	4.5	1.1	44	5	6.7	1.5
As	3.5	0.4	5.1	0.5	1.3	0.2
Se	2.2	0.5	3.4	0.8	1.9	0.5
Br	25	7	23	6	19	5
Rb	3.9	1	8.3	1.4	3.6	0.9
Mo	3.7	0.8	3.5	0.8	3	0.7
Cd	0.58	0.36	0.41	0.26	0.25	0.18
Sb	0.9	0.07	1	0.1	0.71	0.05
Cs	0.27	0.08	0.41	0.09	0.32	0.07
Ba	85	13	190	20	78	9
La	13	1	13	1	11	1
Ce	25	1	25	1	21	1
Sm	2.4	0.2	2.4	0.2	2	0.2
Eu	0.41	0.06	0.37	0.05	0.32	0.04
Yb	1.3	0.2	1.3	0.2	1.1	0.2
Lu	0.2	0.04	0.2	0.04	0.18	0.04
Au*	0.76	0.27	0.99	0.25	0.55	0.14
Hg	0.094	0.023	0.066	0.029	0.026	0.018
Th	4	0.2	4.1	0.2	3.4	0.2
U	1.4	0.1	3.8	0.1	1.6	0.1

* ng/g

	COAL20		COAL21		COAL22	
Element	KY50 (75<d<90)	+/-	IL38 (d<38)	+/-	IL3845 (38<d<45)	+/-
ppm						
Na	310	20	500	30	340	20
Sc	3.4	0.2	2.7	0.2	2.1	0.1
Cr	17	1	17	1	14	1
Fe	2100	100	14000	1000	15000	1000
Co	6.6	0.4	3.9	0.2	3.1	0.2
Zn	8.6	1.7	87	10	94	11
As	3.6	0.4	2.4	0.2	2.6	0.3
Se	3	0.7	1.4	0.3	1.5	0.3
Br	22	6	3.9	1.1	4.2	1.1
Rb	4.8	1.1	18	2	11	2
Mo	3.3	0.7	3.4	0.7	3.7	0.8
Cd	0.24	0.14	0.19	0.09	0.15	0.11
Sb	0.91	0.07	0.37	0.03	0.39	0.03
Cs	0.13	0.06	1.3	0.2	0.84	0.11
Ba	82	10	66	8	36	8
La	12	1	5.6	0.4	3.6	0.2
Ce	22	1	11	1	6.9	0.3
Sm	2.2	0.2	1.1	0.1	0.8	0.07
Eu	0.29	0.04	0.22	0.04	0.16	0.03
Yb	1.2	0.2	0.57	0.09	0.47	0.08
Lu	0.2	0.04	0.1	0.02	0.085	0.018
Au*	0.35	0.12	0.66	0.19	0.8	0.26
Hg	0.037	0.016	0.081	0.014	0.076	0.018
Th	3.7	0.2	2.1	0.1	1.6	0.1
U	1.9	0.1	1.1	0.1	1.7	0.1

* ng/g

	COAL23		COAL24		COAL25	
Element	IL4563 (45<d<63)	+/-	IL6375 (63<d<75)	+/-	IL7590 (75<d<90)	+/-
ppm						
Na	310	20	230	20	310	20
Sc	2	0.1	1.8	0.1	2.1	0.1
Cr	13	1	14	1	15	1
Fe	14000	1000	9200	400	14000	1000
Co	2.9	0.2	2.1	0.1	3	0.2
Zn	97	11	110	10	55 ~~6.8~~	7 ~~6.7~~
As	2.4	0.3	1.9	0.2	2.2	0.2
Se	1.4	0.3	1.6	0.4	1.4	0.4
Br	3.6	1	3.6	1	3.9	1.1
Rb	12	2	7.3	1.2	10	2
Mo	3.5	0.8	2.5	0.6	3	0.7
Cd	0.12	0.07	0.23	0.22	0.29	0
Sb	0.36	0.03	0.44	0.04	0.4	0.03
Cs	0.75	0.1	0.65	0.11	0.82	0.12
Ba	34	6	33	7	32	7
La	3.3	0.2	2.6	0.2	3.5	0.2
Ce	6.6	0.3	6.7	0.3	7.2	0.4
Sm	0.73	0.06	0.71	0.06	0.78	0.07
Eu	0.16	0.03	0.15	0.03	0.17	0.03
Yb	0.43	0.07	0.1	0.07	0.47	0.08
Lu	0.081	0.017	0.077	0.069	0.08	0.02
Au*	0.22	0.11	0.17	0.1	0.14	0.13
Hg	0.084	0.011	0.051	0.012	0.065	0.019
Th	1.5	0.1	1.4	0.1	1.5	0.1
U	1.3	0.1	1.1	0.1	1.4	0.1

* ng/g

	COAL26		COAL18	
Element	IL90106 (90<d<106)	+/-	KY06 (90<d<106)	+/-
ppm				
Na	290	20	240	20
Sc	1.9	0.1	4.2	0.3
Cr	15	1	16	1
Fe	11000	1000	3400	100
Co	2.8	0.2	7.2	0.4
Zn	14	2	9.4	1.4
As	1.8	0.2	4.5	1.9
Se	1.8	0.5	2.9	0.8
Br	3.5	1	26	7
Rb	8.9	1.2	4.8	0.9
Mo	2.8	0.6	2.7	0.6
Cd	0.097	0	1	0.93
Sb	0.39	0.03	1	0.1
Cs	0.76	0.1	0.26	0.06
Ba	36	6	100	10
La	3.2	0.2	14	1
Ce	6.9	0.3	28	1
Sm	0.69	0.06	2.6	0.2
Eu	0.16	0.02		0.05
Yb	0.42	0.07	1.6	0.3
Lu	0.077	0.017	0.24	0.05
Au*	0.32	0.1	0.49	0.17
Hg	0.069	0.012	0.05	0.023
Th	1.4	0.1	4.7	0.3
U	1.4	0.1	1.9	0.1

* ng/g

APPENDIX C
CCSEM Data for Coal Size and Density Fractions

Pittsburgh Coal, 90-106 micron size cut, low density fraction

SAMPLE MIT PT L 90106 COAL 3 2
RUN 1 DATE 28-MAY-97 SUMMARY 104 TOTAL 1199

AVERAGE SPECIES COMPOSITION

#	MINERAL SPECIES	Na	Mg	Al	Si	P	S	Cl	K	Ca	Ti	Fe	Weight %
186	Quartz	0.	0.	0.	98.	0.	1.	0.	0.	0.	0.	0.	17.4
129	Kaolinite	0.	0.	46.	54.	0.	0.	0.	0.	0.	0.	0.	6.9
139	Illite	0.	0.	29.	54.	0.	4.	0.	12.	0.	0.	0.	13.9
3	K-Feldspar	0.	0.	18.	60.	0.	0.	0.	19.	0.	0.	3.	.1
3	Montmorillonite	5.	0.	20.	75.	0.	0.	0.	0.	0.	0.	0.	.0
403	Misc. Silicates	0.	0.	25.	65.	0.	4.	0.	3.	1.	1.	1.	34.3
171	Pyrite	0.	0.	0.	0.	0.	66.	0.	0.	0.	0.	34.	17.5
2	Ferrous Sulfate	0.	0.	0.	0.	0.	51.	0.	0.	0.	0.	49.	.2
28	Misc. sulf.	0.	0.	0.	2.	0.	66.	0.	0.	4.	0.	27.	1.7
3	Apatite	0.	0.	0.	0.	31.	0.	0.	0.	66.	3.	0.	.1
4	Misc. Phosphate	0.	0.	19.	12.	36.	0.	0.	0.	34.	0.	0.	.8
2	Fe-rich	0.	0.	0.	0.	0.	0.	0.	0.	0.	0.	100.	.3
17	Calcite	0.	0.	0.	0.	0.	0.	0.	0.	99.	0.	0.	1.0
7	Mixed Carbonate	0.	0.	1.	15.	1.	1.	0.	0.	82.	0.	0.	.5
6	Ti-rich	0.	0.	4.	8.	0.	5.	0.	0.	1.	82.	0.	2.0
9	Quartz-Sulfate	0.	0.	10.	64.	0.	25.	0.	1.	0.	0.	0.	.1
1	Quartz-Pyrite	0.	0.	0.	39.	0.	41.	0.	1.	0.	0.	19.	.0
35	Sil-sulf	0.	0.	23.	46.	0.	25.	0.	3.	1.	0.	0.	1.0
1	Silicate-Pyrite	0.	0.	14.	27.	0.	31.	0.	0.	0.	0.	29.	.0
1	Alumina-rich	0.	0.	100.	0.	0.	0.	0.	0.	0.	0.	0.	.0
49	Misc. Mixed	0.	0.	16.	40.	5.	12.	1.	2.	21.	2.	1.	2.1
1199	GRAND TOTALS	0.	0.	17.	52.	0.	15.	0.	3.	3.	2.	7.	100.0

WEIGHT DISTRIBUTION

MINERAL SPECIES	WT. %	Size Ranges (Microns) .2 2.5	2.5 5.0	5.0 10.0	10. 20.	20. 40.	40. 80.	80. 500.
Quartz	17.4	12.	53.	20.	13.	0.	1.	1.
Kaolinite	6.9	6.	16.	25.	37.	10.	4.	2.
Illite	13.9	18.	61.	14.	3.	1.	2.	0.
Misc. Silicates	34.3	28.	46.	13.	10.	1.	1.	0.
Pyrite	17.5	1.	14.	14.	39.	13.	17.	1.
MINOR MINERALS	10.0	31.	25.	10.	18.	4.	8.	4.
GRAND TOTALS	100.0	18.	40.	15.	17.	4.	5.	1.

Elkhorn/Hazard Coal, 90-106 micron size cut, low density fraction

SAMPLE MIT KY L 90106 COAL 3 2
RUN 1 DATE 29-MAY-97 SUMMARY 108 TOTAL 1199

AVERAGE SPECIES COMPOSITION

#	MINERAL SPECIES	Na	Mg	Al	Si	P	S	Cl	K	Ca	Ti	Fe	Weight %
103	Quartz	0.	0.	0.	98.	0.	1.	0.	0.	0.	0.	0.	7.1
190	Kaolinite	0.	0.	45.	53.	0.	1.	0.	0.	0.	0.	0.	12.7
230	Illite	0.	0.	31.	54.	0.	3.	0.	9.	0.	1.	1.	15.1
1	K-Feldspar	0.	0.	15.	44.	0.	9.	0.	19.	0.	0.	14.	.1
2	Chlorite	0.	0.	21.	25.	0.	2.	0.	0.	0.	0.	52.	.0
3	Montmorillonite	0.	0.	25.	55.	0.	0.	0.	0.	19.	0.	0.	.2
547	Misc. Silicates	0.	0.	33.	57.	0.	6.	0.	1.	0.	1.	1.	54.0
10	Pyrite	0.	0.	0.	0.	0.	66.	0.	0.	0.	0.	33.	1.6
9	Misc. sulf.	0.	0.	0.	5.	0.	56.	0.	0.	23.	2.	12.	.3
1	Apatite	0.	0.	1.	2.	29.	0.	2.	0.	65.	0.	0.	.0
2	Misc. Phosphate	0.	0.	17.	5.	30.	11.	0.	0.	31.	7.	0.	.1
2	Fe-rich	0.	0.	0.	0.	0.	0.	0.	0.	0.	0.	100.	.3
1	Calcite	0.	0.	0.	0.	0.	0.	0.	0.	100.	0.	0.	.0
5	Mixed Carbonate	0.	0.	1.	0.	12.	3.	1.	0.	83.	0.	0.	.5
3	Ti oxide	0.	0.	0.	0.	0.	0.	0.	0.	0.	100.	0.	.9
9	Ti-rich	0.	0.	2.	4.	0.	5.	0.	0.	0.	86.	0.	1.0
1	Trace-comp	0.	0.	0.	0.	0.	0.	0.	1.	0.	0.	64.	.4
2	Quartz-Sulfate	0.	0.	6.	70.	0.	25.	0.	0.	0.	0.	0.	.1
20	Sil-sulf	0.	0.	28.	46.	0.	25.	0.	0.	0.	0.	0.	1.0
1	Silicate-Pyrite	0.	0.	21.	37.	0.	24.	0.	0.	0.	0.	18.	.1
2	Alumina-rich	0.	0.	95.	0.	0.	2.	0.	0.	0.	3.	0.	.8
55	Misc. Mixed	0.	0.	24.	36.	1.	16.	1.	0.	15.	1.	3.	3.8
1199	GRAND TOTALS	0.	0.	30.	54.	0.	6.	0.	2.	1.	3.	2.	100.0

WEIGHT DISTRIBUTION

MINERAL SPECIES	WT. %	Size Ranges (Microns) .2	2.5	5.0	10.	20.	40.	80.
		2.5	5.0	10.0	20.	40.	80.	500.
Quartz	7.1	6.	36.	34.	17.	3.	1.	3.
Kaolinite	12.7	7.	35.	7.	18.	11.	18.	5.
Illite	15.1	19.	27.	19.	20.	7.	7.	1.
Misc. Silicates	54.0	25.	53.	10.	7.	3.	1.	1.
MINOR MINERALS	11.1	33.	39.	9.	11.	4.	2.	1.
GRAND TOTALS	100.0	22.	44.	13.	12.	5.	4.	1.

Illinois No.6 Coal, 45-63 micron size cut, high density fraction

SAMPLE MIT IL H 4563 COAL 3 2
RUN 1 DATE 2-APR-97 SUMMARY 116 TOTAL 1199

AVERAGE SPECIES COMPOSITION

#	MINERAL SPECIES	Na	Mg	Al	Si	P	S	Cl	K	Ca	Ti	Fe	Weight %
126	Quartz	0.	0.	0.	98.	0.	2.	0.	0.	0.	0.	0.	12.1
46	Kaolinite	0.	0.	47.	50.	0.	2.	0.	1.	0.	0.	0.	3.7
90	Illite	0.	0.	27.	55.	0.	4.	0.	12.	0.	0.	1.	7.9
4	K-Feldspar	0.	0.	18.	48.	0.	7.	0.	20.	0.	0.	6.	.5
1	Montmorillonite	0.	0.	29.	59.	0.	10.	0.	0.	2.	0.	0.	.0
229	Misc. Silicates	0.	0.	22.	64.	0.	9.	0.	4.	0.	0.	1.	19.9
426	Pyrite	0.	0.	0.	0.	0.	65.	0.	0.	0.	0.	35.	42.5
6	Ferrous Sulfate	0.	0.	0.	1.	0.	49.	0.	0.	0.	0.	50.	1.1
2	Gypsum	0.	0.	0.	0.	0.	48.	0.	0.	52.	0.	0.	.1
32	Misc. sulf.	0.	0.	2.	5.	0.	66.	0.	0.	0.	0.	27.	2.0
1	Misc. chloride	0.	0.	0.	13.	0.	21.	66.	0.	0.	0.	0.	.1
4	Fe-rich	0.	0.	0.	0.	0.	1.	0.	0.	0.	0.	99.	.4
61	Calcite	0.	0.	0.	0.	0.	0.	0.	0.	100.	0.	0.	3.4
8	Mixed Carbonate	0.	2.	1.	6.	4.	7.	0.	0.	80.	0.	0.	.5
1	Trace-comp	24.	0.	13.	11.	0.	21.	0.	0.	0.	0.	0.	.0
19	Quartz-Sulfate	0.	1.	8.	52.	0.	34.	0.	4.	0.	0.	0.	.6
1	Quartz-Pyrite	0.	0.	0.	29.	0.	49.	0.	0.	0.	0.	21.	.0
46	Sil-sulf	0.	0.	25.	40.	0.	30.	0.	3.	0.	0.	0.	2.8
6	Silicate-Pyrite	0.	0.	16.	39.	0.	23.	0.	8.	0.	0.	13.	1.0
23	Misc. Mixed	0.	0.	19.	33.	0.	31.	1.	4.	2.	0.	6.	1.3
1132	GRAND TOTALS	0.	0.	10.	34.	0.	34.	0.	2.	4.	0.	17.	100.0

WEIGHT DISTRIBUTION

Size Ranges (Microns)

0 MINERAL SPECIES	WT. %	.1	2.5	5.0	10.	20.	40.	80.
		2.5	5.0	10.0	20.	40.	80.	500.
Quartz	12.1	3.	39.	30.	24.	2.	3.	0.
Illite	7.9	1.	31.	26.	35.	7.	2.	0.
Misc. Silicates	19.9	22.	32.	23.	11.	6.	5.	1.
Pyrite	42.5	1.	0.	8.	18.	27.	44.	2.
MINOR MINERALS	17.6	19.	19.	13.	15.	9.	24.	1.
GRAND TOTALS	100.0	8.	17.	16.	18.	15.	24.	1.

Elkhorn/Hazard Coal, 90-106 micron size cut, high density fraction

SAMPLE MIT KY H 90106 COAL 3 2
RUN 1 DATE 06-MAY-97 SUMMARY 104 TOTAL 1199

AVERAGE SPECIES COMPOSITION

#	MINERAL SPECIES	Na	Mg	Al	Si	P	S	Cl	K	Ca	Ti	Fe	Weight %
111	Quartz	0.	0.	0.	99.	0.	1.	0.	0.	0.	0.	0.	10.9
378	Kaolinite	0.	0.	46.	50.	0.	1.	0.	1.	0.	0.	1.	21.0
197	Illite	0.	0.	32.	53.	0.	3.	0.	10.	0.	1.	1.	12.8
2	K-Feldspar	0.	0.	16.	51.	0.	0.	0.	22.	0.	9.	2.	.1
1	Chlorite	0.	0.	16.	33.	0.	7.	0.	0.	0.	0.	44.	.0
3	Montmorillonite	10.	0.	19.	67.	0.	1.	0.	0.	4.	0.	0.	.2
380	Misc. Silicates	0.	0.	30.	58.	0.	4.	0.	2.	0.	4.	1.	41.0
31	Pyrite	0.	0.	0.	0.	0.	65.	0.	0.	0.	0.	35.	5.1
7	Gypsum	0.	0.	0.	0.	0.	47.	0.	0.	52.	0.	0.	.4
2	Misc. sulf.	0.	0.	0.	0.	0.	52.	0.	9.	0.	0.	39.	.2
2	Misc. Phosphate	0.	0.	12.	45.	35.	0.	0.	0.	7.	0.	0.	1.1
10	Fe-rich	0.	0.	0.	0.	0.	1.	0.	0.	1.	0.	98.	1.8
1	Calcite	0.	0.	0.	0.	0.	0.	0.	0.	100.	0.	0.	.2
8	Mixed Carbonate	0.	1.	0.	5.	1.	7.	0.	0.	60.	0.	25.	.9
9	Ti-rich	0.	0.	1.	9.	0.	2.	0.	0.	0.	88.	0.	2.1
7	Sil-sulf	0.	0.	22.	44.	0.	23.	3.	2.	0.	2.	0.	.2
5	Alumina-rich	0.	0.	76.	11.	5.	5.	0.	0.	0.	0.	2.	.2
27	Misc. Mixed	0.	0.	19.	35.	1.	8.	1.	2.	26.	3.	5.	1.8
1181	GRAND TOTALS	0.	0.	27.	54.	0.	6.	0.	2.	2.	4.	4.	100.0

WEIGHT DISTRIBUTION

0 MINERAL SPECIES	WT. %	Size Ranges (Microns) .2	2.5	5.0	10.	20.	40.	80.
		2.5	5.0	10.0	20.	40.	80.	500.
Quartz	10.9	5.	38.	14.	15.	2.	6.	19.
Kaolinite	21.0	1.	25.	17.	16.	12.	20.	10.
Illite	12.8	15.	49.	12.	2.	10.	12.	0.
Misc. Silicates	41.0	16.	52.	11.	7.	3.	5.	5.
Pyrite	5.1	0.	0.	4.	33.	3.	22.	37.
MINOR MINERALS	9.2	15.	31.	8.	7.	2.	7.	31.
GRAND TOTALS	100.0	10.	40.	12.	10.	5.	10.	11.

Pittsburgh Coal, 90-106 micron size cut, high density fraction

SAMPLE MIT PT H 90106 COALM 3 2
RUN 1 DATE 05-MAY-97 SUMMARY 120 TOTAL 1199

AVERAGE SPECIES COMPOSITION

#	MINERAL SPECIES	Na	Mg	Al	Si	P	S	Cl	K	Ca	Ti	Fe	Weight %
106	Quartz	0.	0.	1.	96.	0.	2.	0.	0.	0.	0.	0.	7.1
175	Kaolinite	0.	0.	46.	51.	0.	1.	0.	1.	0.	0.	0.	7.0
100	Illite	0.	0.	30.	52.	0.	6.	0.	11.	0.	0.	0.	13.0
1	K-Feldspar	0.	0.	16.	57.	0.	4.	0.	18.	0.	0.	5.	.0
5	Montmorillonite	13.	0.	17.	66.	0.	0.	0.	3.	1.	0.	0.	.2
182	Misc. Silicates	0.	0.	18.	66.	0.	10.	0.	4.	0.	0.	1.	18.2
429	Pyrite	0.	0.	0.	0.	0.	65.	0.	0.	0.	0.	35.	36.9
2	Ferrous Sulfate	0.	0.	0.	0.	0.	52.	0.	0.	0.	0.	48.	.1
29	Misc. sulf.	0.	0.	2.	6.	0.	64.	0.	0.	0.	0.	29.	4.0
2	Misc. chloride	0.	0.	0.	13.	0.	5.	59.	5.	0.	7.	11.	.0
1	Apatite	0.	0.	0.	0.	29.	0.	0.	0.	71.	0.	0.	.0
5	Fe-rich	0.	0.	0.	0.	0.	1.	0.	0.	0.	0.	99.	.2
41	Calcite	0.	1.	0.	0.	0.	0.	0.	0.	99.	0.	0.	1.7
7	Mixed Carbonate	0.	0.	3.	9.	6.	0.	0.	0.	64.	0.	18.	.3
15	Quartz-Sulfate	0.	0.	3.	65.	0.	26.	0.	2.	0.	0.	4.	.4
5	Quartz-Pyrite	0.	0.	10.	54.	0.	26.	0.	0.	0.	0.	11.	2.0
33	Sil-sulf	0.	0.	17.	41.	0.	27.	0.	10.	0.	0.	4.	4.4
5	Silicate-Pyrite	0.	0.	15.	39.	0.	30.	1.	2.	1.	0.	12.	1.8
39	Misc. Mixed	0.	0.	15.	46.	1.	15.	1.	4.	7.	2.	4.	2.9
1182	GRAND TOTALS	0.	0.	12.	35.	0.	32.	0.	3.	2.	0.	15.	100.0

WEIGHT DISTRIBUTION

Size Ranges (Microns)

0 MINERAL SPECIES	WT. %	.1 2.5	2.5 5.0	5.0 10.0	10. 20.	20. 40.	40. 80.	80. 500.
Quartz	7.1	8.	59.	17.	7.	2.	5.	2.
Kaolinite	7.0	4.	25.	24.	38.	4.	5.	0.
Illite	13.0	30.	59.	6.	4.	1.	1.	0.
Misc. Silicates	18.2	38.	48.	7.	2.	2.	3.	1.
Pyrite	36.9	2.	0.	3.	7.	5.	37.	46.
MINOR MINERALS	17.8	30.	48.	3.	2.	2.	7.	7.
GRAND TOTALS	100.0	18.	31.	6.	7.	3.	16.	18.

SAMPLE PSI ELKHORN/HAZARD 3 2
RUN 1 DATE 26-JUN-96 SUMMARY 108 TOTAL 1199

AVERAGE SPECIES COMPOSITION

#	MINERAL SPECIES	Na	Mg	Al	Si	P	S	Cl	K	Ca	Ti	Fe	Weight %
122	Quartz	0.	0.	0.	99.	0.	1.	0.	0.	0.	0.	0.	12.0
281	Kaolinite	0.	0.	45.	52.	0.	1.	0.	1.	0.	0.	0.	25.8
195	Illite	0.	0.	31.	52.	0.	2.	0.	11.	0.	1.	2.	14.5
3	K-Feldspar	0.	0.	17.	58.	0.	1.	0.	18.	0.	2.	5.	0.3
1	Montmorillonite	0.	0.	27.	61.	0.	8.	0.	0.	4.	0.	0.	0.0
383	Misc. Silicates	0.	0.	34.	55.	0.	4.	0.	4.	1.	1.	1.	29.2
31	Pyrite	0.	0.	1.	1.	0.	64.	0.	0.	0.	0.	35.	6.1
2	Chalcopyrite	0.	0.	0.	0.	0.	52.	0.	0.	0.	0.	25.	0.5
8	Misc. sulf.	0.	0.	4.	8.	1.	50.	0.	3.	6.	0.	28.	0.4
2	Apatite	0.	0.	2.	0.	27.	0.	1.	0.	70.	0.	0.	0.3
7	Misc. Phosphate	0.	1.	1.	46.	30.	0.	3.	0.	17.	2.	0.	1.5
7	Fe-rich	0.	0.	0.	0.	0.	0.	0.	0.	4.	0.	96.	1.1
4	Calcite	0.	0.	0.	3.	0.	0.	0.	0.	97.	0.	0.	0.8
9	Mixed Carbonate	0.	0.	0.	0.	16.	4.	0.	0.	55.	0.	24.	1.6
1	Ti oxide	0.	0.	0.	0.	0.	0.	0.	0.	0.	100.	0.	0.2
7	Ti-rich	0.	0.	1.	9.	0.	7.	0.	0.	0.	67.	13.	0.9
3	Quartz-Sulfate	0.	0.	0.	39.	0.	31.	19.	11.	0.	0.	0.	0.1
1	Quartz-Pyrite	0.	0.	7.	24.	0.	45.	0.	0.	0.	0.	23.	0.6
29	Sil-sulf	0.	0.	26.	40.	0.	26.	4.	1.	0.	1.	0.	0.5
6	Silicate-Pyrite	0.	0.	16.	23.	0.	28.	1.	4.	1.	0.	26.	0.2
1	Alumina-rich	0.	0.	93.	0.	0.	5.	0.	0.	0.	0.	0.	0.1
81	Misc. Mixed	0.	0.	24.	34.	2.	13.	3.	2.	9.	1.	10.	3.4
1184	GRAND TOTALS	0.	0.	27.	51.	1.	7.	0.	3.	3.	1.	5.	100.0

WEIGHT DISTRIBUTION

Size Ranges (Microns)

0 MINERAL SPECIES	WT. %	0.1 2.5	2.5 5.0	5.0 10.0	10. 20.	20. 40.	40. 80.	80. 500.
Quartz	12.0	10.	24.	16.	12.	10.	5.	24.
Kaolinite	25.8	6.	30.	15.	29.	10.	7.	1.
Illite	14.5	16.	24.	28.	14.	8.	10.	0.
Misc. Silicates	29.2	31.	26.	20.	15.	3.	4.	0.
Pyrite	6.1	8.	22.	15.	41.	7.	7.	0.
MINOR MINERALS	12.4	31.	39.	12.	6.	4.	2.	5.
GRAND TOTALS	100.0	19.	28.	18.	19.	7.	6.	4.

Pittsburgh Coal, 90-106 micron size cut, high density fraction

SAMPLE MIT PT H 90106 COALM 3 2
RUN 1 DATE 05-MAY-97 SUMMARY 120 TOTAL 1199

AVERAGE SPECIES COMPOSITION

#	MINERAL SPECIES	Na	Mg	Al	Si	P	S	Cl	K	Ca	Ti	Fe	Weight %
106	Quartz	0.	0.	1.	96.	0.	2.	0.	0.	0.	0.	0.	7.1
175	Kaolinite	0.	0.	46.	51.	0.	1.	0.	1.	0.	0.	0.	7.0
100	Illite	0.	0.	30.	52.	0.	6.	0.	11.	0.	0.	0.	13.0
1	K-Feldspar	0.	0.	16.	57.	0.	4.	0.	18.	0.	0.	5.	.0
5	Montmorillonite	13.	0.	17.	66.	0.	0.	0.	3.	1.	0.	0.	.2
182	Misc. Silicates	0.	0.	18.	66.	0.	10.	0.	4.	0.	0.	1.	18.2
429	Pyrite	0.	0.	0.	0.	0.	65.	0.	0.	0.	0.	35.	36.9
2	Ferrous Sulfate	0.	0.	0.	0.	0.	52.	0.	0.	0.	0.	48.	.1
29	Misc. sulf.	0.	0.	2.	6.	0.	64.	0.	0.	0.	0.	29.	4.0
2	Misc. chloride	0.	0.	0.	13.	0.	5.	59.	5.	0.	7.	11.	.0
1	Apatite	0.	0.	0.	0.	29.	0.	0.	0.	71.	0.	0.	.0
5	Fe-rich	0.	0.	0.	0.	0.	1.	0.	0.	0.	0.	99.	.2
41	Calcite	0.	1.	0.	0.	0.	0.	0.	0.	99.	0.	0.	1.7
7	Mixed Carbonate	0.	0.	3.	9.	6.	0.	0.	0.	64.	0.	18.	.3
15	Quartz-Sulfate	0.	0.	3.	65.	0.	26.	0.	2.	0.	0.	4.	.4
5	Quartz-Pyrite	0.	0.	10.	54.	0.	26.	0.	0.	0.	0.	11.	2.0
33	Sil-sulf	0.	0.	17.	41.	0.	27.	0.	10.	0.	0.	4.	4.4
5	Silicate-Pyrite	0.	0.	15.	39.	0.	30.	1.	2.	1.	0.	12.	1.8
39	Misc. Mixed	0.	0.	15.	46.	1.	15.	1.	4.	7.	2.	4.	2.9
1182	GRAND TOTALS	0.	0.	12.	35.	0.	32.	0.	3.	2.	0.	15.	100.0

WEIGHT DISTRIBUTION

Size Ranges (Microns)

0 MINERAL SPECIES	WT. %	.1	2.5	5.0	10.	20.	40.	80.
		2.5	5.0	10.0	20.	40.	80.	500.
Quartz	7.1	8.	59.	17.	7.	2.	5.	2.
Kaolinite	7.0	4.	25.	24.	38.	4.	5.	0.
Illite	13.0	30.	59.	6.	4.	1.	1.	0.
Misc. Silicates	18.2	38.	48.	7.	2.	2.	3.	1.
Pyrite	36.9	2.	0.	3.	7.	5.	37.	46.
MINOR MINERALS	17.8	30.	48.	3.	2.	2.	7.	7.
GRAND TOTALS	100.0	18.	31.	6.	7.	3.	16.	18.

APPENDIX D
Microprobe Analyses of Pyrite in Raw Coals

Appendix D. Pyrite Analyses.							PITTSBURGH						
Date	Anal #	Se	Cu	Ni	As	Zn	Cd	Co	Fe	S	Total	Grain	Size (microns)/Form
3/22/97	64	dl	dl	0.01	dl	dl	dl	**dl**	45.28	51.14	96.46	PittsB.1	50x70 subhedral
	67	dl	dl	dl	dl	0.00	dl	**dl**	45.71	53.45	99.20	PittsC.1	100x120 composite-
	68	0.01	dl	dl	0.01	dl	dl	**dl**	45.77	51.78	97.60	PittsC.2	core
	69	0.01	dl	0.00	0.01	dl	dl	**dl**	45.14	52.76	97.96	PittsC.3	
	72	dl	dl	dl	0.00	dl	dl	**0.01**	45.10	51.93	97.08	PittsD.1	40x80 composite-core
	73	0.00	dl	dl	0.01	dl	dl	**dl**	44.66	51.58	96.29	PittsD.2	
	77	0.02	dl	dl	dl	dl	dl	**dl**	46.43	52.45	98.93	PittsE.1	30x70 subhedral
	78	dl	dl	0.02	dl	dl	dl	**dl**	44.91	52.70	97.66	PittsE.2	
	79	0.00	dl	dl	dl	dl	dl	**dl**	45.88	52.07	97.99	Pitts2.1	80x100 subhedral
	80	dl	dl	dl	0.09	dl	dl	**dl**	46.10	52.36	98.59	Pitts2.2	
	81	0.01	dl	0.01	0.01	dl	dl	**dl**	45.55	50.73	96.35	Pitts2.3	
	82	0.02	0.03	dl	0.02	0.01	dl	**dl**	45.16	51.11	96.39	Pitts3.1	40x40 euhedral
	83	dl	0.06	dl	0.01	dl	dl	**dl**	45.09	51.96	97.15	Pitts3.2	
	84	dl	dl	dl	dl	dl	dl	**dl**	44.67	51.52	96.22	Pitts4.1	20x20 euhedral
	85	dl	0.02	dl	0.02	dl	dl	**dl**	45.34	52.19	97.60	Pitts5.1	25x25 euhedral
													on framboid
	86	dl	0.01	dl	dl	dl	dl	**dl**	45.04	54.61	99.70	Pitts6.1	40x50 subhedral
	87	dl	0.03	dl	dl	0.01	dl	**dl**	44.60	51.84	96.50	Pitts6.2	
	88	dl	dl	dl	0.01	dl	dl	**dl**	45.17	50.34	95.54	PittsH.1	150x300 subhedral
	89	dl	dl	dl	0.00	dl	dl	**dl**	45.38	52.07	97.48	PittsH.2	
	90	dl	dl	dl	dl	dl	dl	**dl**	45.19	51.73	96.96	PittsH.3	
	91	dl	dl	dl	dl	dl	dl	**0.01**	45.44	50.66	96.14	PittsH.4	

	92	dl	dl	0.03	0.03	dl	dl	**0.01**	45.63	51.45	97.18	PittsI.1	60x100 composite
	93	dl	dl	0.07	0.02	dl	dl	**dl**	45.48	51.28	96.86	PittsI.2	
	96	0.01	dl	dl	dl	0.00	dl	**0.01**	45.80	51.48	97.33	PittsJ.1	100x110 subhedral
	97	dl	dl	dl	0.02	0.01	dl	**dl**	45.54	51.78	97.38	PittsJ.2	
						PITTSBURGH- continued							
Date	Anal #	Se	Cu	Ni	As	Zn	Cd	Co	Fe	S	Total	Grain	Size (microns)/Form
11/27/96	54		dl	dl	0.08	0.01	dl		45.22	50.75	96.06	Pitts.2.3	60x80 subhedral
	55		dl	dl	0.00	dl	dl		46.06	52.03	98.11	Pitts.3.1	60x60 euhedral
	56		dl	dl	dl	0.01	dl		46.26	52.32	98.60	Pitts.3.2	
	57		0.01	0.02	dl	dl	dl		46.04	52.30	98.36	Pitts.3.3	
	58		dl	dl	dl	dl	dl		45.62	51.23	96.85	Pitts.4.1	40x60 subhedral
	59		dl	dl	dl	dl	dl		45.74	52.10	97.84	Pitts.4.2	
	60		0.01	dl	0.01	dl	dl		45.88	51.34	97.24	Pitts.5.1	25x60 subh./irreg.
	61		dl	dl	dl	dl	dl		46.21	51.48	97.69	Pitts.5.2	
	62		dl	0.01	dl	dl	dl		46.69	52.66	99.36	Pitts.6.1	60x100 subh./irreg.
	63		dl	dl	dl	dl	dl		46.55	52.41	98.96	Pitts.6.2	
	64		dl	dl	0.01	dl	dl		46.39	52.06	98.46	Pitts.6.3	
	65		0.03	dl	dl	dl	dl		46.56	53.84	100.43	Pitts.7.1	120 euhedral
	66		dl	0.06	0.01	dl	dl		45.18	51.51	96.75	Pitts.7.2	
	67		dl	0.02	dl	dl	dl		45.92	51.93	97.86	Pitts.8.1	20x60 cleat?
	68		dl	dl	dl	dl	dl		46.18	51.99	98.17	Pitts.8.2	
	69		0.02	0.01	0.02	dl	dl		46.75	52.76	99.55	Pitts.9.1	15x70 cleat?
	70		dl	dl	0.02	0.01	dl		46.76	52.49	99.28	Pitts.9.2	

	71		dl	dl	0.00	dl	dl		46.61	52.08	98.70	Pitt.10.1	100x100 comp. euh.
	72		0.02	0.02	dl	dl	dl		46.55	52.51	99.10	Pitt.10.2	
	73		0.03	0.01	dl	0.01	dl		46.08	51.68	97.82	Pitt.10.3	
	76		0.19	dl	0.03	0.02	dl		45.98	52.17	98.39	Pitt.13.1	20 euhedral
10/19/96	30		dl	0.01	**0.13**				45.32	52.10	97.56	Pitt.1.1	20x40 subhedral
	31		dl	dl	**0.11**				45.28	51.57	96.95	Pitts.2.1	90 irreg. (round)
						PITTSBURGH -continued							
Date	Anal #	Se	Cu	Ni	As	Zn	Cd	Co	Fe	S	Total	Grain	Size (microns)/Form
10/19/96	33		0.02	0.01	**0.06**				44.06	51.78	95.93	Pitts.3.1	5x15 subhedral
continued													
	34		dl	0.01	**0.08**				44.88	53.07	98.04	Pitts.4.1	20 euhedral
	35		0.02	dl	**0.25**				45.32	52.03	97.61	Pitts.5.1	20x60 subhedral
	36		dl	dl	**0.16**				45.59	52.66	98.41	Pitts.5.2	
	37		0.02	0.01	**0.14**				45.88	52.84	98.90	Pitts.6.1	20 framboidal
	38		dl	dl	**0.12**				46.36	54.42	100.91	Pitts.7.1	50x60 irregular
	39		0.01	dl	**0.10**				45.78	53.70	99.59	Pitts.8.1	40x50 subhedral
	40		0.02	dl	**0.11**				45.63	53.38	99.13	Pitts.8.2	
	41		dl	0.05	**0.08**				43.50	54.30	97.93	Pitts.8.2	
	61		dl	dl	**0.08**				45.41	51.86	97.36	Pitts.9.1	50x60 subhedral
	62		dl	dl	**0.09**				45.19	51.77	97.05	Pitts.9.2	
	63		dl	dl	**0.12**				45.56	51.85	97.54	Pitts.10.1	20x30 euhedral
	64		0.02	dl	**0.10**				46.38	53.57	100.07	Pitts.11.1	25x40 subhedral

9/26/96	42		dl	dl	**0.12**				43.81	51.33	95.25	Pitts.1.3	60 irregular
	44		0.10	0.01	**0.05**				44.40	53.56	98.11	Pitts.3.1	20x20 subhedral
	45		0.11	dl	**0.07**				45.54	54.09	99.82	Pitts.3.2	
	47		dl	dl	**0.04**				45.80	54.60	100.44	Pitts.4.2	25x60 subhedral
	48		dl	dl	**dl**				45.89	54.44	100.36	Pitts.4.3	
	49		dl	dl	**0.08**				45.81	53.68	99.57	Pitts.5.1	40x60 subhedral
	50		dl	dl	**dl**				46.35	53.69	100.09	Pitts.5.2	
	51		dl	dl	**dl**				45.93	53.93	99.85	Pitts.5.3	
	56		0.01	dl	**dl**				44.34	51.48	95.83	Pitts.9.1	100x130 subhedral

PITTSBURGH- continued

Date	Anal #	Se	Cu	Ni	As	Zn	Cd	Co	Fe	S	Total	Grain	Size (microns)/Form
9/26/96	57		dl	dl	**0.06**				45.03	52.28	97.37	Pitts.9.2	
contd.	58		0.01	dl	**dl**				45.63	52.96	98.61	Pitts.9.3	
	59		dl	0.01	**0.06**				45.81	53.12	99.00	Pitts.9.4	
	60		0.02	dl	**dl**				45.22	52.34	97.62	Pitts.9.5	
	61		dl	dl	**0.06**				46.05	54.01	100.12	Pitt. 10.1	30x40 subhedral
	62		0.02	dl	**dl**				45.61	53.36	99.04	Pitts 10.2	
	63		0.01	0.02	**0.06**				44.18	51.86	96.12	Pitts 11.1	20 framboidal
	64		0.04	0.01	**0.06**				44.16	52.19	96.46	Pitts.12.1	10 euhedral on 11.1
	65		dl	0.01	**0.05**				44.88	52.52	97.46	Pitts.13.1	15x20 subhedral
	66		0.04	dl	**0.12**				45.36	53.28	98.79	Pitts.14.1	15x40 subhedral
	67		0.01	dl	**0.09**				45.10	53.26	98.45	Pitts.14.2	

	68		dl	dl	**0.06**				45.37	53.29	98.72	Pitts.15.1	20x30 subhedral
9/13/96	33		0.02	0.01	**0.12**				45.22	52.54	97.91	Pitts.1.1	25 irregular
	45		dl	dl	**0.13**				45.74	53.21	99.09	Pitts.7.2	25 irregular
	46		0.02	dl	**0.13**				45.44	51.67	97.26	Pitts.8.1	30 subhedral
	47		0.03	dl	**0.18**				46.16	53.36	99.73	Pitts.8.2	
	48		0.02	dl	**0.18**				46.04	53.72	99.96	Pitts.8.3	
	50		dl	0.00	**0.13**				45.60	51.51	97.24	Pitts.9.2	20 subhedral
	51		dl	dl	**0.08**				44.52	50.60	95.20	Pitts.10.1	50 subhedral
	52		0.01	0.01	**0.10**				44.45	50.80	95.36	Pitts.10.3	
	53		0.01	dl	**0.12**				44.46	51.42	96.00	Pitts.10.2	
	56		dl	dl	**0.14**				46.38	53.79	100.30	Pitts.11.2	10 euhedral
						PITTSBURGH- continued							
Date	Anal #	Se	Cu	Ni	As	Zn	Cd	Co	Fe	S	Total	Grain	Size (microns)/Form
	57		dl	dl	**0.12**				44.99	51.46	96.57	Pitts.12.1	25 subhedral
	58		dl	0.00	**0.09**				45.76	52.17	98.04	Pitts.12.2	
	59		dl	dl	**0.11**				45.54	52.28	97.93	Pitts.12.3	
	60		dl	dl	**0.12**				45.72	52.53	98.37	Pitts.12.4	
	65		dl	0.01	**0.14**				44.41	50.72	95.29	Pitts.14.1	50 cleat?
	66		dl	dl	**0.14**				45.33	51.80	97.28	Pitts.14.2	
	67		dl	dl	**0.15**				46.21	53.76	100.13	Pitts.14.3	
	*dl= values below detection limit of 100 ± 100 ppm, except arsenic values listed in boldface (dl= 500 ± 500 ppm).												
	Values for Co include a 0.03 wt. percent empirical correction factor subtracted from measured values.												

						ELKHORN-HAZARD							
Date	Anal #	Se	Cu	Ni	As	Zn	Cd	Co	Fe	S	Total	Grain	Size (microns)/Form
3/22/97	102	0.02	0.02	0.01	0.03	dl	dl	**dl**	44.29	50.96	95.36	ELKH B.2	25x30 subhedral
	103	dl	dl	dl	0.64	0.01	dl	**dl**	45.26	50.45	96.38	ELKH C.1	50x90 subhedral
	104	dl	dl	0.00	0.96	dl	dl	**0.01**	45.30	51.10	97.40	ELKH C.2	
	105	dl	0.01	0.01	0.70	dl	dl	**dl**	45.32	49.81	95.88	ELKH C.3	
	106	dl	dl	0.02	dl	dl	dl	**dl**	46.24	52.09	98.38	ELKH D.1	65x100 subhedral
	107	0.01	dl	0.01	0.01	dl	dl	**0.01**	46.01	51.84	97.93	ELKH D.2	
	108	dl	dl	0.02	dl	dl	dl	**dl**	46.04	52.09	98.18	ELKH D.3	
	109	0.02	0.02	0.01	dl	dl	dl	**dl**	46.44	51.44	97.96	ELKH D.4	
	110	dl	0.26	dl	0.01	0.02	dl	**0.01**	46.23	51.59	98.14	ELKH E.1	40x40 subhedral
	111	dl	0.02	dl	dl	dl	dl	**dl**	44.95	51.67	96.67	ELKH E.2	
	112	0.02	dl	0.03	0.02	0.01	dl	**dl**	46.03	51.60	97.74	ELKH 1.1	15 framboidal
11/27/96	29		0.01	dl	0.13	dl	dl		44.46	50.81	95.41	ELk-H.1.1	40x60 irregular
	31		0.02	0.01	0.02	dl	dl		44.95	50.84	95.84	ELk-H.2.1	10x20 irregular
	32		0.02	0.04	0.12	dl	dl		44.98	50.74	95.92	ELk-H.3.1	10 framboidal
	33		0.03	0.04	0.02	dl	dl		45.74	51.57	97.40	ELk-H.4.1	irregular
	34		0.04	0.15	0.02	dl	dl		45.90	52.22	98.32	ELk-H.4.2	
	35		0.01	0.02	0.01	dl	dl		45.64	51.34	97.03	ELk-H.5.1	20 framboidal
	36		0.01	0.02	0.04	dl	dl		45.27	50.38	95.72	ELk-H.5.2	
	38		0.06	0.10	0.05	dl	dl		44.68	51.13	96.03	ELk-H.6.2	30 framboidal
	39		dl	dl	0.01	dl	dl		45.08	50.97	96.06	ELk-H.7.1	15 subhedral
	40		0.03	dl	0.27	dl	dl		45.70	52.14	98.13	ELk-H.8.1	5x30 cleat

ELKHORN/HAZARD- continued

Date	Anal #	Se	Cu	Ni	As	Zn	Cd	Co	Fe	S	Total	Grain	Size (microns)/Form
11/27/96	41		dl	dl	0.01	dl	dl		45.93	52.12	98.06	ELk-H.9.1	70x80 subhedral
continued	42		0.01	dl	dl	dl	dl		45.54	51.20	96.75	ELk-H.9.2	
	43		dl	dl	0.01	dl	dl		46.37	52.49	98.88	ELkH.10.1	80x100 subhedral
	44		dl	dl	dl	dl	dl		46.72	53.48	100.20	ELkH.10.2	
	45		dl	dl	0.01	dl	dl		46.60	52.51	99.12	ELkH.10.2	
	46		0.02	0.02	dl	dl	dl		45.30	51.18	96.52	ELkH.11.1	30x40 subhedral
	48		dl	dl	0.02	0.01	dl		45.51	51.24	96.79	ELkH.12.1	20x35 subhedral/euh.
	49		dl	dl	0.01	dl	dl		45.10	51.46	96.57	ELkH.12.2	
10/19/96	21		0.08	0.01	**0.17**				45.99	52.44	98.69	ELKH.1.1	35 framboidal
	22		0.08	0.02	**0.21**				45.67	52.53	98.52	ELKH.1.2	
	23		0.09	0.02	**0.10**				44.88	52.96	98.05	ELKH.2.1	15 framboidal
	24		dl	0.01	**0.19**				44.93	52.37	97.51	ELKH.3.1	20x20 subhedral
	27		0.04	0.05	**0.23**				45.45	53.26	99.03	ELKH.6.1	20 framboidal
	28		dl	dl	**0.11**				45.55	52.84	98.49	ELKH.7.1	30x70 irregular
	29		dl	0.01	**0.08**				45.37	52.89	98.34	ELKH.7.2	
	53		0.06	dl	**0.10**				45.45	53.86	99.48	ELKH.8.1	20 subhedral
	56		0.12	0.05	**0.15**				44.22	51.26	95.79	ELKH.11.1	15 detrital?
9/26/96	26		dl	dl	**1.80**				45.05	52.00	98.85	ElkH.2.1	30x50 subhedral/euh.
	27		0.01	dl	**1.97**				44.95	51.78	98.71	ElkH.2.2	
	28		dl	dl	**2.10**				44.82	51.74	98.66	ElkH.2.3	
	31		dl	dl	**0.06**				45.65	54.40	100.11	ElkH.4.1	30x40 euhedral
	32		0.01	0.01	**0.05**				45.53	54.27	99.87	ElkH.4.2	

ELKHORN/HAZARD-continued

Date	Anal #	Se	Cu	Ni	As	Zn	Cd	Co	Fe	S	Total	Grain	Size (microns)/Form
9/26/96	37		0.04	0.01	**0.11**				44.18	51.18	95.52	ElkH.8.1	35x40 euhedral
continued													
	74		0.04	dl	**0.12**				44.38	51.80	96.35	ElkH.11.1	40x50 subhedral
	75		0.05	0.01	**0.23**				44.38	51.73	96.39	ElkH.11.2	
	76		dl	dl	**0.12**				44.44	52.03	96.59	ElkH.12.1	45 round
	77		0.02	0.01	**dl**				44.56	51.56	96.20	ElkH.12.2	
	78		0.00	0.01	**dl**				44.47	51.81	96.33	ElkH.12.3	
	81		0.01	0.06	**0.08**				45.52	53.48	99.16	ElkH.14.1	25 round
	82		0.02	0.05	**dl**				45.64	53.49	99.20	ElkH.14.2	
9/13/96	24		dl	dl	**0.23**				45.02	51.58	96.83	ELKH.1.1	50 irregular
	25		dl	dl	**0.19**				44.91	51.30	96.39	ELKH.1.2	
	68		dl	dl	**0.17**				45.25	51.67	97.10	ELKH.8.1	40 subhedral
	69		0.01	dl	**0.22**				45.48	52.03	97.73	ELKH.8.2	
	70		dl	dl	**0.16**				45.09	51.45	96.70	ELKH.8.3	
	77		0.01	dl	**0.37**				44.29	50.49	95.17	ELKH.11.3	80 round
	78		dl	0.01	**0.23**				45.49	51.37	97.09	ELKH.11.4	
	79		0.01	0.02	**0.19**				45.55	51.79	97.55	ELKH.11.5	
	80		0.02	0.02	**0.34**				45.21	51.63	97.22	ELKH.11.6	

*dl= values below detection limit of 100 ± 100 ppm, except arsenic values listed in boldface (dl= 500 ± 500 ppm).

Values for Co include a 0.03 wt. percent empirical correction factor subtracted from measured values.

							ILLINOIS #6					
Date	Anal #	Se	Cu	Ni	As	Zn	Cd	Co	Fe	S	Total	Grain	Size (microns)/Form
3/22/97	23	dl	dl	0.06	dl	dl	dl	**0.01**	45.76	52.52	98.38	Ill6PyD.1	30 subhedral/framb.
	24	0.01	0.02	0.02	dl	dl	dl	**0.02**	45.48	49.75	95.33	Ill6PyD.2	
	27	dl	dl	dl	0.01	dl	dl	**0.01**	45.58	53.75	99.40	Ill6Py1.1	20x25 subhedral/euh.
	28	0.01	0.01	dl	0.02	dl	dl	**dl**	45.02	53.78	98.87	Ill6Py1.2	
	29	dl	dl	dl	dl	dl	dl	**0.01**	44.36	50.71	95.11	Ill6Py2.1	20 framboidal
	30	dl	0.02	0.02	dl	0.01	dl	**0.01**	44.40	51.89	96.38	Ill6Py3.1	17 framboidal
	31	dl	dl	dl	0.00	dl	dl	**0.02**	45.38	52.46	97.89	Ill6Py4.1	20 framboidal
	32	dl	dl	dl	0.02	0.01	dl	**0.01**	45.64	51.78	97.48	Ill6Py5.1	40x60 subhedral
	33	dl	dl	0.01	0.02	0.01	dl	**0.01**	45.37	53.00	98.45	Ill6Py5.2	
	34	dl	0.01	dl	0.01	dl	dl	**0.01**	45.40	52.02	97.48	Ill6Py6.1	30 framboidal
	35	dl		dl	0.00	0.01	dl	**0.01**	44.46	51.26	95.78	Ill6Py6.2	
	36	0.02	0.03	0.02	0.02	0.01	dl	**dl**	44.57	52.01	96.70	Ill6Py7.1	20x30 subhedral
	39	dl	dl	0.01	0.01	0.02	dl	**dl**	43.65	51.19	94.91	Ill6Py8.2	60x60 subhedral/euh.
	41	dl	0.03	0.07	dl	dl	dl	**0.01**	45.30	51.89	97.32	Ill6Py9.1	25 framboidal/euh.
	49	dl	dl	dl	dl	0.01	dl	**dl**	46.03	52.71	98.78	Ill6Py11.2	80x150 plumose
	51	dl	0.02	0.08	dl	dl	dl	**0.01**	45.23	52.24	97.61	Ill6Py12.1	80x90 framb. cluster
	52	dl	0.03	0.40	dl	dl	dl	**0.01**	45.11	51.74	97.32	Ill6Py12.2	
	53	dl	0.02	0.03	0.01	dl	dl	**dl**	45.04	49.72	94.85	Ill6Py12.3	
	54	dl	0.04	0.08	dl	dl	dl	**0.01**	44.95	51.90	97.01	Ill6Py12.4	
	55	dl	0.01	dl	dl	dl	dl	**0.01**	45.83	53.31	99.19	Ill6Py13.1	25x70 cleat?
	56	dl	dl	dl	dl	0.02	dl	**dl**	46.00	48.98	95.03	Ill6Py13.2	
	57	0.02	dl	dl	0.00	dl	dl	**dl**	43.69	52.99	96.73	Ill6Py13.3	

ILLINOIS # 6- continued													
Date	Anal#	Se	Cu	Ni	As	Zn	Cd	Co	Fe	S	Total	Grain	Size (microns)/Form
11/27/96	8		0.03	0.05	dl	dl	dl		45.96	51.45	97.48	ILL-6.1.1	50x60 subhedral
	9		dl	0.04	0.03	0.02	dl		46.17	51.77	98.03	ILL-6.1.2	
	10		0.02	0.04	0.01	dl	dl		45.79	52.38	98.24	ILL-6.1.3	
	11		0.01	dl	0.01	dl	dl		45.62	52.38	98.01	ILL-6.2.1	25 framboidal
	12		0.03	0.01	dl	dl	dl		44.19	51.88	96.11	ILL-6.3.1	20 framboidal
	13		dl	dl	dl	dl	dl		46.66	53.47	100.12	ILL-6.4.1	20x70 cleat?
	14		dl	dl	dl	dl	dl		46.54	53.77	100.31	ILL-6.4.2	
	18		dl	dl	0.01	dl	dl		46.49	53.08	99.59	ILL-6.7.1	20 framboidal
	23		dl	0.01	dl	dl	dl		46.80	53.53	100.34	ILL-6.11.1	20 subhedral
	24		0.01	dl	0.01	dl	dl		46.37	51.83	98.23	ILL-6.12.1	30 framboidal
	25		dl	0.01	dl	dl	dl		46.21	52.37	98.59	ILL-6.12.1	
	26		0.08	0.07	dl	dl	dl		44.27	51.28	95.70	ILL-6.13.1	10 euhedral
	27		0.01	0.06	dl	dl	dl		45.40	51.74	97.22	ILL-6.14.1	20 framboid core
10/19/96	7		0.01	0.02	**0.05**				45.40	53.07	98.56	Ill6.2.1	50 irregular
	8		0.02	0.08	**0.09**				44.75	51.74	96.67	Ill6.3.1	20 framboidal
	9		0.01	0.06	**0.11**				45.57	52.55	98.30	Ill6.3.1	
	10		dl	0.05	**0.17**				45.65	52.86	98.73	Ill6.4.1	30 round
	11		dl	0.05	**0.10**				45.70	52.74	98.60	Ill6.4.2	
	12		dl	dl	**0.08**				45.78	52.04	97.90	Ill6.5.1	130 irregular
	13		dl	dl	**0.08**				46.02	53.19	99.29	Ill6.5.2	
	14		0.02	dl	**0.11**				44.85	51.93	96.90	Ill6.6.1	20x20 subhedral

ILLINOIS #6-continued													
Date	Anal#	Se	Cu	Ni	As	Zn	Cd	Co	Fe	S	Total	Grain	Size (microns)/Form
10/19/96	15		0.01	0.15	**0.13**				45.58	52.47	98.34	Ill6.7.1	20 x20 subhedral
continued													
	16		0.01	0.00	**0.10**				45.91	52.16	98.18	Ill6.8.1	20x30 subhedral
	17		0.01	0.20	**0.12**				44.99	52.69	98.00	Ill6.9.1	10x40 subhedral
	18		0.02	0.15	**0.13**				45.31	52.79	98.40	Ill6.10.1	10x70 subhedral
	19		dl	dl	**0.12**				46.37	53.66	100.15	Ill6.10.1	
	20		0.01	0.01	**0.10**				46.06	53.39	99.57	Ill6.10.2	
	46		0.01	0.12	**0.09**				45.79	53.14	99.15	Ill6.13.1	15x30 subhedral
	47		dl	dl	**0.11**				45.11	52.04	97.26	Ill6.14.1	euhedral on 13.1
	48		dl	dl	**0.11**				45.89	52.80	98.79	Ill6.15.1	20 framboid
	52		0.04	dl	**0.05**				44.97	51.86	96.92	Ill6.18.1	10 framboid
9/26/96	9		dl	dl	**0.10**				45.73	53.20	99.04	Ill6.3.1	20x65 euhedral
	10		0.01	dl	**0.13**				45.74	53.64	99.52	Ill6.3.2	
	11		dl	dl	**0.16**				45.69	53.25	99.10	Ill6.3.3	
	12		dl	dl	**0.08**				45.31	53.52	98.91	Ill6.4.1	20x20 euhedral
	14		dl	dl	**dl**				46.43	54.74	101.20	Ill6.6.1	30x100 subhedral
	15		dl	dl	**dl**				46.28	54.05	100.37	Ill6.6.2	
	16		dl	dl	**0.05**				46.55	54.08	100.68	Ill6.6.3	
	17		0.02	0.01	**0.06**				46.34	53.26	99.68	Ill6.6.4	
	20		0.04	0.26	**0.09**				43.80	52.54	96.74	Ill6.8.1	15 framboid
	83		dl	dl	**0.06**				46.14	54.31	100.52	Ill6.11.1	40x70 subhedral
	84		dl	dl	**0.09**				46.07	54.68	100.85	Ill6.11.2	
	85		dl	0.01	**dl**				45.46	53.14	98.65	Ill6.12.1	20 framboid

ILLINOIS #6-continued													
Date	Anal #	Se	Cu	Ni	As	Zn	Cd	Co	Fe	S	Total	Grain	Size (microns)/Form
9/26/96	86		0.02	dl	**dl**				46.53	53.89	100.44	Ill6.13.1	40 euhedral
continued	87		0.01	dl	**0.06**				46.53	54.11	100.71	Ill6.13.2	
	88		0.04	0.10	**0.08**				44.23	51.94	96.38	Ill6.14.1	10 framboidal
	89		dl	dl	**dl**				46.00	53.82	99.83	Ill6.15.1	20x70 subhedral
	90		0.01	dl	**0.08**				45.88	54.38	100.35	Ill6.15.2	
	91		dl	0.01	**0.07**				46.26	54.86	101.19	Ill6.15.3	
9/13/96	12		dl	dl	**0.06**				44.21	51.18	95.45	ILL6.1.1	50 subhedral
	13		0.01	dl	**0.08**				44.38	51.75	96.22	ILL6.1.2	
	81		dl	dl	**0.06**				47.22	54.33	101.61	ILL6.10.1	40 cleat?
	82		dl	dl	**0.14**				47.09	54.30	101.52	ILL6.10.2	
	83		dl	dl	**0.16**				46.83	54.50	101.50	ILL6.10.3	
	*dl= values below detection limit of 100 ± 100 ppm, except arsenic values listed in boldface (dl= 500 ± 500 ppm).												
	Values for Co include a 0.03 wt. percent empirical correction factor subtracted from measured values.												

WYODAK													
Date	Anal #	Se	Cu	Ni	As	Zn	Cd	Co	Fe	S	Total	Grain	Size (microns)/Form
5/21/97	176	dl	dl	dl	dl	0.03	dl	**0.01**	46.25	51.96	98.28	Cord 1.1	25 x 25 irregular
	177	dl	dl	dl	0.03	0.01	dl	**dl**	45.19	49.04	94.30	Cord 1.2	(composite)
	*dl= values below detection limit of 100 ± 100 ppm, except arsenic values listed in boldface (dl= 500 ± 500 ppm).												
	Values for Co include a 0.03 wt. percent empirical correction factor subtracted from measured values.												

APPENDIX E
Microprobe Analyses of Clay Minerals in Raw Coals

Appendix E. Illite and Kaolinite Analyses												
No.	K_2O	CaO	Na_2O	Al_2O_3	SiO_2	MgO	Cr_2O_3	MnO	FeO	TiO_2	Total	Comment
PITTSBURGH												
111	2.40	7.29	0.24	24.78	48.40	1.01	0.02	0.03	1.79	0.41	86.38	PITTS illite1.1
112	2.69	6.34	0.30	17.97	58.39	0.80	0.03	0.03	1.39	0.23	88.16	PITTS illite1.2
104	dl	0.04	0.05	40.43	48.00	0.10	dl	dl	0.04	dl	88.67	PITTS Kaol1.1
106	0.04	dl	0.02	40.15	47.17	0.02	dl	dl	0.07	dl	87.48	PITTS Kaol2.1
107	0.03	dl	dl	40.20	47.57	dl	0.03	dl	0.04	dl	87.89	PITTS Kaol2.2
108	0.10	dl	dl	40.89	48.22	0.02	0.03	0.02	0.06	0.03	89.38	PITTS Kaol2.3
109	dl	0.02	0.04	39.75	46.83	0.08	dl	dl	0.26	dl	87.01	PITTS Kaol3.1
110	dl	dl	dl	40.47	47.32	0.04	dl	dl	0.10	dl	87.98	PITTS Kaol3.2
115	0.02	0.02	0.04	40.33	47.49	0.04	dl	dl	0.05	dl	87.99	PITTS Kaol4.1
116	0.05	dl	0.05	40.28	47.39	0.02	0.02	dl	0.04	dl	87.85	PITTS Kaol4.2
ELKHORN/HAZARD												
119	1.78	0.06	0.19	38.06	46.91	0.65	dl	dl	1.25	0.04	88.95	ELKHAZ ill1.1
120	1.48	0.06	0.13	38.36	49.79	0.67	dl	0.02	1.27	0.04	91.82	ELKHAZ ill1.2
121	2.26	0.07	0.12	35.09	46.07	0.54	dl	dl	1.07	dl	85.22	ELKHAZ ill1.3
11	0.76	0.07	0.27	35.54	48.81	0.88	dl	dl	1.82	0.05	88.21	ELKHAZ ill1.3
22	1.26	0.15	0.13	37.59	47.15	0.53	0.02	dl	1.48	dl	88.31	ELKHAZ ill2.1
23	1.31	0.14	0.10	36.72	46.87	0.56	dl	dl	1.47	0.02	87.21	ELKHAZ ill2.2
124	0.15	0.02	0.04	40.59	46.74	0.06	dl	dl	0.32	dl	87.92	ELKHAZ Kaol2.1
125	0.05	dl	0.04	41.37	47.94	0.04	dl	0.02	0.28	dl	89.76	ELKHAZ Kaol2.2
25	0.12	0.03	0.03	39.90	48.42	0.03	0.02	dl	0.24	dl	88.79	ELKHAZ Kaol3.1
27	0.05	0.04	0.07	40.08	47.80	0.06	0.02	dl	0.46	dl	88.58	ELKHAZ Kaol3.3
ILLINOIS #6												

130	0.05	0.02	0.03	40.68	48.71	0.18	dl	dl	0.38	dl	90.05	IL#6 illite1.1
131	5.59	0.04	0.16	18.69	51.51	0.84	dl	dl	0.90	0.57	78.29	IL#6 illite1.2
126	dl	dl	0.02	40.23	47.38	dl	dl	0.02	0.07	dl	87.75	IL#6 Kaol1.1
127	dl	0.03	dl	40.66	49.08	0.04	dl	dl	0.14	dl	89.97	IL#6 Kaol1.2
128	dl	dl	dl	40.91	47.80	0.02	dl	dl	0.04	dl	88.79	IL#6 Kaol2.1

APPENDIX F

Example of a mass-balance calculation for arsenic in pyrite, based on electron microprobe (EPMA) data

Example of a mass-balance calculation for arsenic in pyrite, based on electron microprobe (EPMA) data.

Pittsburgh coal: As= 3.96 ppm (whole coal basis)

EPMA: Mean As = 140 + 165 ppm (n = 46)

Pyritic S = 0.91 wt. % * 1.87 = 1.70 wt. % pyrite

As contributed by pyrite = 140 * 0.0170 = 2.38 ppm

Fraction of As contributed by pyrite = 2.38 ppm/3.96 ppm = 60%